TRANSPORT AND FATE OF ACETONE IN AN OUTDOOR MODEL STREAM, STENNIS SPACE CENTER NEAR BAY ST. LOUIS, MISSISSIPPI

By R.E. Rathbun, D.J. Shultz, D.W. Stephens, and D.Y. Tai

U.S. GEOLOGICAL SURVEY

Water-Resources Investigations Report 89-4141

Denver, Colorado
1989

DEPARTMENT OF THE INTERIOR

MANUEL LUJAN, JR., Secretary

U.S. GEOLOGICAL SURVEY

Dallas L. Peck, Director

For additional information
write to:

Chief, Branch of Regional Research
U.S. Geological Survey
Box 25046, Mail Stop 418
Federal Center
Denver, CO 80225-0046

Copies of this report can
be purchased from:

U.S. Geological Survey
Books and Open-File Reports Section
Box 25425
Federal Center
Denver, CO 80225-0425

CONTENTS

FIGURES

TABLES

SYMBOLS AND DEFINITIONS

a_1, a_2	Anemometer readings of the windspeed at times t_1 and t_2, in meters per second
BOD	Biochemical oxygen demand, in milligrams per liter
C	Concentration of an organic compound in the water, in milligrams per liter or micrograms per liter
C_I	Concentration of a solute in an injection solution, in milligrams per liter or micrograms per liter
C_i^{CALC}	Calculated concentration for sample time i, in milligrams per liter or micrograms per liter
C_i^{EXP}	Experimental concentration for sample time i, in milligrams per liter or micrograms per liter
C_0	Concentration of an organic compound in the water at longitudinal position zero, in milligrams per liter or micrograms per liter
C_0^0	Concentration of an organic compound in the water at longitudinal position zero at an arbitrary base time of zero, in milligrams per liter
$\overline{C}$	Equilibrium concentration of an organic compound in the water, in micrograms per liter
$\overline{C}_x$	Equilibrium concentration of an organic compound in the water at longitudinal position x, in micrograms per liter
$C(0,t)$	Concentration of the organic compound in the water at longitudinal position zero at time t, in milligrams per liter or micrograms liter
$C(x,0)$	Concentration of the organic compound in the water at longitudinal position x at time zero, in milligrams per liter or micrograms per liter
$C(x,t)$	Concentration of an organic compound in the water at longitudinal position x at time t, in milligrams per liter or micrograms per liter
$C(x,\infty)$	Concentration of the organic compound in the water at longitudinal position x at infinite time, in milligrams per liter or micrograms per liter
$\overline{C}_1$, $\overline{C}_2$	Equilibrium concentrations of an organic compound in the water at longitudinal positions x_1 and x_2, in milligrams per liter
COD	Chemical oxygen demand, in milligrams per liter

D	Longitudinal-dispersion coefficient, in square meters per minute
erfc(Φ)	Complimentary error function, defined by $(2/\sqrt{\pi})\int_{\Phi}^{\infty}\exp(-z^2)dz$ where z is a dummy variable of integration and π is the constant 3.1416
exp	Indicates an exponential to the base e
$f(x,t)$	Equation giving the concentration at longitudinal position x as a function of time t, the mean velocity, the longitudinal-dispersion coefficient, and the first-order rate coefficients for loss
$f'(x,t)$	Identical to $f(x,t)$ except that $(\Sigma K_i-\gamma)$ has been substituted for ΣK_i; K_i is the first-order rate coefficient for process i and γ is the rate coefficient describing the exponential decrease of the acetone injection rate with time
$f(x,t-\tau)$	Equation giving the concentration at longitudinal position x as a function of time $(t-\tau)$, the mean velocity, the longitudinal-dispersion coefficient, and the first-order rate coefficients for loss; τ is the duration of the injection of the organic compound
H	Henry's constant, in kilopascals · cubic meter per gram mole
H^{AC}	Henry's constant for acetone, in kilopascals · cubic meter per gram mole
H^{TBA}	Henry's constant for t-butyl alcohol, in kilopascals · cubic meter per gram mole
K_D	First-order rate coefficient for bacterial degradation, in minutes^{-1}
K_i	First-order rate coefficient for process i, in minutes^{-1}
K_{OL}	Overall mass-transfer coefficient based on the overall liquid-phase concentration difference driving force, in meters per day
K_{OL}^{AC}	Overall mass-transfer coefficient for acetone, in meters per day
K_{OL}^{TBA}	Overall mass-transfer coefficient for t-butyl alcohol, in meters per day
K_V	First-order rate coefficient for volatilization, in minutes^{-1}
K_V^{AC}	Volatilization coefficient for acetone, in minutes^{-1}
K_V^{θ}	Volatilization coefficient at a water temperature of θ in degrees Celsius, minutes^{-1}
K_V^{25}	Volatilization coefficient at a water temperature of 25.0 degrees Celsius, in minutes^{-1}

k_G	Mass-transfer coefficient for the gas-film, generally called the gas-film coefficient, in meters per day
k_G^{ORG}	Gas-film coefficient for the volatilization of an organic compound, in meters per day
k_G^{TBA}	Gas-film coefficient for the volatilization of t-butyl alcohol, in meters per day
k_G^{WAT}	Gas-film coefficient for the evaporation of water, in meters per day
$k_{G_\theta}^{WAT}$	Gas-film coefficient for the evaporation of water at a water temperature of θ, in meters per day
$k_{G_{26.1}}^{WAT}$	Gas-film coefficient for the evaporation of water at a water temperature of 26.1 degrees Celsius, in meters per day
k_L	Mass-transfer coefficient for the liquid-film, generally called the liquid-film coefficient, in meters per day
k_L^{TBA}	Liquid-film coefficient for the volatilization of t-butyl alcohol, in meters per day
$\log_e$	Natural logarithm
M	Weight of solute injected, in micrograms
n	Number of data points
PR	Percentage recovery of the solute injected
Q	Water discharge, in liters per second
q_A	Acetone injection rate at time t, in milliliters per minute
q_I	Rhodamine-WT dye injection rate, in milliliters per minute
q_0	Acetone injection rate at the arbitrary base time zero, in milliliters per minute
R	Ideal gas constant, in kilopascals · cubic meter per gram mole per kelvin
rms	Root-mean-square
T	Absolute temperature, in kelvins
TBA	t-Butyl alcohol
t	Time, in minutes

t_0	Arbitrary base clock time, in hours
t_s	Clock sampling time, in hours
U	Mean cross-sectional water velocity, commonly called the mean velocity, in meters per minute
V	Windspeed, in meters per second
$\bar{V}$	Integral mean windspeed, in meters per second
V_i, V_{i+1}	Windspeeds at times t_i and t_{i+1}, respectively, in meters per second
V_1, V_2	Windspeeds corresponding to anemometer readings a_1 and a_2, respectively, in meters per second
W	The dimensionless group defined by equation 11
x	Downstream longitudinal position, in meters
Y	Mean water depth, in meters
Z	The dimensionless group defined by equation 10
α	The dimensionless group defined by equation 9
β	Exponential constant in the equation describing the temperature dependence of the volatilization coefficient, in kelvins
γ	Rate coefficient describing the exponential decrease of the acetone injection rate with time, in $minutes^{-1}$
Δt	Traveltime between cross sections, in minutes
Δt_1, Δt_2	Traveltimes between the injection point and cross section 1 and between the injection point and cross section 2, in minutes
δt	Time difference defined by equation 40, in minutes
θ	Water temperature, in degrees Celsius
τ	Length of injection of a solute into the model stream, in minutes
Ψ	Constant in the reference substance concept for the gas film, equal to the ratio of the gas-film coefficient for the volatilization of an organic solute to the gas-film coefficient for the evaporation of water

CONVERSION FACTORS

Metric (International System) units in this report may be converted to inch-pound units by using the following conversion factors:

Multiply metric unit	*By*	*To obtain inch-pound unit*
micrometer (μm)	3.937×10^{-5}	inch (in.)
millimeter (mm)	3.937×10^{-2}	inch (in.)
meter (m)	3.281	foot (ft)
meter per second (m/s)	3.281	foot per second (ft/s)
meter per minute (m/min)	3.281	foot per minute (ft/min)
meter per day (m/d)	3.281	foot per day (ft/d)
square meter per minute (m^2/min)	10.765	square foot per minute (ft^2/min)
microgram (μg)	2.205×10^{-9}	pound (lb)
microgram per liter (μg/L)	6.243×10^{-8}	pound per cubic foot (lb/ft^3)
milligram per liter (mg/L)	6.243×10^{-5}	pound per cubic foot (lb/ft^3)
gram per liter (g/L)	6.243×10^{-2}	pound per cubic foot (lb/ft^3)
milliliter per minute (mL/min)	3.531×10^{-5}	cubic foot per minute (ft^3/min)
liter per second (L/s)	3.531×10^{-2}	cubic foot per second (ft^3/s) (ft^3/s)
kilopascal cubic meter per gram mole (kPa · m^3/g mol)	158.1	standard atmosphere cubic foot per pound mole (atm · ft^3/lb mol)
kilopascal cubic meter per gram mole kelvin [kPa · m^3/(g mol · K)]	87.83	standard atmosphere cubic foot per per pound mole degree rankine [atm · ft^3/(lb mol · °R)]

Temperature in kelvin (K) may be converted to degree Celsius (°C) using:

$$°C = K-273.15$$

Temperature in kelvin (K) may be converted to degree rankine (°R) using:

$$°R = (K-273.15)(1.8) + 491.7$$

Temperature in kelvin (K) may be converted to degree Fahrenheit (°F) using:

$$°F = (K-273.15)(1.8) + 32.0$$

TRANSPORT AND FATE OF ACETONE IN AN OUTDOOR MODEL STREAM, STENNIS SPACE CENTER NEAR BAY ST. LOUIS, MISSISSIPPI

By R.E. Rathbun, D.J. Shultz,
D.W. Stephens, and D.Y. Tai

ABSTRACT

The fate of anthropogenic organic compounds in streams is determined by the interactions of various chemical, biological, and physical processes. The fundamentals of these processes typically are determined in laboratory studies where conditions can be controlled and effects of single variables examined. In such studies, however, reality is lost. An outdoor model stream study, on the other hand, more nearly represents a natural stream and yet permits control of some important physical variables.

The transport and the fate of acetone, rhodamine-WT dye, t-butyl alcohol, and glucose in an outdoor model stream were investigated. Acetone was injected into the stream continuously for 32 days resulting in downstream water concentrations of 20 to 30 milligrams per liter. Rhodamine-WT dye was injected at the beginning of the experiment and again at the end to determine the traveltime and dispersion characteristics of the stream. An injection of t-butyl alcohol was used to determine the volatilization characteristics of the stream. A glucose solution was injected for about 3 days near the middle of the acetone injection period in an attempt to stimulate the bacterial degradation of the acetone. Similarly, a nutrient solution containing bacteria acclimated to acetone in the laboratory was injected for about 1 day in a separate attempt to stimulate the bacterial degradation of the acetone.

Daily acetone concentration data from three cross sections near the upstream, middle, and downstream ends of the stream did not change significantly with time. It was concluded, therefore, that significant bacterial degradation of acetone did not occur during the 32 days of the injection. This result was contrary to laboratory studies which indicated that acetone should be readily degraded by bacteria in streams.

Failure of the acetone to degrade was attributed to a lack of acclimation of bacteria to acetone. This lack of acclimation may be the result of a nutrient limitation because of the small nitrate concentrations in the stream. Preferential use of naturally occurring organic compounds in the stream may also account in part for failure of bacteria to acclimate to acetone.

The limited residence time of the model stream also could restrict the ability of the bacteria to acclimate to the acetone. If free-floating

bacteria dominate the degradation process, then the bacteria, although continuously replenished, would likely be flushed from the system before acclimation could occur. If attached bacteria dominate the degradation process, then the residence time should not be a factor because the bacteria were exposed to acetone continuously for 32 days.

Volatilization coefficients for acetone determined from t-butyl alcohol concentrations were comparable to or larger than coefficients determined from acetone concentrations on day 4 of the experiment. This result supports the conclusion that significant bacterial degradation of the acetone did not occur. Volatilization coefficients for acetone determined by different methods for different time periods usually were in good agreement, although the day 4 values generally were larger. Because the volatilization coefficient increases with windspeed, these larger values were attributed to a greater windspeed on day 4 than was observed during other periods of the study. Measurement of the volatilization coefficients was subject to large errors because of the limited length of the model stream and the slow rate of volatilization of the acetone.

Injection of the glucose solution had no detectable effect on the acetone concentrations. Similarly, injecting the nutrient solution containing bacteria acclimated to acetone also had no measurable effect on the acetone concentrations.

The failure of the acetone to degrade in the model stream was unexpected, based on previous laboratory studies of the fate of acetone in water. This difference in behavior indicates that estimating the fate of an organic compound in a stream on the basis of laboratory studies is subject to error. Thus, the results of this study demonstrate the utility of outdoor model stream studies in estimating such fates.

INTRODUCTION

Organic substances discharged into streams and rivers as components of wastewater affect water quality in various ways. For many years, these effects were defined almost exclusively by collective parameters such as biochemical oxygen demand (BOD) and chemical oxygen demand (COD). These parameters combine the effects of the various components of the wastewater on the quality of the receiving stream. These effects have usually been defined in terms of changes in the dissolved-oxygen concentration.

In 1972, the Federal Water Pollution Control Act known as Public Law 92-500 was passed. Subsequent court cases involving this act resulted in the settlement now commonly known as the Environmental Protection Agency (EPA) Consent Decree (Keith and Telliard, 1979). A component of this Consent Decree was a list of 65 compounds and classes of compounds. This list was then used as the basis for the EPA list of 129 priority pollutants, of which 114 were organic compounds.

These legal actions resulted in a change in emphasis from collective parameters such as BOD and COD to the effects of specific organic compounds on receiving water quality. In particular, processes determining the fate of organic compounds in streams and rivers have received considerable attention.

A number of chemical, biological, and physical processes interact to determine the fate of organic compounds in streams and rivers. Chemical processes include oxidation-reduction, hydrolysis, photolysis, complexation, dissociation, and precipitation-dissolution. Biological processes include bacterial degradation and uptake, accumulation, and release of organic compounds by biota. Physical processes include volatilization, sorption and desorption by particulate and colloidal materials, dispersion, and convective mass transport.

Some of these processes involve transfer of an organic compound between phases of the environment. Other processes involve transformation of the compound into another compound that may be more or less toxic than the parent compound. Not all of these processes will be important for every organic compound. The relative importance depends on the characteristics of both the stream or river and the compound. There are, however, a large number of organic compounds currently in use, and new compounds are placed into use almost daily. Consequently, research on the fate of all compounds that might be present in streams and rivers would be costly and time consuming.

The alternative is research on a specific substance chosen as a model for a class of compounds. This model compound may be selected on the basis of similarities in chemical structure or a physical property. A physical property of importance in several of these processes is water solubility. For example, sorption of various organic compounds on sediments depends on the water solubility (Chiou and others, 1979). Volatilization of organic compounds from water depends on water solubility through its effect on the Henry's constant (Mackay and Yuen, 1980). Bioconcentration factors for organic compounds in fish (Veith and others, 1980) and in alga (Geyer and others, 1981) are related to the water solubility. Because water is the matrix in which the processes occur, solubility is undoubtedly important also in many of the other processes.

Acetone, which is infinitely soluble in water, was chosen in the present study as a model substance for the class of very soluble organic compounds. There were two reasons for selecting acetone. First, acetone is a widely used solvent and, thus, is an environmentally significant compound. In a study (Shackelford and Keith, 1976) of the occurrence of organic compounds in various types of natural waters, it was the compound occurring most frequently. Acetone has been detected in leachates from landfills (Khare and Dondero, 1977), in water effluents from energy-related processes (Pellizzari and others, 1979), and in the drinking waters of 10 U.S. cities (U.S. Environmental Protection Agency, 1975). It may be present in wastewaters from sewage treatment plants operated at above optimum capacity (Abrams and others, 1975). Under some conditions, acetone also may be a precursor in the formation of chlorinated hydrocarbons during chlorination of drinking waters (Stevens and others, 1976).

The second reason for selecting acetone was the suggestion (Abrams and others, 1975; Thom and Agg, 1975; Helfgott and others, 1977) that acetone should be readily degraded by bacteria. This characteristic would permit experiments on the fundamentals of this important biological process to be completed within a reasonable time period.

Laboratory studies on the fate of acetone in water (Rathbun and others, 1982) considered volatilization, sorption by sediments, photolysis, bacterial degradation, and uptake by algae and molds. It was concluded that volatilization and bacterial degradation were the processes most likely to be important in determining the fate of acetone in streams and rivers.

Utility of Model-Stream Studies

Model-stream studies of the fate of organic compounds in streams and rivers have utility in that they provide a situation somewhere intermediate between real-world conditions and controlled laboratory conditions. Laboratory studies are essential in elucidating the fundamentals of the chemical, physical, and biological processes that interact to determine the fate of organic compounds in water. Such studies permit research on individual processes without the complication of synergistic effects. However, while these laboratory studies with a range of possible characteristics permit various controls, the greater the degree of control, the more reality is lost (Warren and Davis, 1971). These differences may result in laboratory coefficients that are not transferable to the field situation (Wilson and others, 1981; Landrum and others, 1984).

Model streams also may have a range of characteristics varying from those located in controlled environmental chambers to those outside and exposed to the naturally variable ambient conditions (Clark and others, 1980). Again, the greater the control, the more reality is lost and the less the model stream approximates a true natural stream.

An outside model stream generally will have a controlled flow and, consequently, a reasonably constant flow velocity and depth. The stream, however, will be subject to ambient variations in sunlight intensity, air temperature, precipitation, windspeed, and water temperature. Such a stream allows a reasonable simulation of the complex hydrologic situation in natural streams, but still permits controls not possible on natural streams. Injections of hazardous or toxic organic compounds into natural streams for the purpose of research on the fate of these compounds generally is not justified environmentally. A model stream where such injections can be made safely thus has utility as a link between laboratory studies and natural streams.

Purpose and Scope

The purpose of this report is to present the results of a study of the transport and fate of acetone in an outdoor model stream located at the Stennis Space Center near Bay St. Louis, Mississippi. The principal element of the experimental design was a 32-day injection of acetone into the model stream. Other elements of the design included injection of glucose for 3 days and injection of a bacteria-nutrient mixture for 1 day in an attempt to stimulate bacterial growth and degradation of the acetone. Rhodamine-WT dye was injected for 1.5 days at the beginning of the test period and for 1.0 day at the end of the test period to determine the overall stream dispersion and traveltime characteristics. t-Butyl alcohol (TBA) was injected for 0.5 day to determine the volatilization characteristics of the stream.

BACKGROUND THEORY

One-Dimensional Convective-Dispersion Equation

The interactions of the various processes that affect the concentration of an organic compound in a stream are generally described by the one-dimensional convective-dispersion equation. This equation has the form (Falco and Mulkey, 1976)

$$\frac{\partial C}{\partial t} + U \frac{\partial C}{\partial x} = D \frac{\partial^2 C}{\partial x^2} - \sum_{i=1}^{n} K_i C \ , \tag{1}$$

where C = the concentration of the organic compound in the water, in milligrams per liter;
t = time, in minutes;
U = the mean cross-sectional water velocity, in meters per minute;
x = the downstream longitudinal position, in meters, relative to the source location;
D = the longitudinal-dispersion coefficient, in square meters per minute; and
K_i = the first-order rate coefficient for the loss of the compound from the stream by process i, in minutes^{-1}.

Equation 1 assumes that these processes act independently on the compound and that the resultant effect is the sum of the individual processes as indicated by the summation term. Equation 1 also assumes there are no sources of the compound along the subject reach of the stream, other than the boundary condition source at the upstream end.

Boundary and initial conditions for an injection of the compound into the stream for a time period τ (in minutes) are

$$C(x,0) = 0 \tag{2}$$

$$C(0,t) = C_0 \quad \text{for } 0 < t \leq \tau \tag{3}$$

$$C(0,t) = 0 \quad \text{for } t > \tau \tag{4}$$

$$\frac{\partial C}{\partial x}(\infty,t) = 0 \ . \tag{5}$$

Following Overman and others (1976) and Van Genuchten (1981), the solution to equation 1 subject to the conditions of equations 2, 3, 4, and 5 is:

$$C(x,t)/C_0 = f(x,t) \text{ for } 0 < t \leq \tau \tag{6}$$

$$C(x,t)/C_0 = f(x,t) - f(x,t-\tau) \text{ for } t > \tau \tag{7}$$

where
$$f(x,t) = \tfrac{1}{2}\left[\exp\{(\sqrt{1+\alpha}+1)\frac{Ux}{2D}\}\ \text{erfc}\ (\frac{Z+2W}{2\sqrt{W}}) + \exp\{-(\sqrt{1+\alpha}-1)\frac{Ux}{2D}\}\ \text{erfc}\ (\frac{Z-2W}{2\sqrt{W}})\right] , \tag{8}$$

and $$\alpha = \frac{4D}{U^2} \sum_{i=1}^{n} K_i \tag{9}$$

$$Z = \frac{Ux}{2D} \left(1 + \frac{4D}{U^2} \sum_{i=1}^{n} K_i\right)^{0.5} \tag{10}$$

$$W = \frac{U^2 t}{4D} \left(1 + \frac{4D}{U^2} \sum_{i=1}^{n} K_i\right). \tag{11}$$

In equations 6 and 7, C_0 is the concentration of the compound in the water in the stream at the source location where x is zero.

The steady-state solution is obtained by allowing t and τ to go to infinity (∞) in equation 7. The result is:

$$C(x,\infty)/C_0 = \exp\left[\frac{Ux}{2D}\{1-(1+\alpha)^{0.5}\}\right] . \tag{12}$$

Because α generally is small for streams and rivers, it can be shown by Taylor series expansion of equation 12 (Overman and others, 1976) that the steady-state distribution is given by:

$$C(x,\infty)/C_0 \cong \exp\left[-\frac{x}{U} \sum_{i=1}^{n} K_i\right] . \tag{13}$$

Laboratory studies of the fate of acetone in water (Rathbun and others, 1982) concluded that volatilization and bacterial degradation were the processes most likely to be important in determining the fate of acetone in streams. Therefore, $\sum_{i=1}^{n} K_i$ in these equations can be replaced by:

$$\sum_{i=1}^{n} K_i = K_V + K_D \tag{14}$$

where K_V = the first-order rate constant for volatilization; and

K_D = the first-order rate constant for bacterial degradation.

These equations are for a one-dimensional system. Consequently, it is assumed that there are no concentration variations in the vertical or lateral direction.

Volatilization of Organic Compounds from Water

Volatilization of organic compounds from water generally is described by the two-film model (Lewis and Whitman, 1924). This model assumes uniformly mixed water and air phases separated by thin films of water and air in which

mass transfer is by molecular diffusion. A dynamic steady-state equilibrium is assumed at the interface, with the equilibrium expressed by Henry's law.

The basic equation of the two-film model is:

$$1/K_{OL} = 1/k_L + RT/Hk_G \tag{15}$$

where K_{OL} = the overall mass-transfer coefficient, in meters per day, based on the overall liquid phase concentration difference driving force;

k_L = the mass-transfer coefficient for the liquid film, generally called the liquid-film coefficient, in meters per day;

R = the ideal gas constant, in kilopascals · cubic meter per gram mole per kelvin;

T = the absolute temperature, in kelvins;

H = the Henry's constant, in kilopascals · cubic meter per gram mole; and

k_G = the mass-transfer coefficient for the gas film, generally called the gas-film coefficient, in meters per day.

The overall mass-transfer coefficient, K_{OL}, of equation 15 is related to the volatilization coefficient, K_V, of equation 14 by the equation (Rathbun and Tai, 1982):

$$K_{OL} = K_V Y \tag{16}$$

where Y = the mean water depth, in meters.

Analysis of equation 15 (Rathbun and Tai, 1982) has indicated that the relative importance of the resistances of the gas film and the liquid film to volatilization depends on the Henry's constant of the organic compound. Organic compounds with large Henry's constants have virtually all the resistance in the liquid film. Compounds with small Henry's constants such as acetone and TBA have resistances in both the liquid film and the gas film. For these compounds, the gas-film and liquid-film coefficients of equation 15 cannot be measured directly. In this case, the reference-substance concept must be used.

The reference-substance equation for the gas-film coefficient is (Rathbun and Tai, 1986)

$$k_G^{ORG} = \psi\, k_G^{WAT} , \tag{17}$$

where k_G^{ORG} = the gas-film coefficient for an organic compound;

k_G^{WAT} = the gas-film coefficient for water; and

ψ = the reference-substance constant.

This constant is assumed to be independent of mixing conditions in the air phase. These mixing conditions usually are characterized by the windspeed. Equation 17 has been verified with ethylene dibromide as the organic compound (Rathbun and Tai, 1986).

Values of ψ are determined in the laboratory by measuring the volatilization fluxes of the pure organic compounds and water under identical windspeed conditions. The basis of this procedure is the rationalization that there can be no concentration gradient in a pure liquid. Therefore, this volatilization process must be controlled completely by the gas-film resistance, and the measured mass-transfer coefficient is the gas-film coefficient. A procedure for measuring these fluxes has been described (Rathbun and Tai, 1984b).

The reference substance concept is applied by calculating the gas-film coefficient for evaporation of water, k_G^{WAT}, from the stream of interest. This coefficient is then combined through equation 17 with the laboratory-determined ψ value to give the gas-film coefficient for the organic compound for the stream. Gas-film coefficients for the evaporation of water from a stream may be calculated from the equation (Rathbun and Tai, 1983):

$$k_{G_{26.1}}^{WAT} = 416 + 156V \tag{18}$$

where $k_{G_{26.1}}^{WAT}$ = the gas-film coefficient, in meters per day, at 26.1 degrees Celsius; and

V = the windspeed, in meters per second.

Gas-film coefficients may be adjusted to the desired water temperature using the equation (Rathbun and Tai, 1983):

$$k_{G_\theta}^{WAT} = k_{G\ 26.1}^{WAT} \exp\ [0.00934\ (\theta\text{-}26.1)] \tag{19}$$

where $k_{G_\theta}^{WAT}$ = the gas-film coefficient, in meters per day, for water evaporation at water temperature θ, in degrees Celsius.

The reference-substance equation for the liquid-film coefficient (Rathbun and Tai, 1984a) cannot be applied to acetone and TBA because no limiting case exists for which the acetone and TBA liquid-film coefficients can be measured directly. However, the acetone and TBA liquid-film coefficients can be determined by difference from equation 15 using measured values of the overall mass-transfer coefficient and gas-film coefficients determined as just described (Rathbun and Tai, 1988).

The two-film model used to describe volatilization of organic compounds from water assumes transport through the films is by molecular diffusion. Because molecular diffusion is temperature dependent, it is expected that the volatilization coefficient also will be temperature dependent. The temperature dependence of the volatilization coefficients of acetone and TBA have been determined (Rathbun and Tai, in 1988). This dependence relative to a base temperature of 25.0 °C has the form:

$$K_V^{\theta} = K_V \quad \exp\left[\beta \left(\frac{1}{25.0+273.2} - \frac{1}{\theta+273.2}\right)\right] \tag{20}$$

where θ = the water temperature, in degrees Celsius; and
β = a constant having a value of 4,420 K for acetone and 6,550 K for TBA (Rathbun and Tai, in 1988).

Equation 13 indicates that the total loss of acetone from the model stream will be described by the sum of the volatilization and bacterial degradation losses as indicated by equation 14. Thus, the effects of these two processes will not be separable unless some procedure is developed for independent measurement of one of these two coefficients.

The procedure adopted was to select a compound that would have volatilization characteristics similar to those of acetone but that would be much more resistant to bacterial degradation. The compound selected for this purpose was TBA which, like acetone, is infinitely soluble in water. Therefore, TBA was expected to have volatilization characteristics similar to those of acetone. However, because of its branched structure, TBA was expected to be much more resistant to bacterial degradation. Justification for this expectation is discussed in more detail in the next section.

Finally, equation 1 and equations 9 through 14 assume that the processes of volatilization and bacterial degradation are first order. This assumption has been verified for the volatilization of two chlorinated hydrocarbons from water (Rathbun and Tai, 1984a). Evidence in support of this assumption for bacterial degradation will be discussed in the next section.

Bacterial Degradation of Organic Compounds in Water

Bacterial degradation of organic compounds in the water of streams and rivers is a complex process. A complete discussion of this process is beyond the scope of this report. However, a brief discussion of the general principles of bacterial degradation as they relate to acetone and TBA is presented.

The degradation of organic compounds in streams occurs as the result of the use of the compounds by bacteria as energy for cell growth (Dugan, 1972). Bacterial degradation of organic compounds can be described by the equation (Tinsley, 1979):

$$C = C_0 \exp(-K_D t) , \tag{21}$$

where C = the concentration of the organic compound in the water at time t, in milligrams per liter;
C_0 = the concentration at time zero, in milligrams per liter; and
K_D = the first-order rate coefficient, in minutes^{-1}, for bacterial degradation.

Equation 21 is a simplified representation of a complex process. Many transformations actually may be occurring simultaneously, with the overall process only approximately described by equation 21. It has been determined (Paris and others, 1981) that a second-order equation may be more appropriate

for describing bacterial degradation in natural waters. This equation has the degradation rate proportional to the concentration of bacteria, as well as the concentration of organic compound. We conclude, however, that the present state of our knowledge of this complex process is such that a second-order equation cannot be used in all situations to describe the bacterial degradation process.

Degradation reactions are catalyzed by an enzyme (or enzymes) specific to a particular reaction. In such cases, the ability of bacteria to degrade a specific organic compound depends on the chemical structure of the compound and the ability of the bacteria to acclimate to this structure. Acclimation may have already occurred as a result of prior exposure of the bacteria in the stream water to the specific organic compound. If not, then acclimation may occur (Dugan, 1972) by a temporary change in the characteristics of the bacteria allowing production of the necessary enzyme or by mutation resulting in a permanent change in the bacteria. Other mechanisms possibly contributing to the acclimation and lag phase time periods have been discussed (Wiggins and others, 1987). These include the time necessary for small populations of the bacteria to become large enough to cause a significant consumption of the compound, insufficient concentrations of inorganic nutrients, the preferential use of other organic compounds in the natural water before the compound of interest, the time needed for the bacteria to acclimate to toxins or other inhibitors present in the water, and predation of bacteria by protozoa.

The development of acclimated bacteria is the most important factor in the degradation of anthropogenic organic compounds in streams. Other factors are important, however. These include the temperature and pH of the water, and the concentrations of nutrients, dissolved oxygen, trace elements, and other organic compounds present in the water. Organic compounds may sometimes be added to the water as a supplemental carbon source to enhance bacterial activity. Compounds which are readily available sources of carbon and energy such as glucose generally are used for this purpose (Pfaender and Alexander, 1973; Subba-Rao and others, 1982; Schmidt and Alexander, 1985), although increased bacterial degradation is not always observed.

One way to introduce desired bacteria into the natural water is by addition of laboratory-acclimated organisms. This procedure results in enhanced degradation in some cases and no enhancement in others. Possible reasons for failure of acclimated bacteria to enhance degradation in the natural water have been summarized (Goldstein and others, 1985). These include a concentration of the compound too small to sustain growth of the bacteria, organic or inorganic compounds that inhibit or arrest the bacterial process, a rate of predation of the bacteria by protozoa that is faster than the rate of growth, and preferential use of other organic compounds in the water.

Acetone was expected to degrade readily in the model stream on the basis of the laboratory studies (Rathbun and others, 1982) and on the basis of the literature. Thom and Agg (1975) classified acetone as easily degradable in a biological sewage treatment plant, although they stressed the importance of acclimation. Abrams and others (1975) similarly classified acetone as having low persistence. Finally, Helfgott and others (1977) measured a refractory index of 0.8 for acetone, resulting in a classification of readily degradable

for acetone. It was on the basis of the expectation that acetone would degrade readily in the model stream that acetone was selected as the model substance for the class of very soluble organic compounds.

Conversely, TBA was expected to be relatively resistant to bacterial degradation because of its branched structure. This expectation was supported by the literature. Tallon (1969) noted that branching in the structure of a molecule greatly increased resistance to bacterial degradation in the treatment of sewage, with TBA having considerable resistance to degradation but with n-butyl and sec-butyl alcohols degrading readily. Stover and McCartney (1984) compared two BOD tests of 20 organic compounds using both acclimated and nonacclimated bacteria. They found no degradation of TBA with the nonacclimated bacteria and only very limited degradation with the acclimated bacteria. Acetone was degraded rapidly in all tests.

The resistance of TBA to bacterial degradation also was supported by limited experimental data from two tests. The first test used the respirometer procedure and the same strain of bacteria developed in the laboratory study of the bacterial degradation of acetone (Rathbun and others, 1982). The acetone concentration was reduced to about 10 percent of its initial value in 1.0 day and to virtually zero after 1.25 days. The TBA concentration, however, was virtually unchanged after 25 days. The second test consisted of the incubation of 10 g of sediment and water from the model stream with acetone and TBA. Periodic monitoring of the concentrations showed that the acetone began to degrade after about 3.8 days and the concentration was reduced to virtually zero after 21 days. The TBA concentration was virtually unchanged after 21 days, however. A parallel study with sterile sediment and water from the model stream resulted in no loss of either acetone or TBA. This supports the conclusion that the loss of acetone under the nonsterile conditions was the result of bacterial processes rather than sorption processes.

These results indicate that the TBA was much more resistant to bacterial degradation than acetone for these two studies. The results do not necessarily mean that TBA is recalcitrant, that is, completely resistant to degradation by all bacteria. It does, however, support the assumption that TBA is reasonably inert to bacterial degradation. Also, because only a relatively limited injection of TBA is necessary to determine the volatilization characteristics of the model stream, exposure of the bacteria to TBA would be minimal, thus reducing the possibility of acclimation.

It was concluded, therefore, that TBA could be used to measure the volatilization characteristics of the model stream without interference from bacterial degradation. Transfer of the measured TBA volatilization coefficients to coefficients for acetone thus requires knowledge of the relative volatilization characteristics of acetone and TBA.

Relative Volatilization Characteristics of Acetone and t-Butyl Alcohol

The relative volatilization characteristics of acetone and TBA and the temperature dependences of the volatilization coefficients were studied previously (Rathbun and Tai, 1988). Therefore, only a brief summary of the results of that study pertinent to the present work will be presented here.

The equation relating the overall mass-transfer coefficient for volatilization of acetone to the several coefficients describing the volatilization of TBA is (Rathbun and Tai, 1988):

$$K_{OL}^{AC} = 1.30 \left[K_{OL}^{TBA}\right] \left[\frac{H^{AC}}{H^{TBA}} \quad \frac{(H^{TBA} k_G^{TBA}/k_L^{TBA}) + RT}{(1.08\ H^{AC}\ k_G^{TBA}/k_L^{TBA}) + 1.20RT}\right], \qquad (22)$$

where AC = a superscript denoting acetone; and
TBA = a superscript denoting t-butyl alcohol.

Equations 22 and 16 permit calculation of the acetone volatilization coefficient from information on the TBA volatilization characteristics and the depth of water in the stream. Thus, the computed coefficient is independent of any effects of bacterial degradation of the acetone.

The various coefficients in equation 22 are determined as follows. The overall mass-transfer coefficient, K_{OL}^{TBA}, for TBA is calculated from equation 16. The mean flow depth, Y, is determined from cross-section measurements. The TBA volatilization coefficient is determined from the experimental data in two ways.

First, for the limiting case of only volatilization and a long time such that steady-state conditions have been established in the model stream, equation 13 reduces to:

$$\bar{C}_x/C_0 = \exp\left(-\frac{K_V}{U}\,x\right) . \qquad (23)$$

Taking logarithms gives:

$$\log_e\ [\bar{C}_x] = \log_e\ (C_0) - \left(\frac{K_V}{U}\right) x \qquad (24)$$

which indicates that a plot of the logarithm of the concentration in the model stream as a function of longitudinal position has a slope of $-K_V/U$. Thus, the volatilization coefficient is calculated from this slope and the mean water velocity. Such data are the type that would be obtained in a synoptic sampling survey along the length of the model stream.

Second, equation 13 can be written for any two longitudinal positions in the model stream, x_1 and x_2. Combining these equations, replacing x/U with Δt, the traveltime to the cross section, and taking logarithms gives:

$$\log_e\ (\bar{C}_2/\bar{C}_1) = -\ K_V\ (\Delta t_2 - \Delta t_1) . \qquad (25)$$

Equation 25 shows that the volatilization coefficient can be calculated from the equilibrium plateau concentrations at any two cross sections and the traveltimes to these cross sections. Because these traveltimes are relative, $\Delta t_2 - \Delta t_1$ is the traveltime between the cross sections.

The Henry's constants in equation 22 are calculated from equations from the literature (Rathbun and Tai, 1988) expressing the constant as a function of temperature.

The gas-film coefficient is determined from the reference substance equation (eq. 17). The gas-film coefficient for water evaporation from the model stream is determined from windspeed and water temperature measurements and equations 18 and 19. A value of ψ for TBA at 25.0 °C of 0.452 was determined in laboratory studies (Rathbun and Tai, 1988).

Finally, the liquid-film coefficient is determined from equation 15 and the values of the overall mass-transfer coefficient, Henry's constant, and the gas-film coefficient obtained as just described.

Substituting these various values into equation 22 gives an overall mass-transfer coefficient for acetone. This coefficient can be converted to a volatilization coefficient using equation 16 and the mean flow depth determined from cross-section measurements. The result is an acetone volatilization coefficient that is independent of acetone concentration measurements in the model stream.

Modeling Considerations

Equations 8, 9, 10, 11, and 14 can be considered as expressing the concentration at longitudinal position, x, as a function of time, t, and four parameters. These parameters are the mean water velocity, U, the longitudinal-dispersion coefficient, D, the volatilization coefficient, K_V, and the bacterial degradation coefficient, K_D.

The general procedure when modeling nonconservative solutes is to use a conservative solute for determining the flow parameters U and D (Bencala, 1983; Jobson and Rathbun, 1984). Several limiting forms of equation 8 are useful in obtaining initial estimates of the velocity and dispersion coefficient from experimental concentration-versus-time data for a conservative solute. Ogata and Banks (1961) determined for points relatively far downstream from the source location that the first term on the right of equation 8 is negligible with respect to the second. The point at which this approximation is valid depends on the relative magnitudes of the distance, the velocity, the dispersion coefficient, the loss coefficients, and the observation time. If conditions are such that the first term can be neglected, then equation 8 for a conservative solute reduces to:

$$C(x,t)/C_0 = \tfrac{1}{2} \operatorname{erfc} \left[\frac{x - Ut}{\sqrt{4Dt}}\right] . \qquad (26)$$

Ogata (1970) described a procedure for computing the dispersion coefficient from equation 26 and concentration-versus-time data.

Equation 26 also can be used to obtain an initial estimate of the velocity. At the time at which $t = x/U$, the argument of the erfc is zero. Because erfc (0) is 1.0, it follows from equation 26 that

$$C(x,t)/C_0 = 0.5 \ . \tag{27}$$

Therefore, an initial estimate of the velocity between the source and the downstream position x can be computed from the time at which the concentration is 0.5 of the source concentration, C_0.

Initial estimates of the dispersion coefficient and velocity obtained using these limiting forms of equation 8 are used in equation 8 to obtain best-fit values for the concentration-versus-time data for the conservative solute. The root-mean-square (rms) error was used as a measure of the degree of fit. This error is defined as:

$$\text{rms error} = \frac{\sum_{i=1}^{n} \left[(C_i^{EXP} - C_i^{CALC})^2 / n \right]^{0.5} (100)(n)}{\sum_{i=1}^{n} C_i^{EXP}} \ , \tag{28}$$

where EXP = a superscript denoting an experimental concentration;
$CALC$ = a superscript denoting a calculated concentration; and
n = the number of concentrations considered.

The general procedure is to vary the velocity and the dispersion coefficient until this rms error is minimized.

The velocity and dispersion coefficient determined in this way from the conservative solute then are used in equation 8 to model the nonconservative solute acetone. The acetone volatilization coefficient can be estimated from the TBA volatilization coefficient as described previously, leaving the bacterial degradation coefficient as the single parameter to be fitted to the experimental concentration-versus-time data. Thus, it should be possible to determine unique values of the bacterial degradation coefficient.

Equation 13 indicates that the concentration of a conservative solute in a stream system in equilibrium is C_0 at all points in the stream, where C_0 is the concentration of the solute in the water at the source location. Few solutes are completely conservative, however, and the percentage of the solute recovered can be calculated by comparing observed equilibrium concentrations in the stream with this expected value of C_0. An expression for C_0 can be derived by applying the principle of conservation of mass at the source location. The result is:

$$C_0 = q_I C_I / Q \ , \tag{29}$$

where q_I = the injection rate into the stream of the solution of the solute, in liters per second;
C_I = the concentration of the solute in the solution being injected, in micrograms per liter; and
Q = the water discharge in the stream, in liters per second.

The percentage recovery of the solute, PR, is calculated from:

$$PR = \frac{\bar{C}_x}{C_0} (100) \ , \tag{30}$$

where $\bar{C}_x$ = the observed equilibrium concentration in the stream, in micrograms per liter, at longitudinal position x.

Combining equations 29 and 30 gives:

$$PR = \frac{\bar{C}_x Q}{q_I C_I} (100) \ . \tag{31}$$

The percentage recovery of the solute also can be calculated from:

$$PR = \frac{Q \int_0^\infty C \, dt}{M} (100) \ , \tag{32}$$

where $\int_0^\infty C \, dt$ = the area under the concentration-versus-time curve for the solute, in microgram · seconds per liter; and

M = the weight of solute injected, in micrograms.

DESCRIPTION OF THE OUTDOOR MODEL STREAM

The experiments were conducted in an outdoor model stream located at the Stennis Space Center near Bay St. Louis, Mississippi. Figure 1 is a schematic representation of the stream showing the general arrangement and location. The stream was 234 m long, and cross sections along the stream were designated by the distance in meters from the water source at the upstream end.

The water source was an artesian well with a flow of about 1.2 L/s. Water input to the stream was measured with a rotameter (fig. 2). Prior to the experiment, the rotameter was calibrated in place using a volumetric procedure. The water level at the downstream end of the stream was controlled by a concrete weir (fig. 3). Water output from the stream was determined volumetrically by placing a plastic container under the trough on the weir (fig. 3) and collecting the flow for a specific time period.

The upper part of the stream from the point where the water entered the stream (fig. 4) to a point about 25 mi downstream was deeper and wider than the rest of the stream. Because the characteristics of this part of the stream differed considerably from those of the rest of the stream, the injection point for the experiment was located at cross section 33 (fig. 1). To provide a control section for biological and chemical experiments, a 30-m section of the stream beginning at a point 3 m upstream of the injection point

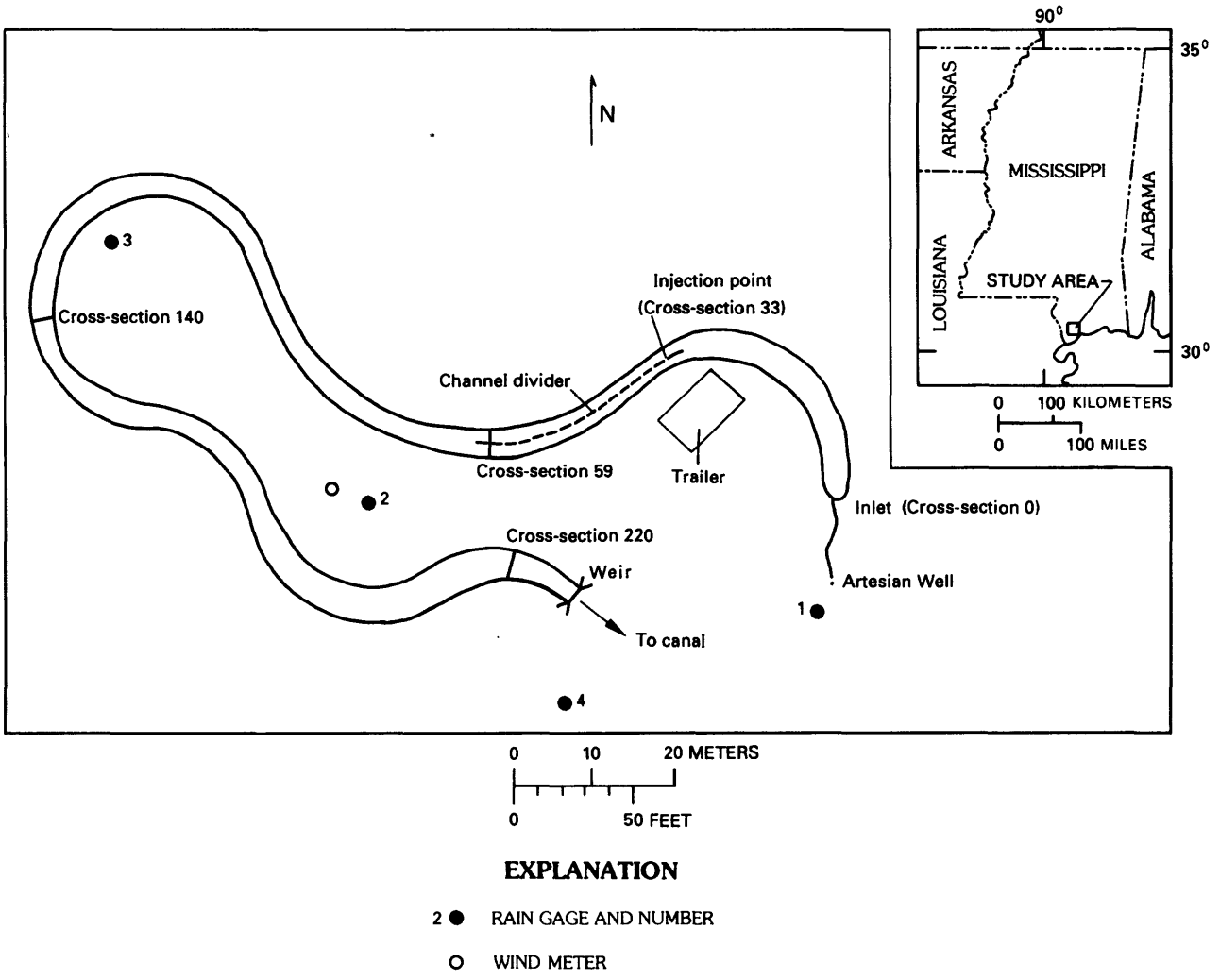

Figure 1. Schematic representation of the outdoor model stream.

Figure 2. Rotameter used to measure water input to the model stream from the artesian well.

Figure 3. Weir at the downstream end of the model stream.

was divided lengthwise into two channels with a piece of galvanized sheet metal (fig. 5). The left channel (facing downstream) was the experimental section into which the injections were made, and the right channel was the control section. To facilitate mixing of the two streams downstream from the partition, a 0.2-m-long galvanized sheet metal baffle was used. This baffle was placed on the left bank 2 m downstream from the partition so as to direct the flow into the center of the channel.

Figure 4. Upstream end of the model stream showing water input.

The primary sampling cross sections were at 59 m, 140 m, and 220 m. Cross section 59 was 1.0 m upstream from the downstream end of the channel partition. Thus, sampling at this cross section was in the divided part of the stream (fig. 5). Cross sections of the stream from the injection point to cross section 220 generally were U-shaped, with the bottom of the cross section filled with a floc of organic detritus. This floc was relatively immobile, as evidenced by no apparent movement during periods of high flow

Figure 5. Divided section of the model stream looking downstream toward cross section 59.

after intense rainfall. Cross sections at 60 m, 140 m, and 220 m are presented in figures 6, 7, and 8. These figures indicate the depths both to the top of the floc layer and to the bottom of the stream.

Cross-section measurements at 10-m intervals from the injection point to cross section 220 gave a mean stream top width of 1.57 m, a mean hydraulic flow depth to the top of the floc of 0.085 m, and a mean depth to the stream bottom of 0.155 m. The mean cross-sectional area to the top of the floc was 0.141 m^2. The water-surface slope from the injection point to cross section 220 was 7.58×10^{-5} m/m. The mean water velocity was about 0.5 m/min. The small water velocity and flat slope are characteristic of many streams and rivers in the coastal region of the southeastern United States. Figure 9 is a view of the stream looking downstream toward cross section 140, and figure 10 is a view of the stream looking upstream toward cross section 220.

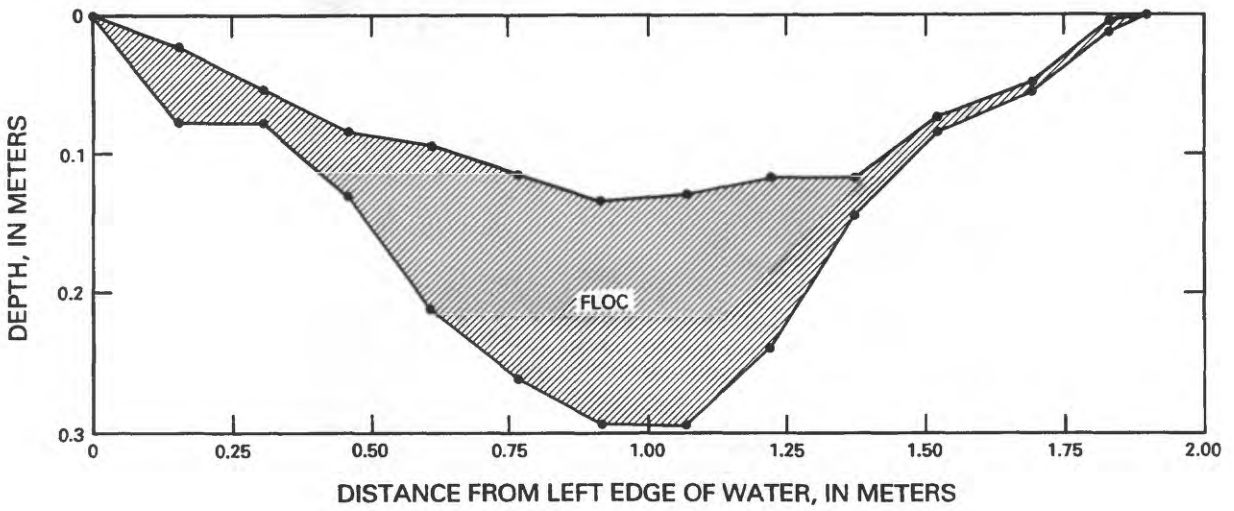

Figure 6. Cross-section measurement for cross section 60.

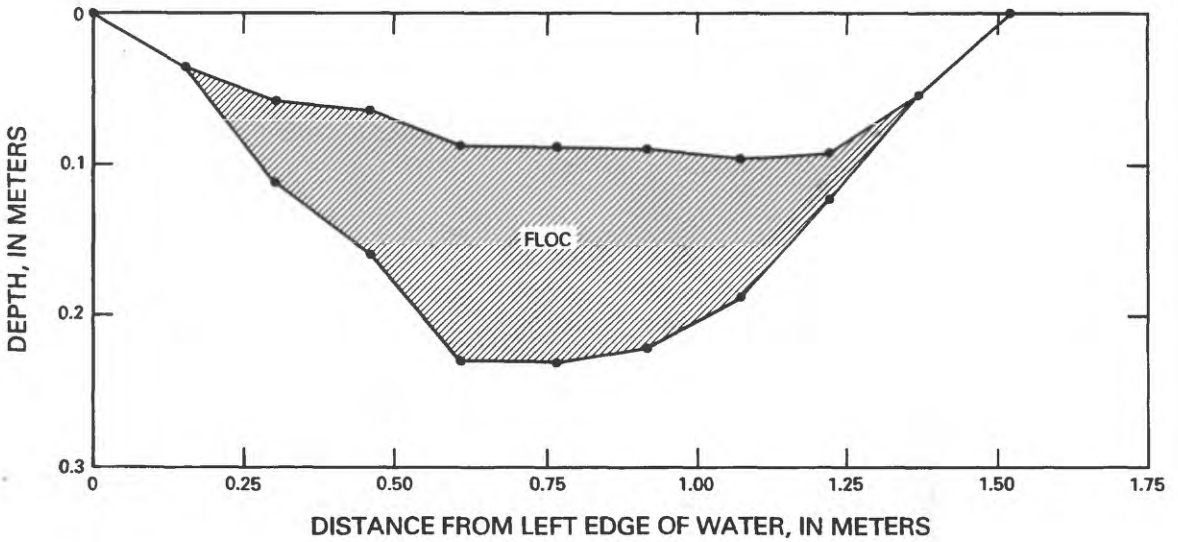

Figure 7. Cross-section measurement for cross section 140.

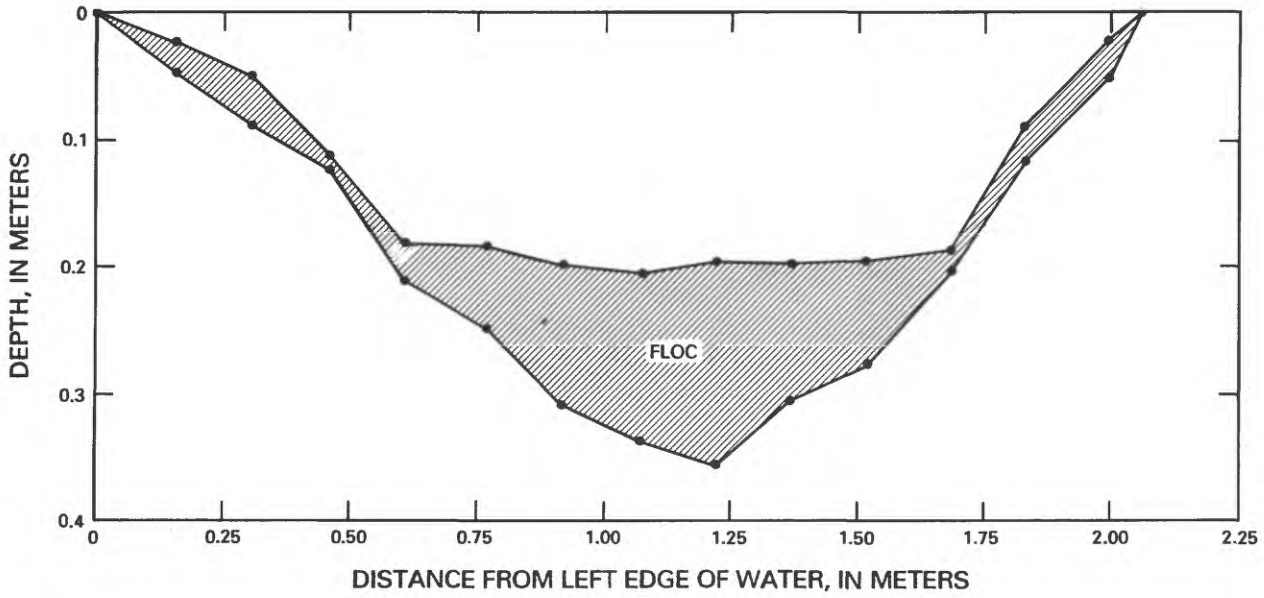

Figure 8. Cross-section measurement for cross section 220.

Figure 9. Model stream looking downstream toward cross section 140.

Figure 10. Model stream looking upstream toward cross section 220.

Four rain gages of the graduated-cylinder type were placed in the area of the model stream (fig. 1). A nonrecording anemometer was located near the center of the stream layout (fig. 1) to measure windspeed. A trailer was positioned near the injection point (fig. 1) to serve as a field laboratory. All injection equipment was housed in this trailer. It also was used for field monitoring of the rhodamine-WT and field processing of all samples.

The stream appeared to be a biologically rich community. It contained large numbers of small mosquito fish, numerous frogs, and several turtles and water snakes. The stream bottom along both banks from about cross section 150 to the downstream end (fig. 10) supported a profuse growth of a rooted macrophyte. Frequent cutting and raking were necessary to control these plants. Also, clumps of moss and algae were present on the surface of the stream along the entire length (figs. 5, 9, and 10). Large amounts of this material were evident at the upstream end of the stream (fig. 4). This material appeared to come from the floc layer. As the water temperature increased during the day, gas bubbles from the floc dislodged small clumps of this material which moved to the water surface. These small clumps moved downstream; however, because of the low hydraulic gradient of the stream, the slightest obstruction was sufficient to stop the movement. The clumps then accumulated

until such time as the mass became large enough to break free of the obstruction and move on downstream. This cycle was repeated until the material passed over the weir and out of the system. A taxonomic identification of this material was not attempted.

PRELIMINARY DATA REQUIREMENTS AND RESULTS

Rhodamine-WT Dye Study

A preliminary study using rhodamine-WT dye was conducted 24 days prior to the start of the acetone-injection experiment. The objectives of this study were to determine the division of the flow by the partition (fig. 5), to determine how well the two streams were mixed laterally at a point 20 m downstream from the end of the partition, and to estimate the injection time required to establish a plateau concentration at the downstream end of the stream.

A water-dye solution was injected continuously for 700 min on the experimental side of the partition (fig. 5). The solution was injected just above the water surface at a point 1.0 m downstream from the upstream end of the partition. A Fluid Metering, Inc.,[1] positive displacement metering pump powered by a 12-volt battery was used. The dye solution was pumped from a 250-mL graduated cylinder so that the injection rate could be monitored. This cylinder was refilled periodically with dye solution from a bucket. Samples of this solution were collected at the beginning and at the end of the injection for later analysis in the laboratory to determine the concentration of the solution injected.

Dye samples were collected in glass vials with screw caps as a function of time at cross sections 59, 140, and 220 (fig. 1). Samples of the stream water also were collected prior to the injection of the dye to permit correction of the dye concentrations for background. Synoptic sampling surveys were done four times during the latter stages of the experiment. These surveys consisted of samples collected at 10-m intervals between cross sections 30 and 59 and at 20-m intervals between cross sections 80 and 220. Dye samples also were collected three times at four points across the stream at cross section 80 to determine how well the flows from the two sides of the partition had mixed. All samples were stored in the dark in an incubator at constant temperature until analysis. Dye concentrations were determined using a Turner model 111 fluorometer and standard fluorometric techniques (Wilson and others, 1984).

[1]Use of brand, firm, and trade names in this report is for identification purposes only and does not constitute endorsement by the U.S. Geological Survey.

Rhodamine-WT dye concentrations at cross sections 59, 140, and 220 are presented in figure 11 as a function of elapsed time from the start of the dye injection. Three apparent plateau concentrations were observed at cross section 59. The first plateau concentration of 20.60 µg/L with a coefficient of variation of ±1.75 percent persisted from 125 min to 295 min. The coefficient of variation used in this report is the standard deviation of the data divided by the mean and multiplied by 100 to express the coefficient as a percentage. The second plateau concentration of 18.76 µg/L with a coefficient of variation of ±2.33 percent persisted from 305 min to 570 min. The final plateau concentration of 19.61 µg/L with a coefficient of variation of ±1.59 percent persisted from 580 min to the last sample at 689 min. Cross section 140 showed a plateau concentration of 10.14 µg/L with a coefficient of variation of ±0.95 percent which persisted from 500 min to the last sample at 688 min. The dye concentration at cross section 220 did not reach a plateau concentration, but appeared to be approaching about the same value as the plateau concentration at cross section 140. This behavior is as expected if the stream is approximately at steady state and the dye is reasonably conservative.

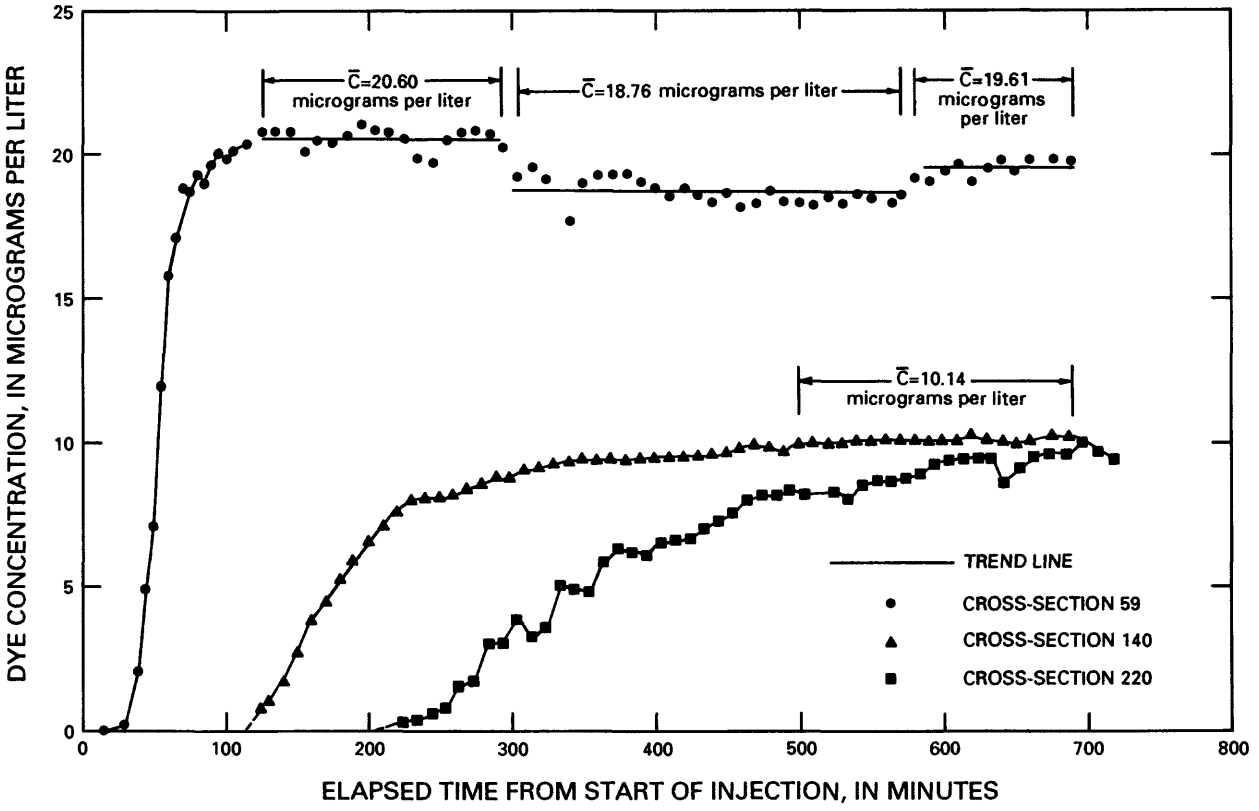

Figure 11. Rhodamine-WT dye concentrations at cross sections 59, 140, and 220 as a function of elapsed time from the start of the injection, preliminary dye study.

Comparison of the plateau concentration at cross section 140 with the plateau concentrations at cross section 59 gives a direct measure of the division of the flow by the partition (fig. 5). The flow division factor, defined as the fraction of the flow on the experimental side of the partition, was 0.492, 0.541, and 0.517 for the three plateau concentrations at cross section 59. It was concluded on the basis of these results that the partition divided the flow about equally.

This analysis presumes the dye is conservative. Because the dye is not completely conservative, these factors would be larger if corrections were made for dye loss because dye loss increases with distance downstream. The magnitude of the increase would be dependent on the extent of the dye loss. Because the concentration at cross section 220 appears to be approaching about the same value as the plateau concentration at cross section 140 (fig. 11), dye loss probably was minimal in the preliminary dye study. Dye loss will be discussed in more detail later.

There are several possible explanations for the change in the plateau concentration at cross section 59. The constancy of plateau concentrations in an injection experiment in a stream depends on the constancies of the concentration of the solute being injected, the injection rate, and the water discharge in the stream (eq. 29). In the preliminary dye study, one dye solution was used for the entire injection; therefore, the concentration of the injected dye should have been constant. The injection rate of the dye solution as a function of elapsed time from the start of the injection is presented in figure 12. The rates oscillate about the mean rate from 0 min to about 150 min, are below the mean from about 150 min to about 375 min, and then generally are above the mean for the rest of the injection. The times of these changes, however, do not correspond to the times in the changes in the plateau concentrations at cross section 59. For example, because the travel-time of the leading edge of the dye to cross section 59 is about 30 min (fig. 11), the decrease in the injection rate at about 150 min should have affected the concentration at cross section 59 at about 180 min. However, the decrease in concentration did not occur until about 300 min. Similarly, the increase in the injection rate at about 375 min should have affected the concentration at about 405 min. However, the increase in the concentration did not occur until about 575 min.

The magnitudes of the changes also suggest that the changes in the plateau concentrations were not the result of the changes in the injection rate. The coefficient of variation of the dye injection rate was ±3.12 percent. However, the decrease in the plateau concentration was about 9 percent. Therefore, the observed variation in the dye injection rate does not appear to be large enough to produce the observed change in the plateau concentrations. Also, had the concentration changes been the result of changes in the dye injection rate, then the concentrations at cross sections 140 and 220 should have been affected also.

The water discharge in the model stream was approximately constant; however, changes in the division of this discharge by the partition could cause changes in the plateau concentration. If the division of the flow by the partition changed temporarily such that the discharge on the experimental side was increased about 9 percent, then the plateau concentration at cross

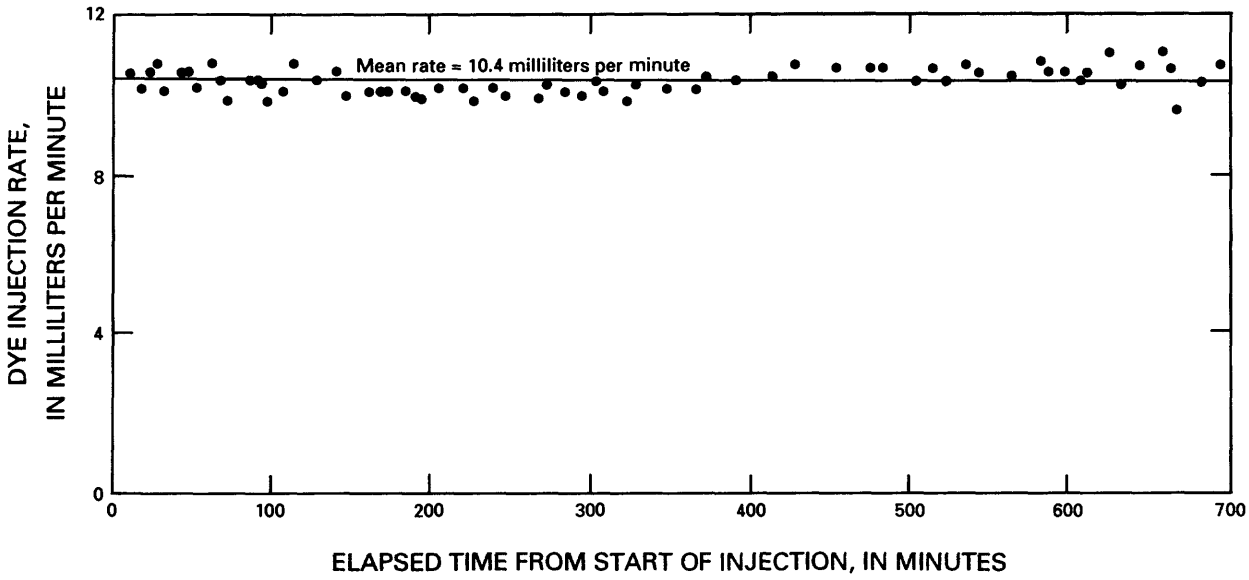

Figure 12. Injection rate of the rhodamine-WT dye solution as a function of elapsed time from the start of injection, preliminary dye study.

section 59 would be decreased as shown in figure 11. This explanation is supported by the observation that the concentrations at cross sections 140 and 220 apparently were not affected by the change in the flow division. Presumably, the increased flow on the experimental side of the partition with the reduced dye concentration combined with the decreased flow on the control side to give the same average concentration at the downstream end of the partition.

It was not anticipated that the flow division factor would vary; and unfortunately, the variation of the plateau concentration at cross section 59 in the preliminary dye study was not recognized initially as a flow division change. Variations in the flow division factor were not recognized until after the first 9 days of the acetone-injection experiment. This problem will be discussed in more detail later.

Results of the synoptic sampling surveys are presented in figure 13. The concentration increased with time at each cross section and, also, there was a trend toward a constant rate of decrease of concentration with distance downstream such as would be observed for a slightly nonconservative solute. The last sample set at 615 min indicates the stream was not yet in equilibrium because the concentrations at cross sections 200 and 220 are smaller than those predicted on the basis of the samples for cross sections 80 through 180.

The concentrations at cross sections 59 and 80 from the synoptic surveys also provide a direct measure of the flow division factor, assuming the stream between these cross sections is in equilibrium. This assumption is supported by the fact that the coefficient of variation of the four concentrations at cross section 59 was ±1.16 percent and the coefficient of variation at cross section 80 was ±2.68 percent. These small coefficients of variation indicate

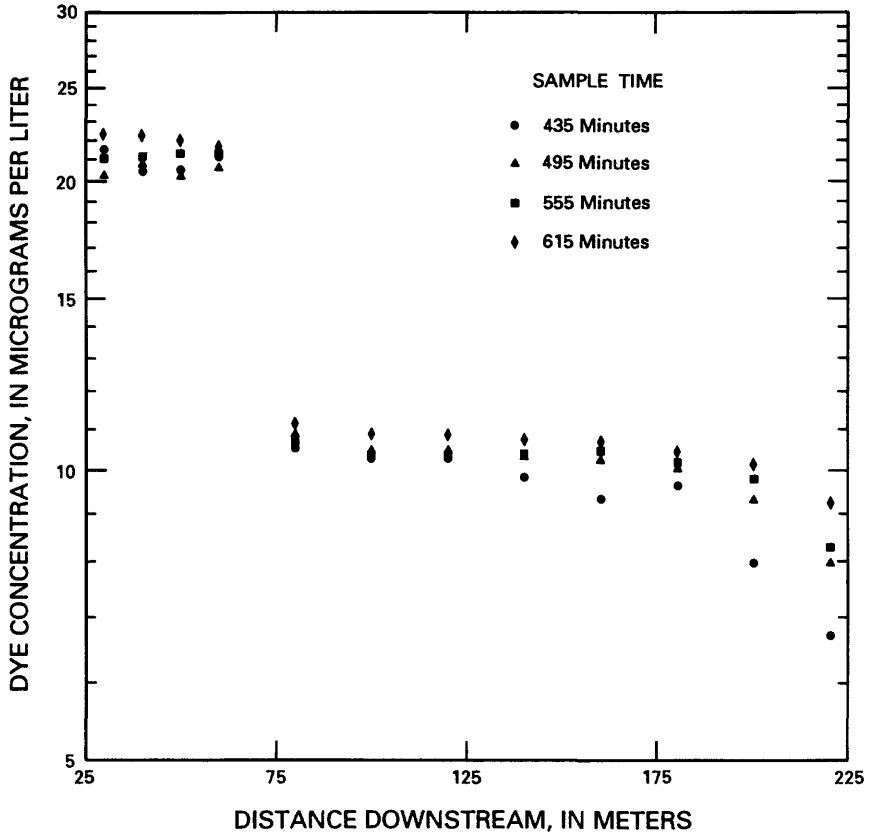

Figure 13. Rhodamine-WT dye concentration on a logarithmic scale as a function of distance downstream for synoptic samples, preliminary dye study.

approximately uniform concentrations. Taking ratios of the concentrations gives flow division factors of 0.499, 0.520, 0.504, and 0.522, in agreement with values presented previously.

Lateral distributions of the dye concentrations at cross section 80 for three sample times are presented in table 1. These results indicate that the dye was reasonably mixed across the width of the stream at this cross section. Therefore, it was concluded that the baffle and the natural mixing characteristics of the stream were sufficient to mix the two streams in a relatively short distance downstream from the end of the partition.

The 700-min injection in the preliminary dye study resulted in a plateau concentration at cross section 140 and a concentration at cross section 220 that was approaching this value. Consequently, it was concluded that an injection period longer than 700 min was necessary to establish plateau concentrations at cross sections 140 and 220 in the model stream.

Table 1.--*Rhodamine-WT dye concentrations across the model stream at cross section 80 for three sample times, preliminary dye study*

Clock time (hours)	Dye concentration (micrograms per liter)				Coefficient of variation (percent)
	Left edge	Left quarter	Right quarter	Right edge	
1301	10.54	10.56	10.15	9.92	±3.03
1640	9.61	10.02	10.67	10.61	±4.94
1800	11.30	11.10	11.28	11.28	±0.83

Nutrient Monitoring

Nutrients were monitored in the model stream for approximately 15 months (Oct. 1977 to Jan. 1979) prior to the acetone-injection experiment. Grab samples were collected at mid-depth near the center of the stream. Flow conditions during this monitoring were about the same as during the acetone-injection experiment. Orthophosphate concentrations were determined using the ascorbic acid method (American Public Health Association, 1971). Nitrate-nitrogen and nitrite-nitrogen were determined using the cadmium reduction column and diazo dye spectrophotometric method (Strickland and Parsons, 1968).

Results of the preliminary nutrient monitoring are present in table 2 for orthophosphate, in table 3 for nitrate-nitrogen, and in table 4 for nitrite-nitrogen. Minimum, maximum, and mean concentrations are presented for the inlet artesian well water and water from four cross sections in the stream for 13 sample times. Unfortunately, these times were not uniformly distributed during the approximately 15-month monitoring period. One measurement was in May, four were in October, and the rest were in the months from November through February. Thus, the results are weighted toward the months when water temperatures were low, biological and bacterial activity might be expected to be minimal, and nutrient concentrations larger than average. Conversely, heavy rains preceding several of the sampling times may have affected the nutrient concentrations, and one measurement was not included because of heavy rain during the actual sampling. Rain could decrease the concentrations in the model stream through dilution and could increase the concentrations through runoff from the surrounding land surfaces.

The orthophosphate concentrations in the model stream (table 2) were reasonably consistent with the concentration in the inlet water from the well, and also varied little with position in the stream. The coefficients of variation indicate the variability introduced as a result of the 13 sampling times during the 15-month monitoring period and, also, variability resulting from the sampling and analytical techniques. The fact that these coefficients are small indicates the orthophosphate concentration varied little with time during the monitoring period.

The nitrate-nitrogen concentrations in the model stream (table 3) varied considerably. Also, the concentrations in the stream were much larger than the concentration in the inlet water. Some of the nitrate in the stream could

Table 2.--*Orthophosphate concentrations in the model stream during the preliminary monitoring period, October 1977 to January 1979*

Cross section (meters)	Concentration (micrograms per liter)			Coefficient of variation (percent)
	Minimum	Maximum	Mean	
0 (Inlet)	260	321	280	±5.16
20	246	330	268	±7.76
40	232	293	264	±6.20
140	210	315	263	±11.2
234 (Weir)	224	353	272	±13.1

Table 3.--*Nitrate-nitrogen concentrations in the model stream during the preliminary monitoring period, October 1977 to January 1979*

Cross section (meters)	Concentration (micrograms per liter)			Coefficient of variation (percent)
	Minimum	Maximum	Mean	
0 (Inlet)	0.0	17.7	5.7	±86.8
20	60.8	248	157	±37.5
40	56.4	227	151	±32.1
140	5.6	127	57.0	±58.1
234 (Weir)	0.0	154	39.1	±124

Table 4.--*Nitrite-nitrogen concentrations in the model stream during the preliminary monitoring period, October 1977 to January 1979*

Cross section (meters)	Concentration (micrograms per liter)			Coefficient of variation (percent)
	Minimum	Maximum	Mean	
0 (Inlet)	0.1	13.7	2.0	±182
20	1.8	16.0	8.0	±52.8
40	2.4	19.7	8.2	±54.0
140	1.2	16.3	5.0	±82.4
234 (Weir)	1.0	11.7	2.9	±99.0

have resulted from runoff from the surrounding land surfaces during rain events. The nitrate-nitrogen concentration at cross section 234 varied considerably, as indicated by the large coefficient of variation. Also, the concentration generally was small. Of the 13 values, two were 0.0 and five others were less than 11 µg/L. The average of 39.1 µg/L was influenced considerably by the maximum value of 154 µg/L and another large value of 104 µg/L

that occurred after about 62 mm of rain. The large coefficient of variation at cross section 0 probably is a result of the low concentrations being measured. Also, the analytical technique used for nitrate-nitrogen has a larger error than the techniques used for the other two nutrients.

The nitrite-nitrogen concentrations were small and highly variable (table 4), as indicated by the large coefficients of variation. Nitrite in water containing dissolved oxygen generally undergoes nitrification to nitrate, and this could explain the decrease in the mean concentrations with distance downstream from cross section 40. Conversely, because the inlet water generally had zero or a very small dissolved-oxygen concentration, denitrification of some of the nitrate material in the upstream end of the stream could explain the increase in nitrite concentration between the inlet and cross section 20. These conclusions are tenuous, however, based on limited data with considerable variability. Some of this variability is undoubtedly because all the concentrations are small, approaching the limit of detectability of 1.0 µg/L of the analytical technique (American Public Health Association, 1971).

AUXILIARY DATA REQUIREMENTS AND RESULTS

Various auxiliary data were necessary for the analysis and interpretation of the experimental results. These data include rainfall, water temperature, water discharge, and windspeed.

Rainfall

Rainfall occurred a number of times during the acetone-injection experiment. Amounts measured with each of the four rain gages (fig. 1) are presented in table 5. Because of the small flow in the model stream, heavy rain could appreciably affect the concentrations of the various solutes in the stream and also the water temperature.

Table 5.--*Rainfall during the acetone-injection experiment*

Day of experiment	Time gages emptied (hours)	Rainfall at gage number, in millimeters			
		1	2	3	4
1	--	Trace	Trace	Trace	Trace
5	--	Trace	Trace	Trace	Trace
6	1637	9.0	10.1	9.8	9.8
7	0900	3.0	3.0	3.0	3.0
14	1655	20.8	21.0	22.5	21.0
15	1745	2.0	3.0	3.0	2.5
25	0830	40.0	45.0	45.0	45.0
32	1520	29.0	33.2	34.0	33.8
33	0822	5.0	5.0	5.0	5.0

Water Temperatures

Water temperatures measured at cross sections 59, 140, and 220 during the morning, noon, and afternoon sampling for acetone are summarized in table 6. These temperatures reflect the characteristics of the model stream. Cross section 59 (fig. 5) was shaded much of the time and this is reflected by maximum temperatures which were smaller than the corresponding maximum temperatures at cross sections 140 and 220. Conversely, the minimum temperatures at cross section 59 were, with one exception, larger than the corresponding minimum temperatures at cross sections 140 and 220. This occurred because of the moderating effect of the temperature of the inlet water from the well which varied only in the narrow range between 26.8 °C and 27.0 °C. Cross section 140 (fig. 9) was not shaded; consequently, the maximum temperatures were, with one exception, larger than the corresponding maximum temperatures at cross sections 59 and 220. The minimum temperatures also were larger than the corresponding minimums at cross section 220 which was shaded part of the time (fig. 10). However, in addition to the extent of shading, water temperatures at the downstream cross sections also were influenced by the temperature of the water received from upstream sections of the stream.

Table 6.--*Summary of water temperatures at cross sections 59, 140, and 220*

[°C, degree Celsius]

Cross section (meters)	Mean sample time (hours)	Temperature			Number of values	Coefficient of variation (percent)
		Minimum (°C)	Maximum (°C)	Mean (°C)		
59	0823	21.5	26.8	24.2	29	±5.44
	1216	24.5	31.2	28.6	24	±7.04
	1607	24.0	31.6	28.8	32	±5.95
140	0824	20.0	27.0	23.9	29	±6.75
	1217	23.8	34.8	30.4	24	±9.13
	1609	24.0	35.8	31.6	32	±9.18
220	0826	17.9	25.8	21.9	29	±9.81
	1216	21.6	32.9	28.2	24	±9.68
	1612	23.9	36.3	31.8	32	±10.0

The largest changes in the mean water temperature occurred between the morning and noon sample times, with smaller changes occurring between the noon and afternoon sample times. The coefficients of variation were largest for cross section 220, reflecting the partial shading of this cross section and also the dependence on the temperature of the water received from the upstream parts of the stream. The coefficients of variation were smallest for cross section 59, reflecting the shading of this cross section and the moderating effect of the inlet water temperature.

The moderating effect of the approximately constant temperature of the inlet water is evident in the synoptic temperature surveys for day 10 presented in figure 14. The temperature at 0815 hours decreased with cross-sectional distance downstream, a result of the low nighttime air temperatures. The temperature at 1250 hours increased with distance downstream to cross section 140, was approximately constant for 40 m, and then decreased. The temperature at 1608 hours increased with distance downstream to cross section

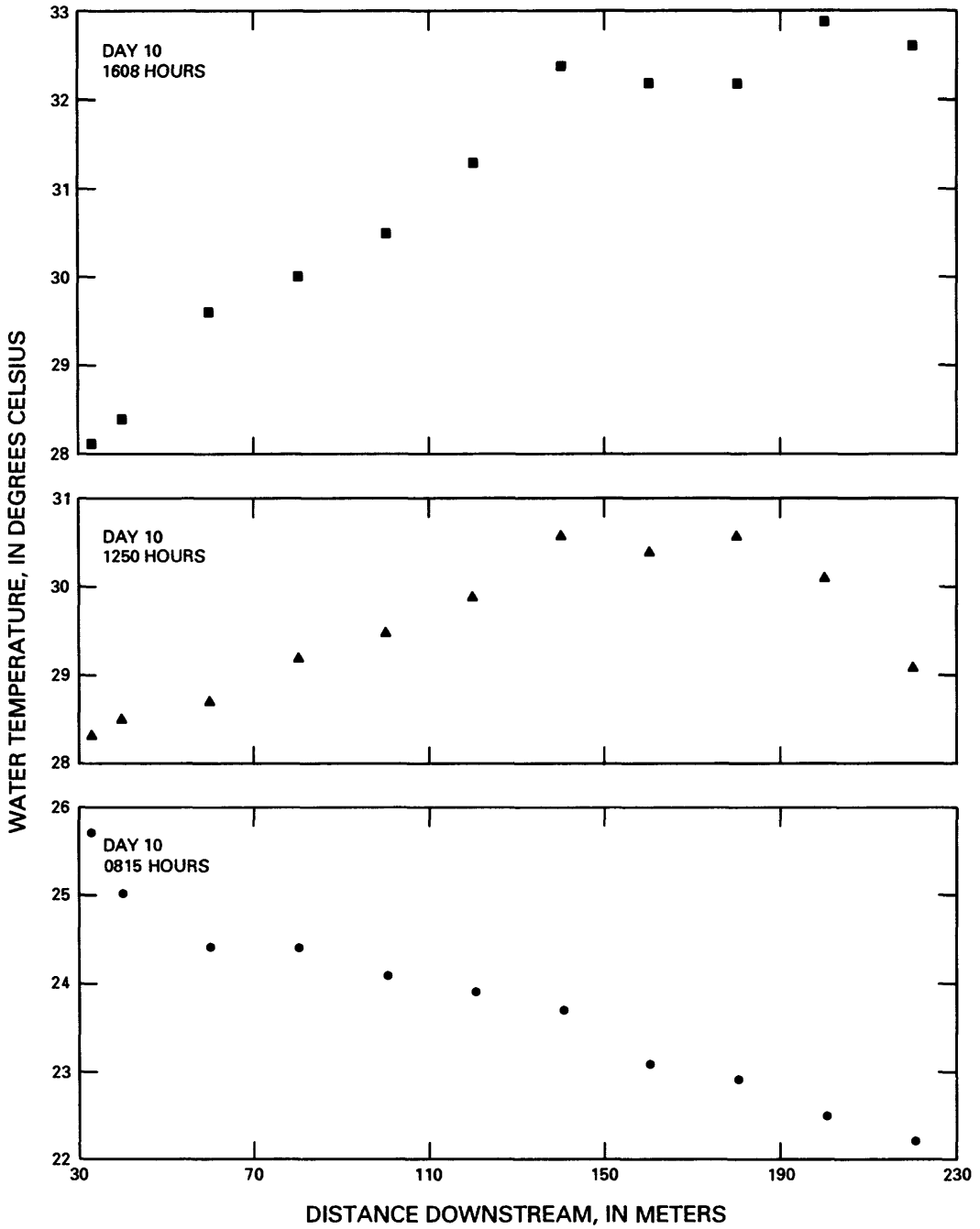

Figure 14.--Synoptic temperature surveys for times of 0815 hours, 1250 hours, and 1608 hours on day 4.

140 similar to that observed at 1250 hours; from cross section 140 on downstream, the temperature was approximately constant. This temperature pattern (fig. 14) was observed throughout the acetone-injection experiment, with the temperature changes decreased somewhat on cloudy or rainy days.

A gradual increase in water temperature during the experiment was expected because the acetone-injection experiment was conducted from late April to early June, a period when the air temperature was expected to be increasing. To check this expectation, least-square analyses of the water temperatures as a function of the day of the experiment were calculated. The regression slopes were all positive, indicating increasing temperature with time. However, the slopes also were small and, with one exception, not significantly different from zero at the 5-percent level. The slope of the morning data for cross section 59 was just significantly different from zero at the 5-percent level but was not significantly different at the 2.5-percent level. The conclusion, therefore, must be that water temperatures, within the scatter of the data, did not increase significantly with time during the experiment.

This analysis was affected by two factors. First, a weather front passed through the area on the evening of day 14, and this moderated temperatures for several days thereafter. Second, much of the rainfall received during the experiment occurred during the latter half of the study (table 5), and water temperatures were decreased appreciably on several days. Both of these factors would contribute to lower water temperatures than might be expected during the middle and latter half of the study. Consequently, these factors also would reduce the rate of increase of the water temperature with time.

As an example of daily variations, water temperatures at cross sections 59, 140, and 220 are presented in figure 15 as a function of time for day 4. Weather conditions on day 4 were cloudy, resulting in water temperatures about intermediate between the minimum and maximum temperatures given in table 6. The water temperature at cross section 59 changed less relative to the variations at cross sections 140 and 220. Also, there is a slight tendency for the time of the peak temperature to increase with distance downstream. This apparently is indicative of the increasing temperature of a water parcel as it moves through the stream system.

Water Discharge

Daily mean water discharges at the inlet and outlet of the model stream are presented in figure 16 as a function of the day of the experiment. The ranges of water discharges at the outlet on days when measurable rainfall occurred (table 5) also are indicated on figure 16. These ranges indicate the maximum measured discharges which are not necessarily the maximums of the storm events because the complete events were not sampled.

The mean daily inlet water discharge decreased about 4 percent during the first 5 days of the experiment and then was approximately constant. The overall mean inlet discharge was 1.195 L/s with a coefficient of variation of ±1.94 percent for 213 determinations. The outlet water discharge approximately paralleled the inlet discharge but was almost always less than the inlet discharge. The overall mean outlet discharge excluding those days

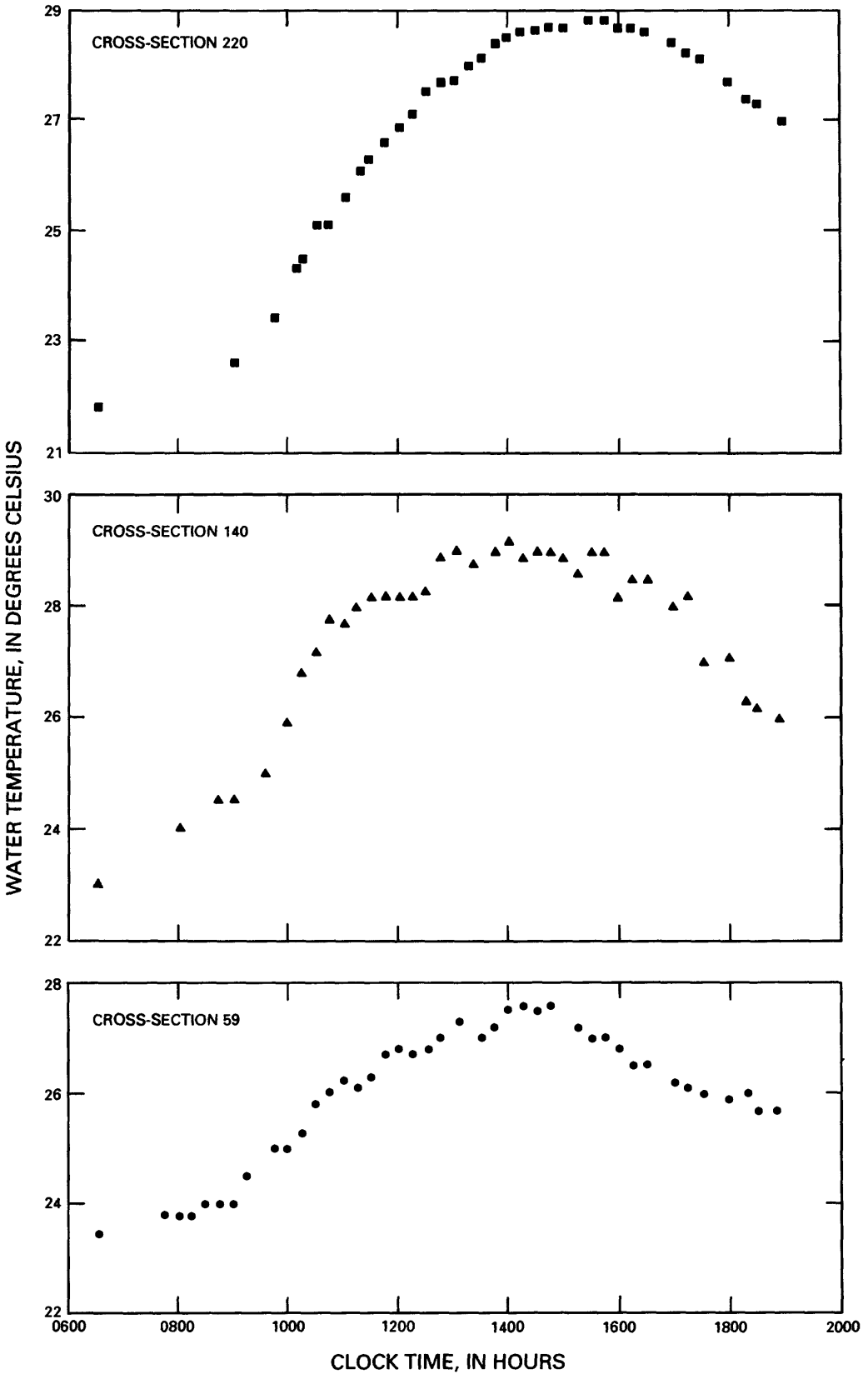

Figure 15.--Variation with time of the water temperature at cross sections 59, 140, and 220 for day 4.

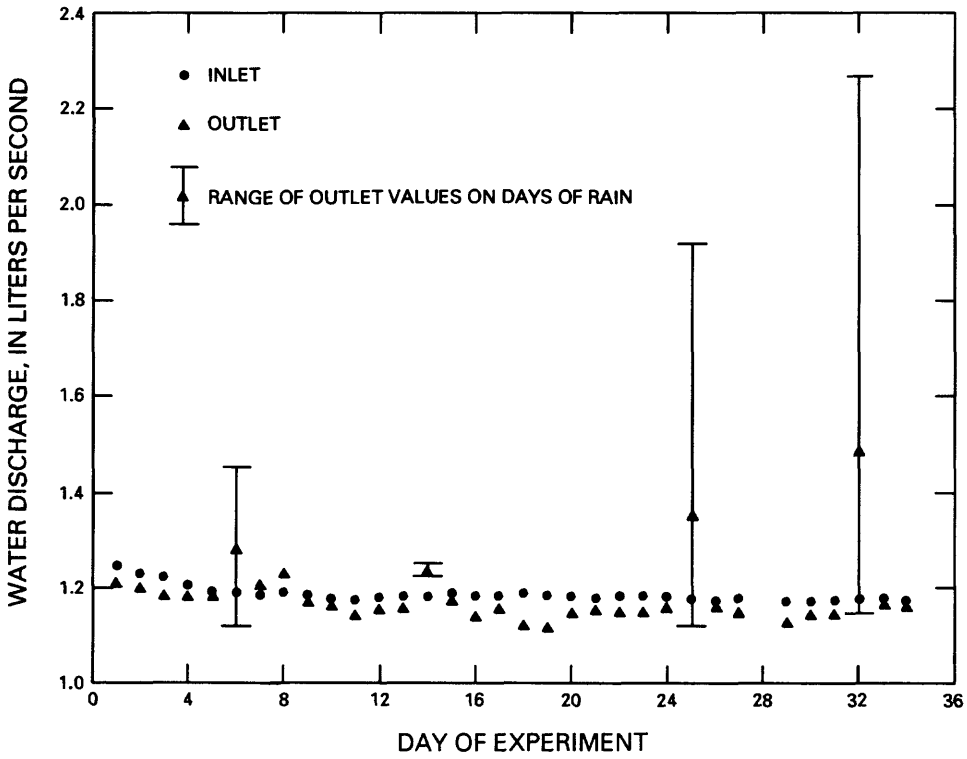

Figure 16.--Daily mean water discharges at the inlet and outlet as a function of the day of the experiment.

affected by rain was 1.171 L/s, with a coefficient of variation of ±3.29 percent for 193 measurements. The 2.0-percent difference between the inlet and outlet means was attributed to evaporation and evapotranspiration.

Experimental problems to be discussed later were experienced with the division of the flow by the partition on days 6 to 9. Consequently, some data analyses were limited to the time period from day 10 to the end of the experiment. For this period, the overall mean inlet water discharge was 1.181 L/s, with a coefficient of variation of ±0.48 percent for 135 determinations. Similarly, the overall mean outlet discharge was 1.155 L/s, with a coefficient of variation of ±2.16 percent for 121 measurements.

Windspeed

The windspeed data for 28 daytime and 27 nighttime periods are summarized in table 7. The daytime values are integral mean values for the period with a mean starting time of 0828 hours and a mean ending time of 1614 hours. The integral mean values were calculated from:

$$\bar{V} = \frac{0.5}{t_n - t_1} \sum_{i=1}^{n} (t_{i+1} - t_i)(V_{i+1} + V_i) , \qquad (33)$$

where V_{i+1} = the windspeed at time t_{i+1};
V_i = the windspeed at time t_i;
t_1 = the time of the first windspeed measurement; and
t_n = the time of the last windspeed measurement.

The windspeeds were calculated from:

$$V_i = \frac{a_2 - a_1}{t_2 - t_1} \tag{34}$$

where a_2 = the anemometer reading at time t_2;
a_1 = the anemometer reading at time t_1.

The time t_i corresponding to V_i is the mean of times t_1 and t_2. Equation 33 uses the trapezoid rule to compute the area under the windspeed-versus-time curve.

Table 7.--*Summary of windspeed data*

[h, hours; m/s, meters per second]

Time period	Mean starting time (h)	Mean ending time (h)	Windspeed			Number of values	Coefficient of variation (percent)
			Minimum (m/s)	Maximum (m/s)	Mean (m/s)		
Daytime	0828	1614	0.322	1.42	0.739	28	±43.7
Nighttime	1617	0829	0.094	0.894	0.311	27	±56.5

The nighttime values are single overall mean values computed from equation 33 because anemometer readings were obtained only for the starting and ending times of the observation period. Mean value of the starting time was 1617 hours and of the ending time was 0829 hours (table 7).

The mean daytime windspeed was 0.739 m/s compared with a mean nighttime value of 0.311 m/s, indicating that the daytime windspeeds on the average were more than twice the nighttime values. Similar differences exist in the maximum and minimum windspeeds also. Finally, the daytime and nighttime mean windspeeds both had large coefficients of variation, demonstrating the high variability and intermittent nature of the wind.

The coefficients of variation in table 7 indicate the variability of mean windspeeds for approximately 8-hour daytime and 16-hour nighttime periods. The variability of the windspeed within a daytime period is demonstrated in figure 17, in which the windspeed for day 4 is presented as a function of time. The windspeed oscillated about an approximately constant value until 0947 hours, increased between 0947 hours and 1354 hours, and then decreased. The variability of the windspeed is apparent.

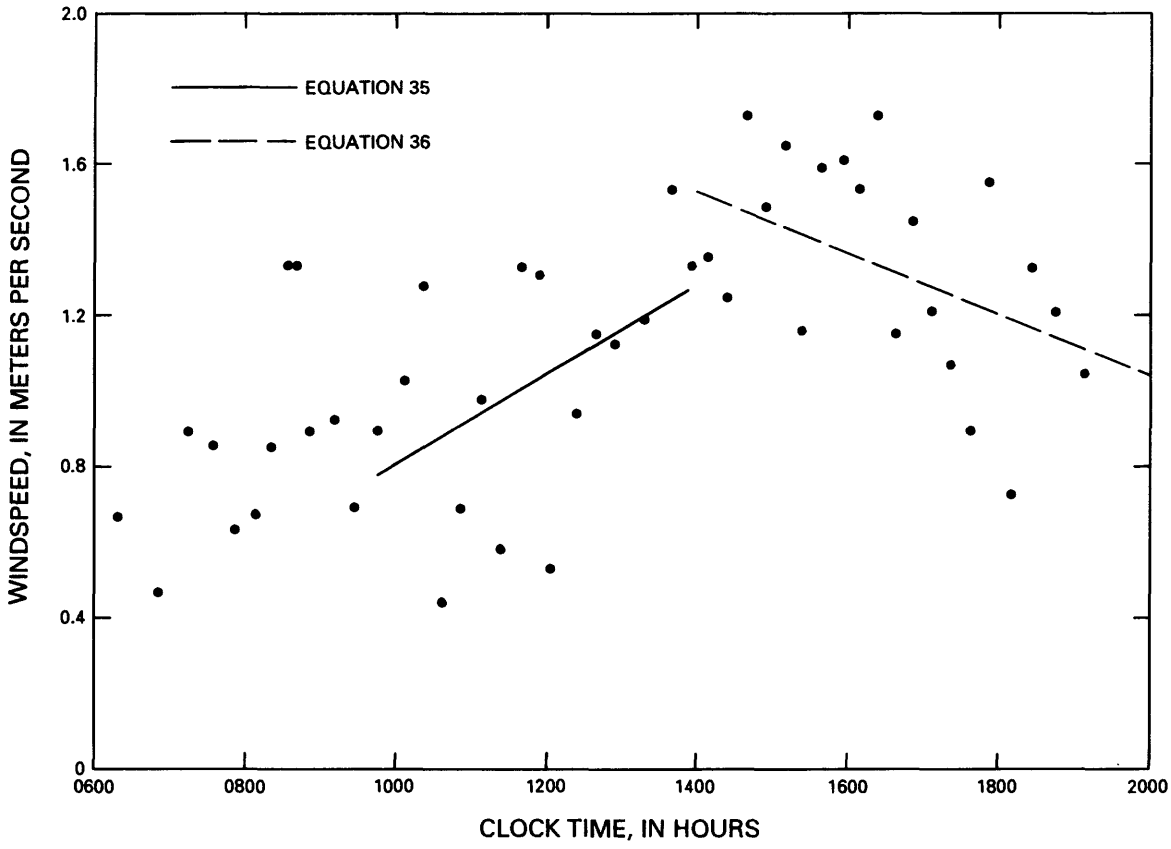

Figure 17.--Windspeed as a function of time for day 4.

To facilitate computation of integral mean windspeeds for specific time periods during the afternoon of day 4, the windspeed was assumed to vary linearly with time between 0947 hours and 1354 hours and between 1354 hours and 1906 hours. The resultant least-squares equations are:

$$V_{0947\text{-}1354} = (0.120)(t) + 0.202 \quad (35)$$

and

$$V_{1354\text{-}1906} = (-0.0820)(t) + 2.27 \quad (36)$$

where V = the windspeed, in meters per second; and
t = the elapsed time, in hours relative to 0500 hours.

The equations are used later in the analysis of the results from day 4 of the experiment.

EXPERIMENTAL PROCEDURES FOR THE ACETONE TRANSPORT AND FATE STUDY

The acetone transport and fate experiment consisted of injections of several solutes into the model stream over a 34-day period from late April to early June, 1979. The time periods of these injections are given in table 8. A primary productivity study was conducted on days 11 and 12. Qualitative

time in this experiment was measured in terms of the "day of experiment," beginning with the initiation of the rhodamine-WT dye injection at 0600 hours on day 1.

Table 8.--*Schedule for the acetone transport and fate experiment*

Day of experiment	Clock time (hours)	Solute	Action
1	0600	Rhodamine-WT dye	Begin injection
2	0600	Acetone	Begin injection
2	1802	Rhodamine-WT dye	Stop injection
4	0700	t-Butyl alcohol	Begin injection
4	1905	t-Butyl alcohol	Stop injection
17	1500	Glucose	Begin injection
18	1025	Glucose	Increase concentration
19	1155	Glucose	Increase concentration
20	1607	Glucose	Stop injection
23	1603	Bacteria and nutrients	Begin injection
24	1615	Bacteria and nutrients	Stop injection
30	0600	Rhodamine-WT dye	Begin injection
31	0540	Rhodamine-WT dye	Stop injection
34	0831	Acetone	Stop injection

The rhodamine-WT dye was used to determine the traveltime and dispersion characteristics of the model stream at the beginning and at the end of the experiment. The TBA was injected to determine the volatilization characteristics of the stream. It was expected that TBA would have volatilization characteristics similar to those of acetone but would be much more resistant to bacterial degradation. The glucose was injected in an attempt to stimulate the growth of bacteria in the stream and, thus, to promote bacterial degradation of the acetone. Similarly, on days 23 and 24, a nutrient solution containing bacteria acclimated to acetone in the laboratory was injected in an attempt to induce bacterial degradation of the acetone in the stream. Procedures used for the injection, sample collection and handling, and analysis of these various solutes are described in the following paragraphs.

Acetone

Technical grade acetone was pumped from a calibrated 13-L glass carboy using a Fluid Metering, Inc., positive displacement AC-powered metering pump. The carboy and the pump were located in the trailer (fig. 1). The acetone was pumped through 6.4-mm OD stainless steel tubing to a point 1.0 m downstream from the upstream end of the partition on the experimental (left) side

(fig. 5). The acetone was injected 100 mm below the water surface. Most of the acetone is assumed to have dissolved, although a small surface "boil" at this point suggested the possiblity of some loss through volatilization.

The carboy was usually filled daily, and levels recorded at about 0800 hours and 1600 hours, permitting calculation of the acetone injection rate. The acetone injection rate also was determined volumetrically at various times by raising the end of the stainless steel tubing from the water and placing a 10-mL graduated cylinder over the end for 1.0 min. After determining the volume, the acetone was poured into the stream a short distance downstream from the injection point.

Acetone samples were collected in 4-mL glass vials with Teflon-faced septum caps. The vials were about half-filled with sample and then frozen in liquid nitrogen. Samples were stored in a freezer at -20 °C until analysis.

Sampling for acetone determination was concentrated at cross sections 59, 140, and 220. However, several acetone synoptic sampling surveys were completed. These surveys consisted of samples at 20-m intervals from cross section 40 through cross section 220. Samples were collected in as short a time period as possible so as to obtain an instantaneous distribution of the acetone in the model stream.

Sampling frequency at cross sections 59, 140, and 220 varied, depending on the objective of the sampling. During the transient period on day 2, samples were collected at about 15-min intervals at cross section 59 and at about 30-min intervals at cross sections 140 and 220. As the concentrations tended toward equilibrium conditions, these sampling intervals were lengthened to 30 min at cross section 59 and 60 min at cross sections 140 and 220. Acetone samples also were collected at about the same frequency on day 4 during the TBA injection, at about 2-hour intervals on day 30, and at about 1-hour intervals on day 33. Acetone sampling on the other days was limited to samples at approximately 0800 hours, 1200 hours, and 1600 hours.

Acetone concentrations in the samples were determined using a purge-and-trap procedure followed by analysis in a Varian 2700 gas chromatograph equipped with a flame ionization detector. The purge-and-trap apparatus consisted of an eight-port valve with two U-tube traps packed with Tenax-GC. The heated injection port was constructed from a 6.35-mm stainless steel Swagelok tubing tee, a Teflon-coated septum, a heating tape, and a needle guide as used for injection ports of gas chromatographs. Direct aqueous injection of from 1.0 µL to 5.0 µL aliquots of the samples was used. Purging was at room temperature for 10 min with a helium flow of 20 mL/min. Desorption into the chromatograph was with a heating cup at 170 °C to 180 °C. The gas chromatographic column was a 1.83-m length of 6.35-mm OD stainless steel tubing packed with Chromosorb 103. The oven was operated isothermally at 150 °C, and the detector temperature was 200 °C. Six replicates with a concentration of 50 mg/L had a coefficient of variation of ±3.4 percent. Complete details of the procedure have been presented previously (Tai, 1978).

Rhodamine-WT dye

Procedures for the rhodamine-WT dye injections on days 1 and 2 and on days 30 and 31 (table 8) were basically the same as those used in the preliminary dye study. The main differences were in the procedures used to determine the dye-solution injection rates. In the preliminary dye study, the dye solution was pumped from a graduated cylinder. Manpower limitations precluded using this procedure in the acetone-injection experiment. Consequently, in the days 1 and 2 injection, the dye solution was collected periodically in a 10-mL graduated cylinder for 1.0 min. After determination of the volume, the solution was poured into the stream just downstream from the injection point. In the days 30 and 31 injection, the dye solution was pumped from a calibrated reservoir, and the injection was determined from the volume changes as a function of time.

t-Butyl alcohol

A water solution containing 3.47×10^5 mg/L of reagent grade TBA was pumped from a 500-mL graduated cylinder using a Fluid Metering, Inc., positive displacement metering pump powered by a 12-volt battery. Pumping from the graduated cylinder, which periodically was refilled, permitted monitoring of the injection rate. The TBA solution was pumped through 6.4-mm OD polypropylene tubing to a point 1.2 m downstream from the upstream end of the partition on the experimental side (fig. 5). The solution was injected 100 mm below the water surface, and the injection was continued for 725 min (table 8).

The sampling procedure and sampling frequency were the same as those described previously for acetone. Also the analytical technique was the same, so that the TBA and acetone concentrations could be determined simultaneously in the same samples. The coefficient of variation for six replicates with a concentration of 50 mg/L was ±1.7 percent.

Glucose

Glucose solutions were prepared from distilled water and reagent grade anhydrous D-glucose. Concentrations of the three solutions injected (table 8) were 106 g/L, 228 g/L, and 371 g/L, giving concentrations in the model stream ranging from 76 mg/L to 277 mg/L at cross section 40 (divided section) and from 23 mg/L to 72 mg/L at cross section 80 (undivided section). As discussed previously, the objective of the glucose injection was to increase bacterial growth in an attempt to induce bacterial degradation of the acetone.

The glucose solution was injected through 6.4-mm OD polypropylene tubing using a Fluid Metering, Inc., positive displacement metering pump powered by a 12-volt battery. The solution was pumped from a calibrated reservoir and injected just above the water surface at a point 1.2 m downstream from the upstream end of the partition on the experimental side (fig. 5). The glucose injection was continued for slightly more than 3 days (table 8).

Samples for the determination of the glucose concentration were collected in glass vials or plastic bottles and frozen with liquid nitrogen. They were stored in a freezer at -20 °C until analysis. Sampling the glucose injection was limited to synoptic surveys at 20-m intervals from cross section 40 through cross section 220. Seven surveys were completed; however, two of these were relatively short time periods after the increases in the concentration of the injection solution, and the stream system probably was not in equilibrium.

Glucose concentrations were determined using a modified form of the phenol-sulfuric acid method (Dubois and others, 1956; Handa, 1966). The modification consisted of adding the sulfuric acid immediately after the phenol was added to the sample and also doubling the reagent amounts and the sample aliquot taken for analysis. The coefficients of variation for two sets of six samples each at a concentration of 8.0 mg/L in distilled water were ±1.30 percent and ±1.34 percent. The coefficient of variation of six samples of the same concentration in water from the model stream was ±2.60 percent. The increased variability in the stream water samples was caused by the color of the water, which resulted in a high background in the spectrophotometric method.

Loss of glucose in the stream water samples was noted, with only about 10 percent of a concentration of 8.0 mg/L remaining after 24 hours. No losses in distilled water samples occurred over a 2-week period. Analysis of preservation methods showed that refrigeration, freezing, and 1 mL of 2 percent sulfuric acid per 100 mL of sample were effective. Freezing was used in the present study, as discussed previously.

Bacteria and nutrients

The bacteria and nutrients were injected through 6.4-mm OD polypropylene tubing using a Fluid Metering, Inc., positive displacement metering pump powered by a 12-volt battery. The solution was pumped from a calibrated reservoir and injected just above the water surface at a point 1.2 m downstream from the upstream end of the partition on the experimental side (fig. 5). The bacteria-nutrient solution injection was continued for slightly more than 1 day (table 8).

A description of the bacteria, of the method used to acclimate the bacteria to acetone, and of the nutrient mixture was presented previously (Rathbun and others, 1982). Briefly, the bacteria were selected from a primary sewage sample using an enrichment-culture technique. The bacteria in a medium especially designed for growth of bacteria (Montgomery and Gardiner, 1971) were initially fed glucose, then a mixture of glucose and acetone, and finally acetone alone. The resultant bacteria effectively degraded acetone in laboratory studies (Rathbun and others, 1982). Although the specific genera of the bacteria were not determined, electron photomicrographs showed the bacteria were rod shaped and about 1 μm in length.

The bacteria-nutrient solution was not sampled. However, sampling for the determination of the acetone concentration was continued at cross sections 59, 140, and 220 on the regular sampling schedule of approximately 0800 hours, 1200 hours, and 1600 hours.

Diel Oxygen Study

A diel oxygen study was conducted on day 11 and day 12 of the acetone-injection experiment to determine net daytime productivity and nighttime respiration values for the model stream. Samples were collected at approximately 1-hour intervals from 0700 hours on day 11 to 0700 hours on day 12. Sampling points were on the experimental and control sides of the partition at cross section 59 and at cross sections 140 and 220.

Dissolved-oxygen concentrations were determined using a micro-Winkler technique (Carpenter, 1965) in which the titrations are done directly in the sample bottle. Samples were fixed with the Winkler reagents immediately after collection, and usually were titrated within 1 hour. Inorganic carbon concentrations were determined using a Beckman 915-A carbon analyzer. The pH values were determined with a Corning Model 130 pH meter. Water temperatures were measured with a mercury thermometer with 0.1 °C divisions.

RESULTS OF THE ACETONE TRANSPORT AND FATE STUDY

Experimental Problems

As in any experimental study and, in particular, a field study, experimental problems occurred. Two problems significantly complicated the interpretation of the experimental results. These were a variable division of the flow by the channel partition and a declining acetone injection rate during the daytime hours.

Flow Division Problem

Interpretation of the experimental results was complicated by the fact that the division of the flow by the partition was not constant during the acetone-injection experiment. As discussed previously, the preliminary dye study showed that the partition divided the flow about equally. A small perturbation in the data did occur, but this was not recognized as a flow division problem at the time. Therefore, the acetone-injection experiment was designed on the basis that the streamflow was divided about equally by the partition.

Analysis of the acetone samples from the first 10 days of the acetone-injection experiment indicated otherwise, however. The general course of the experiment was followed with the morning, noon, and afternoon acetone samples at cross sections 59, 140, and 220. Weekend samples were analyzed on the following Monday. On day 9, the weekend samples from days 7 and 8 indicated much larger acetone concentrations at cross section 59 than had previously been determined. Also, the field notes indicated a large accumulation of moss and algae on the water surface on the experimental side of the partition on the afternoon of day 7. When these large acetone concentrations were determined on day 9, the moss and algae were removed from the water surface with a rake, and the acetone concentrations decreased rapidly to about the same values determined previously.

Acetone concentrations at cross sections 59, 140, and 220 are presented as a function of the day of the experiment for days 3 through 12 in figures 18, 19, and 20. The times are the mean sample times for the morning, noon, and afternoon samples. Not all samples were analyzed because of the finite amount of time available for laboratory analysis.

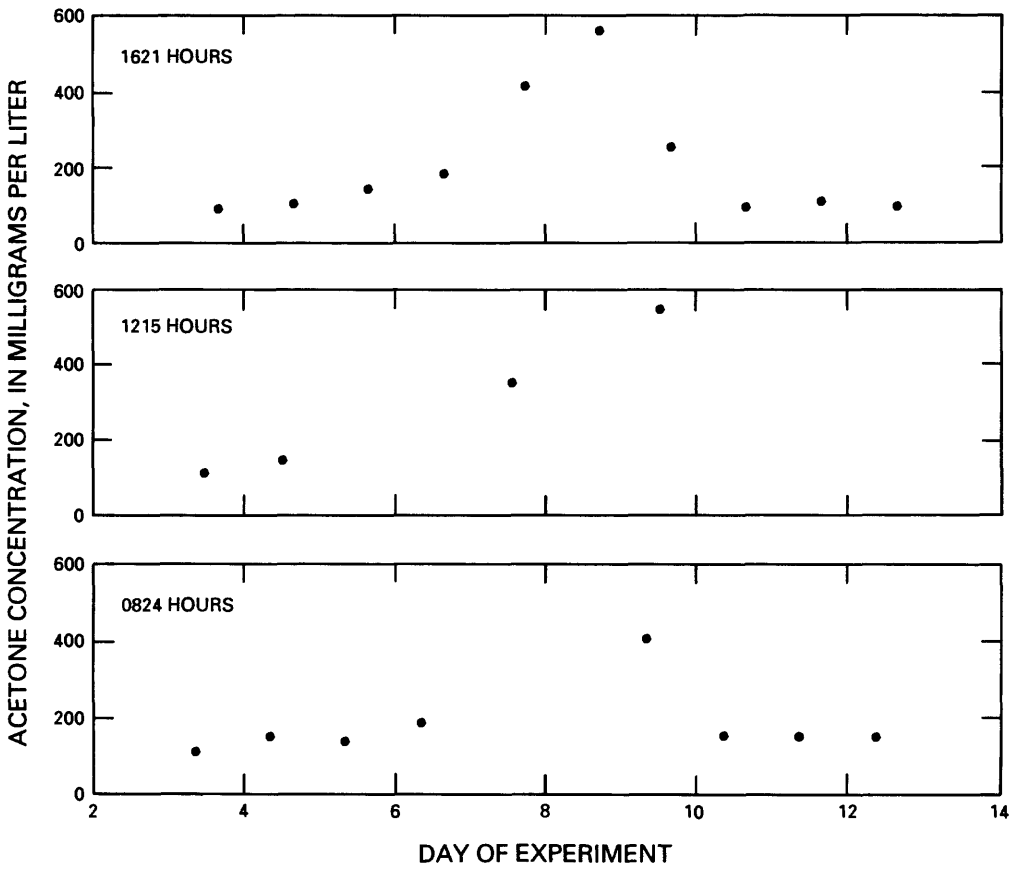

Figure 18.--Acetone concentration as a function of the day of the experiment for days 3 through 12, cross section 59; 0824 hours, 1215 hours, and 1621 hours are the average times of the morning, noon, and afternoon samples.

The concentrations at cross section 59 (fig. 18) were reasonably constant on days 3 to 5, then increased considerably on days 6 to 9. The surface blockage was removed about 60 min before the afternoon sample on day 9, and this sample had already shown a large decrease in concentration relative to the previous sample. Concentrations for days 10 to 12 were approximately constant and also about the same as the concentrations on days 3 to 5 prior

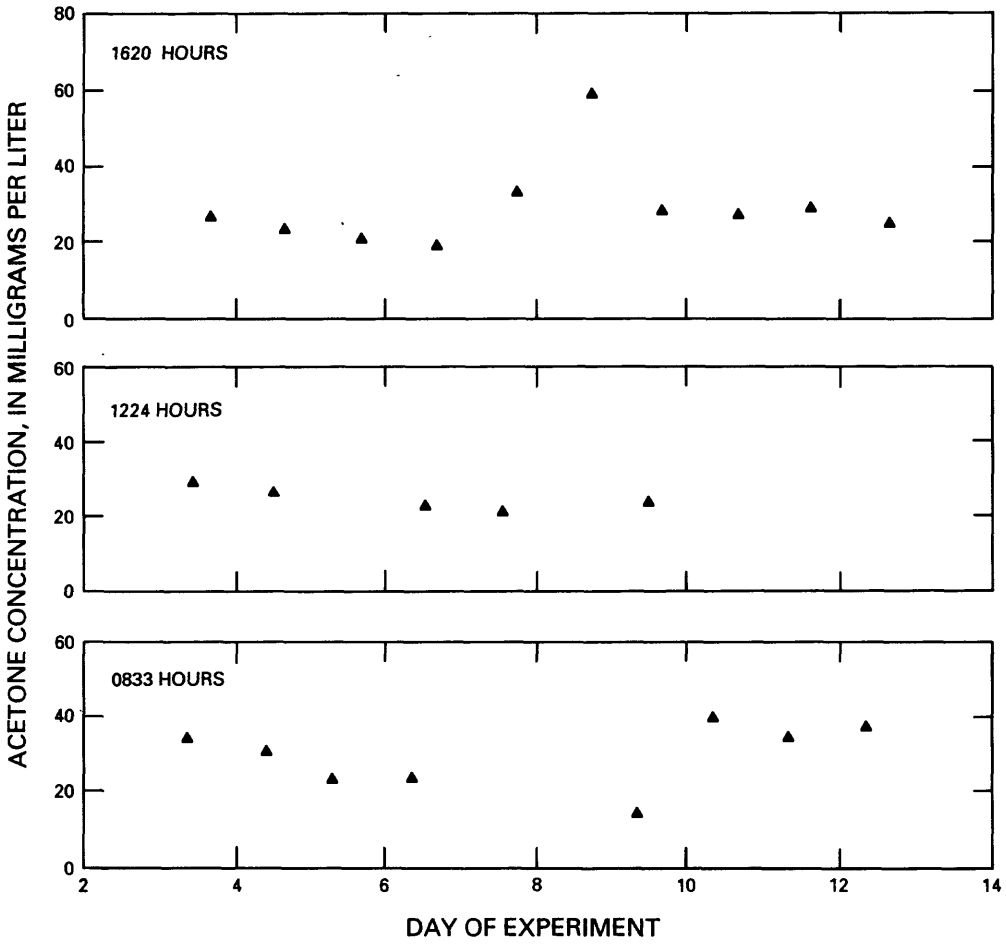

Figure 19.--Acetone concentration as a function of the day of the experiment for days 3 through 12, cross section 140; 0833 hours, 1224 hours, and 1620 hours are the average times of the morning, noon, and afternoon samples.

to the blockage problem. As will be discussed shortly, the concentrations on days 10 to 12 also were about the same as the mean concentrations for the rest of the experiment.

The concentrations at cross sections 140 and 220 (figs. 19 and 20) generally decreased after day 5 and then increased to about the mean concentrations after the blockage was removed on day 9. This behavior occurred because of the accumulation of the injected acetone on the experimental side of the partition. As a result, smaller quantities were transported downstream. Exceptions to this behavior at cross section 140 were the large concentration in the afternoon sample on day 8 and the approximately mean

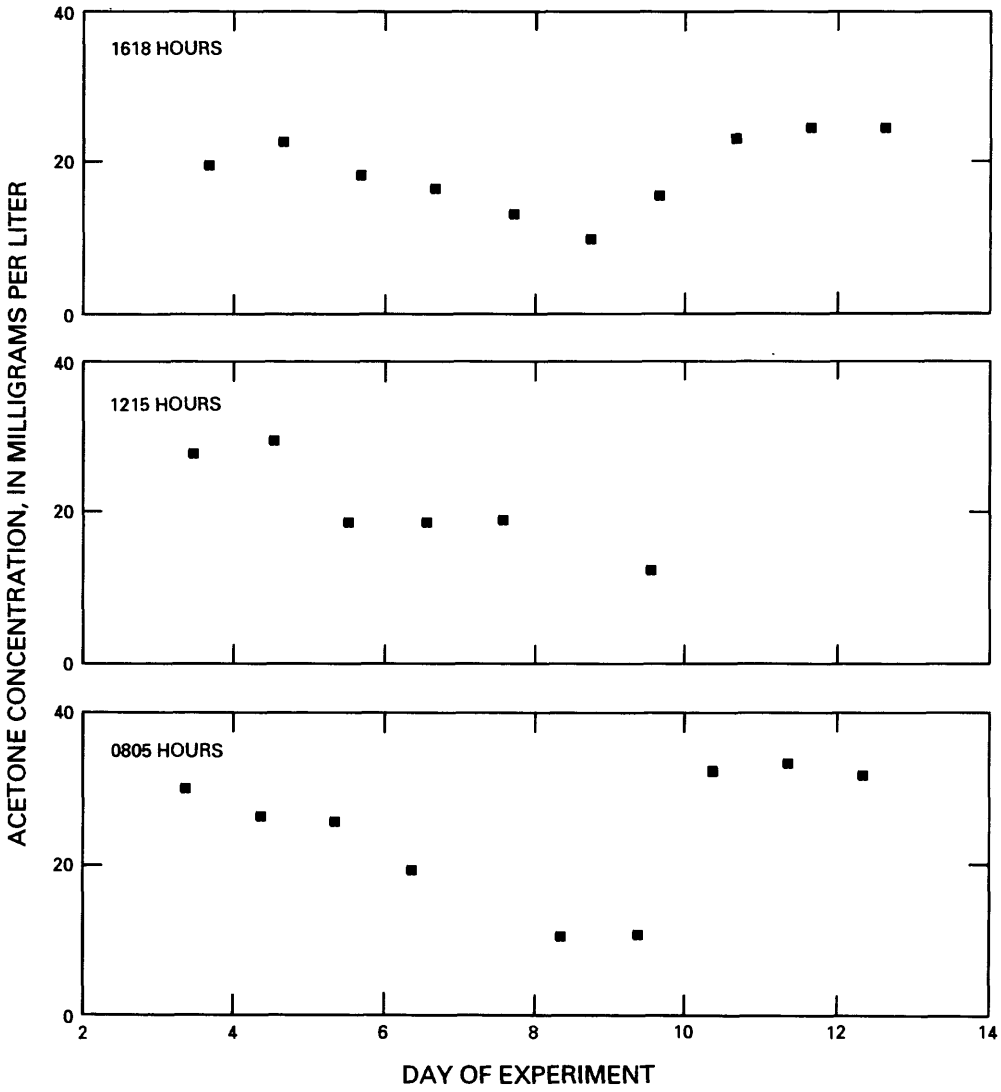

Figure 20.--Acetone concentration as a function of the day of the experiment for days 3 through 12, cross section 220; 0805 hours, 1215 hours, and 1618 hours are the average times of the morning, noon, and afternoon samples.

concentration in the afternoon sample on day 7. These perturbations could have been the result of a short term release of a slug of acetone from the experimental side of the partition.

The flow division problem apparently occurred because of an accumulation of moss and algae on the experimental side of the partition. This resulted in a greater fraction of the flow on the control side where the resistance to flow was less. Because of this problem, the moss and algae were removed periodically thereafter from the water surface on the experimental side of the partition, and no major changes in the flow division occurred for the rest of the experiment.

Small changes in the flow division factor did occur, however. This factor was determined by comparing the concentrations of the various solutes at cross sections 59 and 80 as determined from the synoptic samples. Concentrations of the nonconservative solutes were corrected for losses between cross sections 59 and 80 using observed concentrations from the synoptic samples for cross sections 80, 100, 120, and 140. This procedure assumes that the loss characteristics of the stream between cross sections 59 and 80 are the same as those between cross sections 80 and 140. This should be a valid assumption because the physical characteristics of the stream from cross sections 59 to 140 were reasonably uniform.

Acetone concentration ratios for cross sections 80 and 100, 100 and 120, and 120 and 140 for seven synoptics ranged from 0.904 to 1.13 and averaged 1.024, with a coefficient of variation of ±5.60 percent for the 21 values. This mean value was used to correct the acetone concentrations at cross section 80 for losses between cross sections 59 and 80. There was considerably more variation in these values for glucose. The ratios for seven synoptics ranged from 0.786 to 1.41 and averaged 1.082, with a coefficient of variation of ±13.6 percent for the 21 values. Only one TBA synoptic was determined and the cross sections 80/100, 100/120, and 120/140 ratios were 1.064, 1.038, and 1.063, giving a mean ratio of 1.055. These mean ratios for glucose and TBA were used to correct the concentrations at cross section 80 for losses between cross sections 59 and 80. Finally, the ratios for seven rhodamine-WT dye synoptics ranged from 0.864 to 1.065 and averaged 0.999 with a coefficient of variation of ±4.67 percent for the 21 values. The mean value of nearly 1.0 is consistent with the fact that the dye is nearly conservative. Therefore, no correction was applied to the dye concentrations.

Flow division factors calculated from the ratios of the concentrations at cross sections 80 and 59 are given in table 9. Values ranged from 0.225 to 0.453 and averaged 0.296 with a coefficient of variation of ±24.1 percent. The mean flow division factor of 0.296 is considerably less than the approximately equal flow division determined in the preliminary dye study.

Also, the coefficient of variation of ±24.1 percent indicates considerable variation in the division of the flow by the partition. Some of this overall variability was the result of the variability of the six day 2 values where the flow division factor varied by almost a factor of 2. Precautions were taken after day 10 to prevent major blockages on the experimental side of the partition. If only values after day 10 are considered, the mean of 0.290 is about the same as that of all values in table 6; however, the coefficient of variation is decreased to ±18.4 percent.

The procedure used for calculating the flow division factors assumes that any change that occurs is for a time period long enough for equilibrium conditions to be established downstream to cross section 140. The average flow time from the injection point to cross section 140 was about 120 min. Therefore, any flow division changes of less than 120-min duration would contribute to the scatter in the results.

Table 9.--*Flow division factors determined from the synoptic samples*

Day of experiment	Solute	Clock time (hours)	Flow division factor
2	Rhodamine-WT dye	0535	0.296
		1030	.239
		1215	.230
		1415	.374
		1600	.453
		1800	.427
3	Acetone	0830	.229
4	Acetone	1900	.227
	t-Butyl alcohol	1900	.243
10	Acetone	0800	.289
18	Glucose	0930	.332
		1530	.256
19	Glucose	0915	.282
		1530	.256
20	Glucose	0830	.225
		1235	.250
		1530	.304
23	Acetone	1550	.327
31	Rhodamine-WT dye	0545	.416
34	Acetone	0830	.255

Acetone injection problem

The acetone injection rate showed two unexpected characteristics during the experiment. First, the mean daytime injection rates determined from volume changes in the calibrated supply reservoir were consistently smaller than the mean nighttime injection rates. Second, the instantaneous injection rate determined using the graduated cylinder procedure decreased with time during the daytime hours. These two effects, which are undoubtedly interrelated, resulted in an approximately periodic variation with time of the acetone injection rate. This variation persisted throughout the 32 days of the acetone injection; however, the amplitudes of the variations changed from day to day.

The acetone level in the supply reservoir usually was determined daily at about 0800 hours and at about 1600 hours. The mean daytime injection rate determined from these measurements was 3.11 mL/min with a coefficient of variation of ±10.8 percent for 26 measurements. The mean nighttime rate was 3.96 mL/min with a coefficient of variation of ±6.28 percent for 26 measurements. Consequently, the nighttime rate was, on the average, 27 percent larger than the daytime rate.

After the conclusion of the model stream experiment, the acetone injection system was set up in the laboratory in an attempt to determine the explanation for the difference in rates. Head differentials between various

parts of the system were the same as for the model stream injection. The only difference was that water was pumped rather than acetone. Comparison of the daytime and nighttime rates over a 3-day period showed no significant differences. The injection system then was set up again in the trailer at the model stream, and water was pumped for a 3-day period. Again, no significant differences between the daytime and nighttime water injection rates were found.

Acetone, however, is much more volatile than water; therefore, the possiblity of a temperature effect on the injection process was considered. The acetone reservoir and pump were located in the trailer. The stainless steel discharge line ran from the pump out the north end of the trailer and then just under the surface of the ground to the bank of the stream. The last 2 m of the discharge line were exposed to the air, and the last 100 mm were submerged to facilitate injecting the acetone at a point 100 mm below the water surface as described previously. Consequently, air temperature variations may have had an effect on the pumping of a volatile liquid using this system.

Air temperatures were not measured during the experiment; therefore, the water temperature at cross section 59 was used as an indicator of the air temperature in the vicinity of the injection point. The water depth in the stream was shallow enough that significant diurnal variations in temperature occurred. These variations were moderated somewhat by the fact that the temperature of the inlet water from the artesian well was always within the narrow range between 26.8 °C and 27.0 °C. Thus, it was assumed that changes in the air temperature were indicated by changes in the water temperature. However, it also was expected that the changes in the water temperature were less than the corresponding changes in the air temperature because of the heat capacity of the water and the moderating effect of the constant inlet water temperature.

The daytime acetone injection rate as a function of the water temperature at cross section 59 is presented in figure 21 for mean observation times of 1219 hours and 1609 hours. There is considerable scatter in the data; however, in each case, the slopes of the least-squares lines were significantly different from zero at the 5-percent level. Consequently, a significant relation existed between the acetone injection rate and the water temperature.

The instantaneous acetone injection rate was determined numerous times using the graduated cylinder procedure described previously on days 2, 4, 13, 30, and 33, and a limited number of times on other days. The variation of the injection rate with time was expressed by

$$q_A = q_0 \exp\left[-\gamma(t-t_0)\right] \tag{37}$$

where q_A = the instantaneous acetone injection rate, in milliliters per minute, at time t, in minutes;

q_0 = the injection rate, in milliliters per minute, at an arbitrary base time of t_0, in minutes; and

γ = the rate coefficient, in minutes^{-1}, describing the exponential decrease of the acetone injection rate with time.

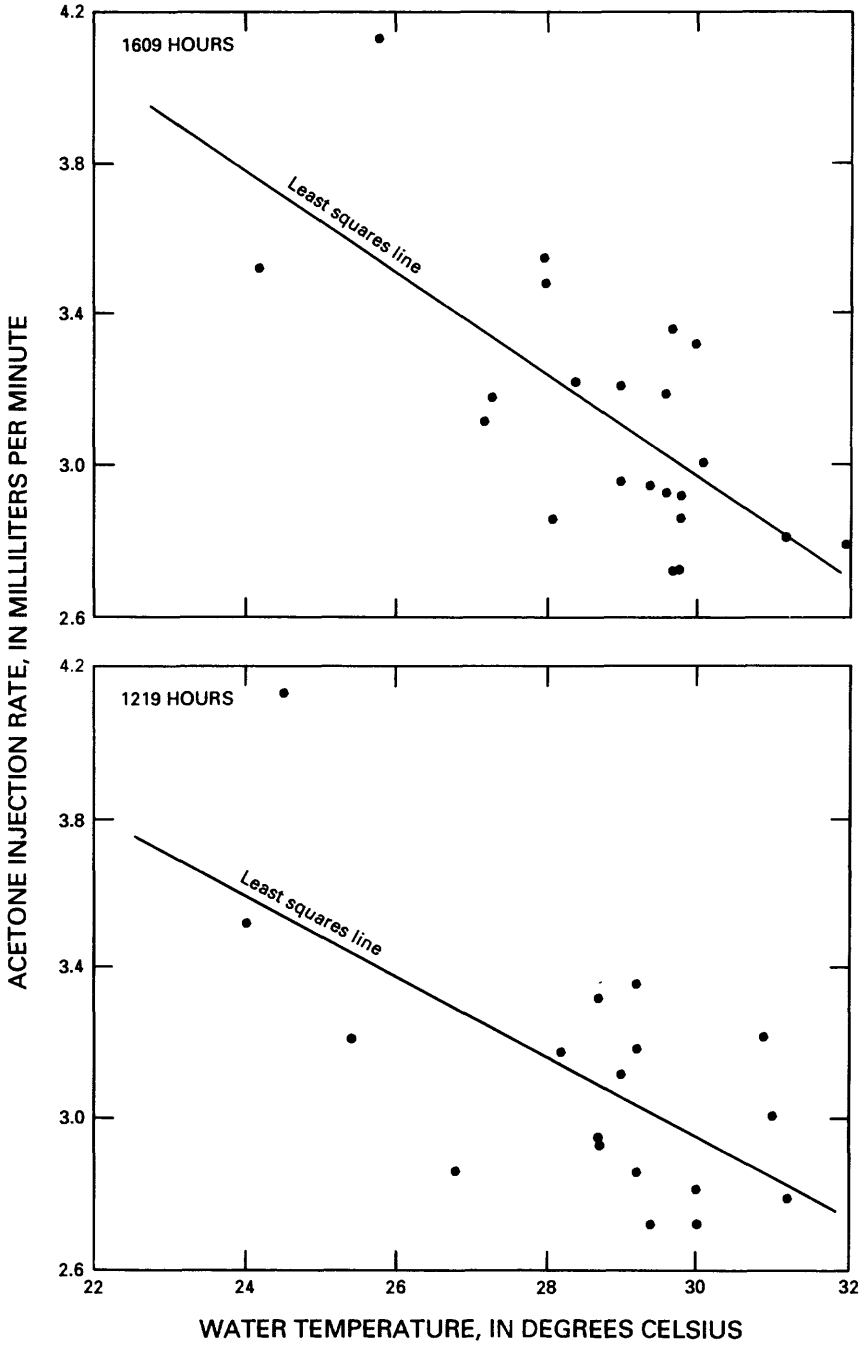

Figure 21.--Daytime acetone injection rate as a function of water temperature for mean times of 1219 hours and 1609 hours.

Values of the rate constant, γ, were determined from least-squares regressions of the logarithm of the injection rate as a function of time, and the results are presented in table 10. Also given in table 10 are the root-mean-square errors of the regression fit calculated from an equation of the form of equation 28.

Table 10.--*Values of the rate coefficient γ determined from linear regressions of the logarithm of the acetone injection rate as a function of time, and the root-mean-square errors of fit*

Day of experiment	Rate coefficient γ $\times 10^4$ (minutes^{-1})	Root-mean-square error (percent)
2	2.88	±6.93
4	2.67	±17.2
13	9.15	±17.8
30	6.44	±9.85
33	6.83	±9.92
Overall	2.83	±16.8

The γ constants for days 2, 30, and 33 were significantly different from zero at the 5-percent level. The slopes for days 4 and 13 were not significantly different from zero at the 5-percent level. Presumably, the slopes were not significant because of the greater scatter in the data indicated by the larger rms errors for days 4 and 13 (table 10). The instantaneous acetone injection rates for days 2 and 4 are plotted on a logarithmic scale in figure 22 as a function of elapsed time from 0500 hours as examples of data with large and small rms errors. The decrease of the injection rate with time is apparent for each day. The difference in the scatter in the data also is apparent. The reason for this difference is unknown.

There is no physical basis for combining all the instantaneous acetone injection rates in a single correlation because it was rationalized previously that the rates depended on air temperature which undoubtedly varied from day to day. However, in the analysis of the long-term mean acetone concentration data at cross sections 59, 140, and 220, to be discussed shortly, some measure of the overall average rate of change of the acetone injection rate with time was needed. Therefore, an overall least-squares fit was computed using the 91 values from days 2, 4, 13, 30, and 33 and the 98 values from the other days. The result was a γ value of 2.83×10^{-4} min^{-1} with a coefficient of variation of ±16.8 percent (table 10). This large coefficient of variation indicates considerable scatter and probably is partly a result of combining the data for the different days with different air temperature conditions. However, the γ constant was significantly different from zero at the 5-percent level and the correlation coefficient was significant at the 5-percent level. Therefore, the γ value for the overall correlation (table 10) was used as an indicator of the mean overall rate of change of the daytime acetone injection rate with time during the experiment.

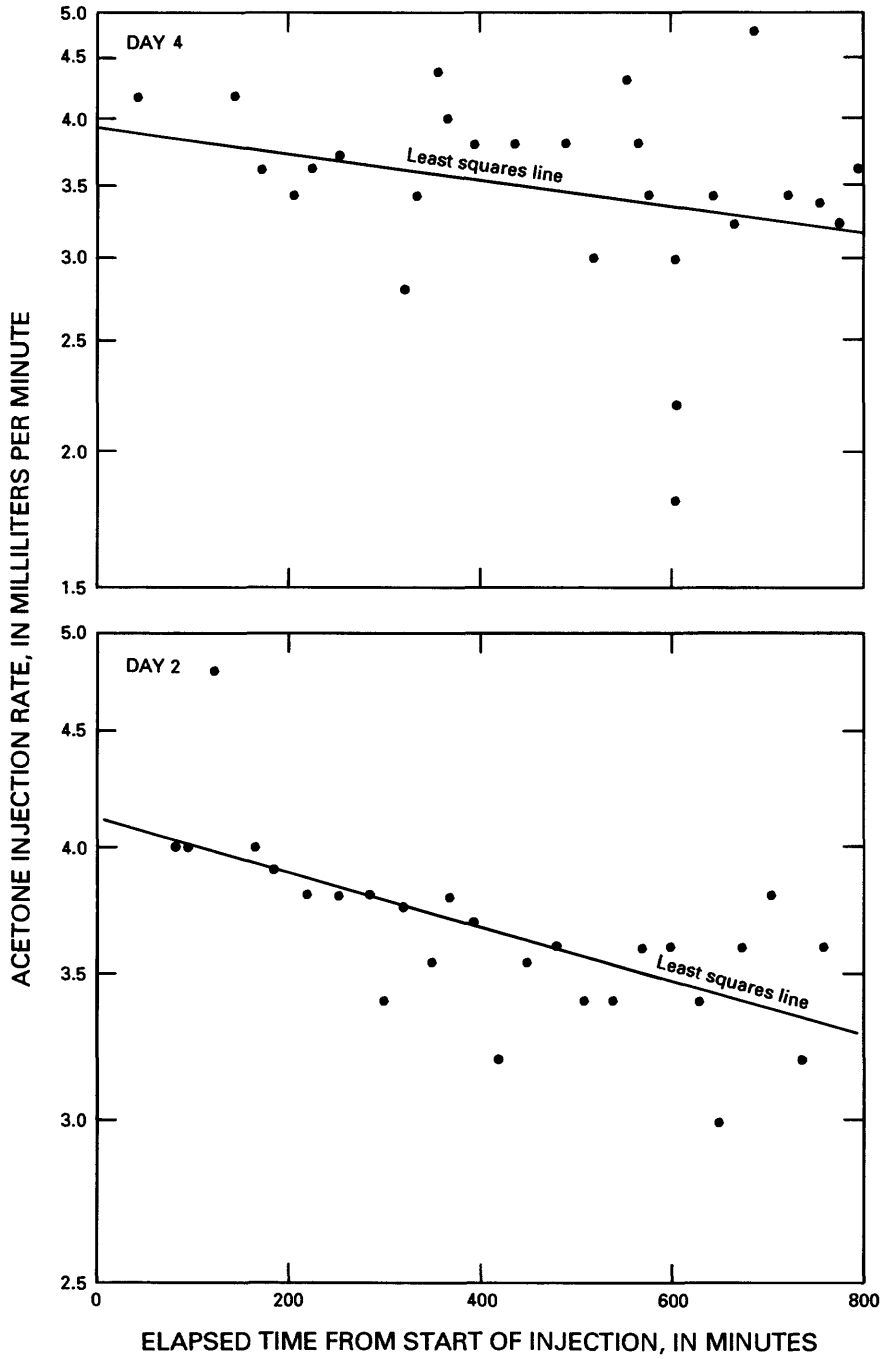

Figure 22.--Instantaneous acetone injection rate on a logarithmic scale as a function of elapsed time relative to 0500 hours for days 2 and 4.

The γ values in table 10 represent the rate of change of the acetone injection rate with time. If the acetone injection rate depends on air temperature as hypothesized, then the slopes should be largest on those days on which the air temperature changed the most. Again using the water temperature as an indicator of the air temperature, the maximum afternoon water temperature at cross section 59 on day 2 was 29.0 °C; on day 4 it was 28.1 °C; on day 13 it was 31.0 °C; on day 30 it was 30.5 °C; and on day 33 it was 29.8 °C.

The γ values in table 10 are quantitatively in the same order, with the exception of the values for days 30 and 33. This observation supports the argument that the acetone injection rate was affected by the air temperature.

Acetone Results

Results of the laboratory study (Rathbun and others, 1982) indicated that volatilization and bacterial degradation were the processes most likely to be important in determining the fate of acetone in streams. It was also expected on the basis of this laboratory study and the literature (Wiggins and others, 1987) that some acclimation period would be necessary before bacterial degradation would begin in the model stream. Therefore, it was hypothesized that the acetone injected into the model stream would first establish equilibrium concentrations on the basis of the volatilization characteristics of acetone and the stream. Then, after the acclimation period, the length of which may depend on a number of mechanisms (Wiggins and others, 1987), bacterial degradation of the acetone would begin. The spatial distribution of the degradation process was expected to depend on the relative importance of free-floating and attached bacteria. If free-floating bacteria dominated the process, then degradation was expected to be observed first at the downstream end of the stream because of the longer period of exposure of the bacteria to the acetone. If attached bacteria dominated, then the spatial distribution of degradation rates was expected to be variable, depending on such factors as numbers of bacteria, availability of nutrients, and the levels of other factors influencing degradation rates.

Daily Acetone Concentrations

Acetone concentrations at cross sections 59, 140, and 220 for the morning, noon, and afternoon samples are presented in figures 23, 24, and 25 as a function of the day of the experiment for day 10 through day 34. Also presented in these figures are the time periods of the glucose and bacteria-nutrient injections. Acetone concentrations for day 3 through day 12 were presented previously (figs. 18, 19, and 20).

The acetone concentrations did not change appreciably during the glucose and bacteria-nutrient injections, with the possible exception of the smaller concentrations in most of the samples on day 25. These samples were collected on the day after the completion of the injection of the bacteria-nutrient solution and, thus, could have been the result of increased degradation with the increased bacterial population. However, 40 to 45 mm of rain occurred during the evening hours of day 24 and the early morning hours of day 25 (table 5), considerably increasing the water discharge in the stream and diluting the acetone concentrations.

Discharge data are not available for the nighttime hours; therefore, the exact decrease in acetone concentration as a result of the increased flow cannot be computed. However, discharge at the outlet of the stream at 0830 hours on day 25 was still relatively high (1.92 L/s) compared with the overall mean discharge of 1.155 L/s (for days 10 through 34). If this were the maximum discharge, then the concentrations would be decreased by a factor of

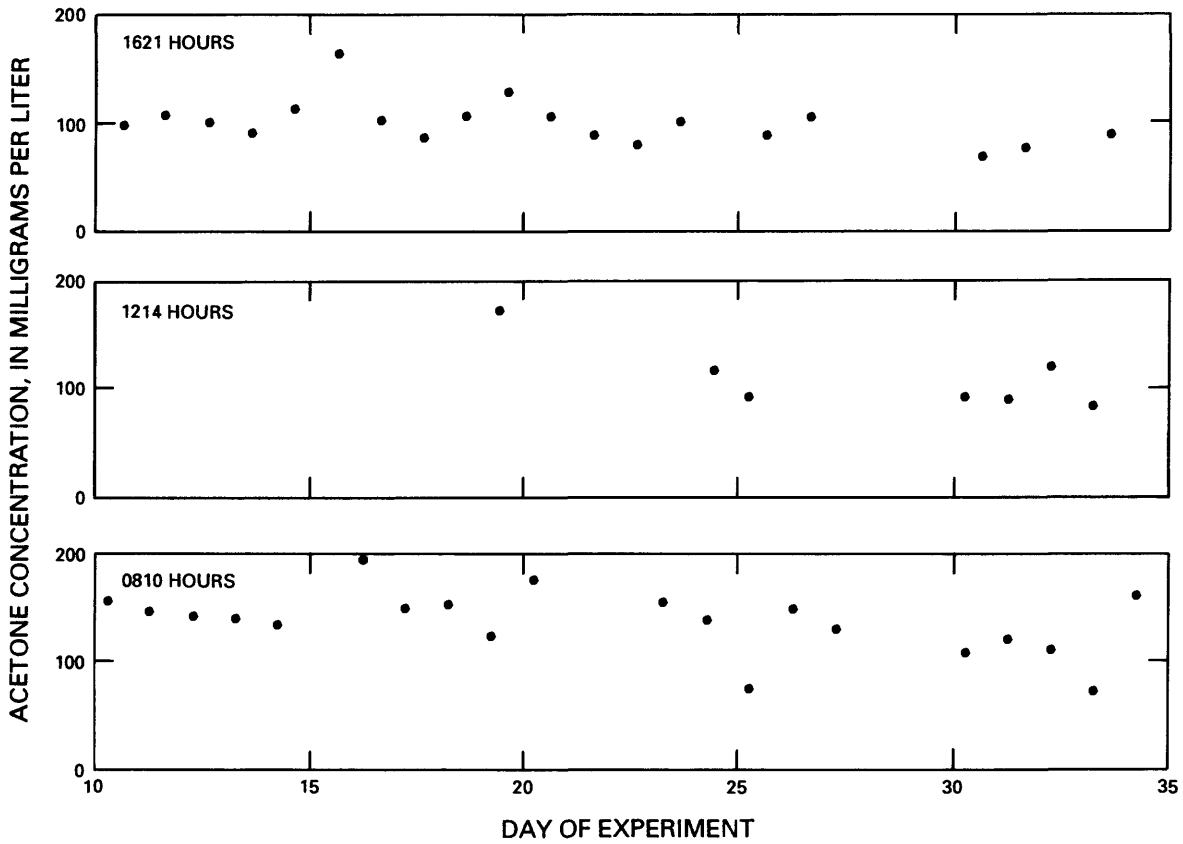

Figure 23.--Concentration of acetone at cross section 59 as a function of the day of the experiment for day 10 through day 34; 0810 hours, 1214 hours, and 1621 hours are the average times of the morning, noon, and afternoon samples.

1.155/1.92 or 0.60. The smallest concentration ratio from day 24 to day 25 was 0.53 for the morning samples at cross section 59. The morning and afternoon samples at cross section 220 had ratios of 0.58, which are comparable to those predicted by the discharge alone with no bacterial degradation. The fact that these concentration ratios are about the same as the discharge ratios indicates that little degradation occurred as a result of the injection of the bacteria-nutrient solution. However, uncertainties regarding the magnitude of the maximum discharge and its time relative to the sampling times preclude the conclusion that acetone degradation did not occur as a result of the injected bacteria.

Possible explanations for the failure of bacteria injected into a natural water to degrade an organic compound, when the same bacteria efficiently degraded the compound in a laboratory culture, were analyzed by Goldstein and others (1985). Of the explanations proposed, those appropriate to the model-stream study include concentrations of acetone too small to sustain growth, susceptibility of bacteria to toxins and predators, and preferential use of other organic compounds in the stream.

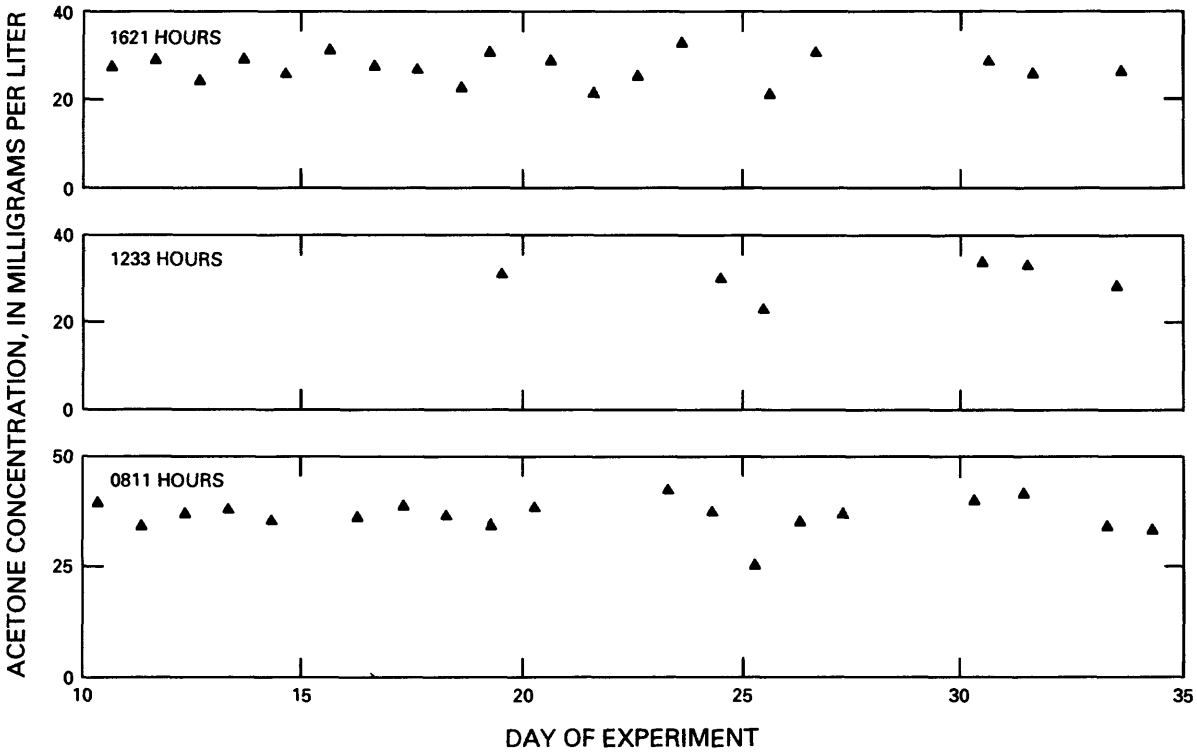

Figure 24.--Concentration of acetone at cross section 140 as a function of the day of the experiment for day 10 through day 34; 0811 hours, 1233 hours, and 1621 hours are the average times of the morning, noon, and afternoon samples.

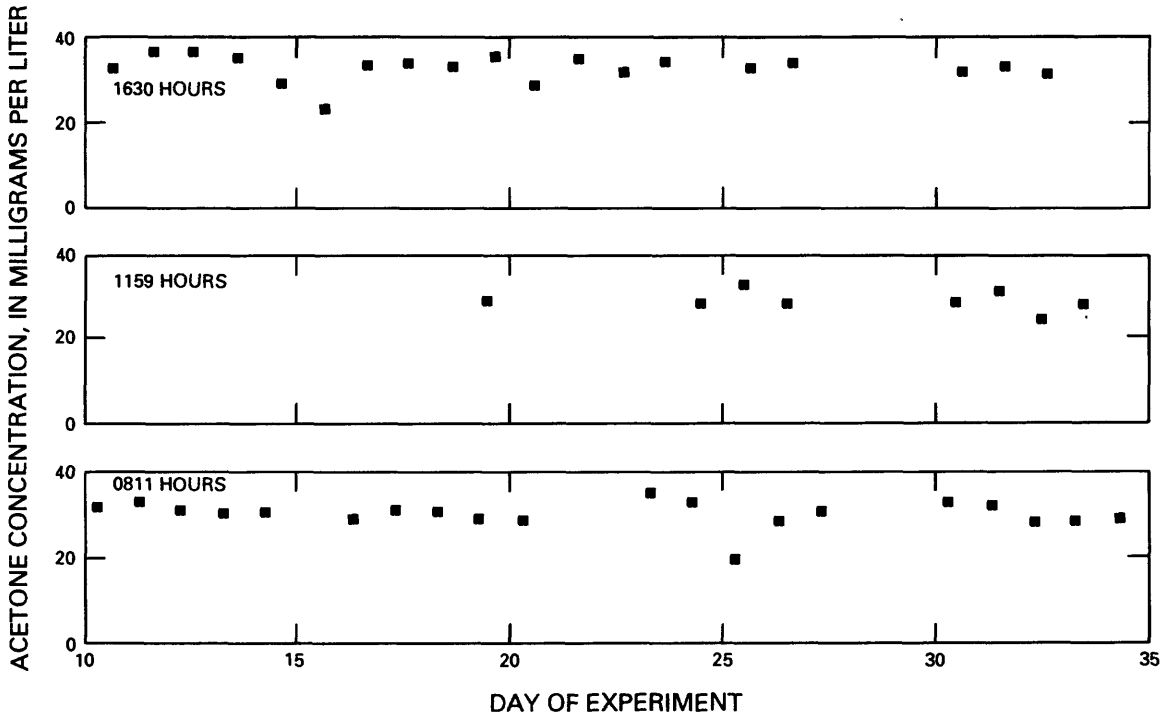

Figure 25.--Concentration of acetone at cross section 220 as a function of the day of the experiment for day 10 through day 34; 0811 hours, 1159 hours, and 1630 hours are the average times of the morning, noon, and afternoon samples.

The concentrations of acetone in the model stream were in the 20 to 200 milligram per liter range (figs. 23, 24, and 25). These were comparable to the intial concentrations in the laboratory biodegradation studies (Rathbun and others, 1982) where rapid degradation was observed. Consequently, the concentrations in the model stream should have been sufficiently large to suport growth of the bacteria. The possibility of toxins inhibiting the growth and the effect of predators on the bacteria were not investigated. However, these factors were not expected to be important because of the nature of the model stream. The preferential use of other organic compounds was a possibility and this is discussed in more detail later in the report. Finally, another factor that could have been important was the limited residence time in the model stream system. This factor also is discussed in more detail later in the report.

Least-square slopes of the acetone concentration-time data presented in figures 23, 24, and 25 were computed to determine if the acetone concentrations were changing significantly with time. Concentrations obviously affected by rainfall (day 25 and day 33) were excluded from these regressions. With the exception of the noon samples at cross section 59, the least-squares slopes were not significantly different from zero at the 5-percent level. These results indicate that the acetone concentrations were not changing significantly with time; therefore, the model stream appeared to be in a steady-state condition.

Mean acetone concentrations, the coefficients of variation, and the number of data points included are presented in table 11. The mean acetone concentration at each cross section decreased with time during the day. This decrease was a result of the decreasing acetone injection rate with time during the daytime hours discussed previously and an increasing volatilization rate with increasing water temperature.

Table 11.--*Mean acetone concentrations and coefficients of variation for day 10 through day 34*

Cross section (meters)	Mean sampling time (hours)	Acetone concentration		
		Mean (milligrams per liter)	Number of values	Coefficient of variation (percent)
59	0810	144.3	18	13.4
	1214	110.9	7	17.2
	1621	101.1	19	18.3
140	0811	37.6	18	6.65
	1233	29.9	6	11.8
	1621	27.4	19	11.3
220	0811	31.1	19	6.25
	1159	29.5	7	7.21
	1630	25.3	18	8.65

The coefficients of variation were largest for cross section 59 and generally smallest for cross section 220. The problems with the flow division by the partition discussed previously probably contributed to the large variability at cross section 59 because small changes in the flow division caused direct changes in the acetone concentration. The smaller variability for cross section 220 relative to cross section 140 was unexpected because of differences in the physical characteristics of the stream at these points (figs. 9 and 10). Scatter in the increasing dye concentration-versus-time data was noted previously (fig. 11), and this was attributed to the effects of the weeds at the downstream end of the stream. Similar effects were expected in the mean acetone concentrations, but were not observed. This difference suggests that perhaps the dead zones created by the weeds were acting as a buffer against concentration fluctuations or were improving mixing conditions.

The mean concentrations presented in table 11 can be used to estimate how long an injection period is necessary to establish equilibrium in the stream with the dead zones created by the floc layer and the weeds at the downstream end. Comparison of nine concentrations each on day 3 and day 4 with the corresponding mean concentrations in table 11 gave mean differences of -7.91 percent for day 3 and -3.98 percent for day 4. Some of this difference is caused by the fact that the water discharge decreased about 4 percent during the first 5 days of the experiment, as discussed previously. Consideration of these results indicates the stream system probably was not in equilibrium on day 3 but was on day 4. Because the acetone injection was begun on day 2 (table 8), this indicates a time period of somewhat less than 2 days was necessary to establish equilibrium. Difficulties with the division of the flow by the partition precluded a quantitative determination of the exact time necessary to establish equilibrium conditions.

On day 10, the average difference from the mean concentrations in table 11 was +1.19 percent. Because this difference is within the analytical error, the system was assumed to be in equilibrium at this time. This result is in agreement with the previous conclusion that the acetone concentration was not changing significantly with time between day 10 and day 34 when the injection was stopped. Finally, the fact that the stream appeared to be in equilibrium on day 10 showed that the system recovered quickly from the changes in concentration caused by the flow division problem on day 6. This indicates the stream was nearly in equilibrium prior to the problem.

No large decreases in acetone concentration occurred at any time during the experiment, but there were minor decreases at cross sections 140 and 220 (figs. 19 and 20) as a result of the flow division problem. It is concluded on the basis of this result that significant bacterial degradation of the acetone did not occur during the 32 days of the injection. All losses of acetone observed in the model stream consequently were attributed to volatilization. Thus, equation 14 reduces to:

$$\Sigma K_i = K_V \tag{38}$$

where K_V = the acetone volatilization coefficient, in minutes^{-1}.

Acetone Volatilization Coefficients

Acetone volatilization coefficients were calculated for the reaches between cross sections 59 and 140, 140 and 220, and the overall reach between 59 and 220. Coefficients also were computed for the reaches between the injection point and cross sections 59, 140, and 220. The computations between cross sections have the advantage that the concentrations of the solutes at the injection point are not needed. Consequently, some of the effects of the injection problems discussed previously are eliminated.

Various types of data collected in the experiment were used. These included the TBA plateau concentrations on day 4, the TBA synoptic concentrations on day 4, the daily acetone concentrations (table 11), the approximately steady-state acetone concentrations on day 4 and day 30, and the acetone synoptic concentrations on day 4.

Calculation of the acetone volatilization coefficients was complicated by the flow division problem and the daytime decreasing acetone injection problem discussed previously. Values of the flow division factor were determined from the synoptic sampling surveys as described previously and presented in table 9. The effect of the decreasing acetone injection rate was reduced using two approaches. The first approach was to limit the analysis to data based on samples collected at the same point and same time of day but on different days. This approach was subject to some error because the variation of the injection rate was not truly periodic, but changed from day to day, apparently depending on the air temperature, as hypothesized previously. The second approach was to use a Lagrangian approach in which a parcel of acetone injected into the stream was followed through the system at the mean flow velocity of the stream. Both approaches were used in the data analysis.

Temperature also was a problem because the volatilization coefficient depended on temperature, and water temperature in the model stream varied with time at a specific cross section (fig. 15) and with longitudinal position at a specific time (fig. 14). Variations in water temperature were accounted for by assuming the computed volatilization coefficient was for the mean temperature of the water parcel passing through the reach. This Lagrangian parcel temperature was obtained by averaging the water temperature at the upstream end of the reach at a specific time with the water temperature at the downstream end of the reach one reach mean traveltime later. To facilitate comparison of volatilization coefficients, they were converted from this average Lagrangian temperature, θ, in °C to a base temperature of 25.0 °C using equation 20.

t-Butyl alcohol plateau concentrations on day 4

The preliminary dye study suggested that a plateau concentration was almost attained at cross section 220 (fig. 11) with a 700-min injection. On this basis, TBA was injected for 725 min on day 4 (table 8) to determine the volatilization characteristics of the model stream. Concentration-versus-time curves for TBA are presented in figure 26 for cross sections 59, 140, and 220.

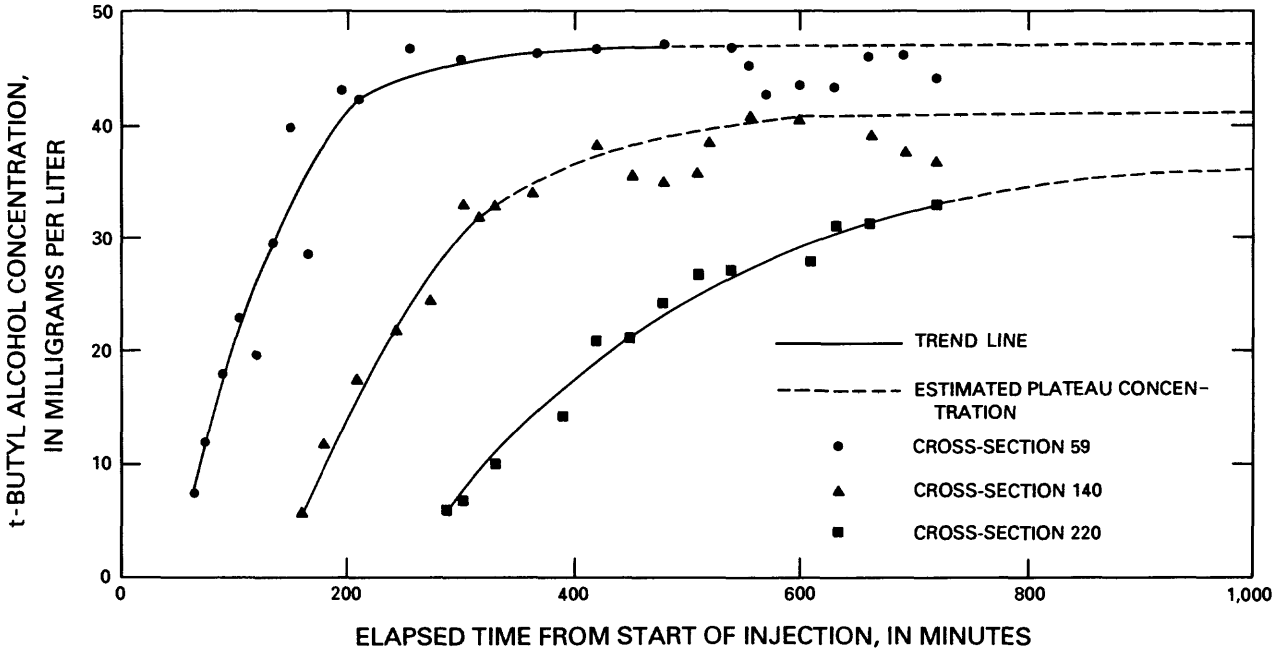

Figure 26.--Concentrations of t-butyl alcohol (TBA) as a function of time at cross sections 59, 140, and 220 on day 4.

The concentrations for cross section 59 have been adjusted for the division of the flow by the partition using the average flow division factor for day 4 of 0.235 (table 9).

Plateau concentrations were established at cross sections 59 and 140 but not at cross section 220. There is scatter in the data at cross sections 59 and 140; thus, some error could result in the determination of the plateau concentrations. Some of this scatter appears to be actual concentration variations because several concentrations were involved. These changes, particularly at cross section 59, could be caused by small perturbations in the division of the flow by the partition.

The failure to establish a plateau concentration at cross section 220 using an injection period based on the results of the preliminary dye study was probably the result of the observed increase in weed density at the downstream end of the stream. The preliminary dye study was done in early April and the TBA injection was done 28 days later. Thus, there was a considerable time period for weed growth between the injections, and this was the time of the year when the weeds were actively growing. Some weed cutting and cleaning of the stream was done prior to the start of the acetone-injection experiment. However, it was difficult to maintain exactly the same conditions.

TBA volatilization coefficients between cross sections were computed from equation 25 using mean water velocities to be presented shortly and the estimated plateau concentrations indicated by the dashed lines in figure 26. Volatilization coefficients between the injection point and specific cross sections were computed from equation 25 with the injection point as the

upstream cross section. The concentration of TBA at the injection point was computed from equation 29. The mean TBA solution injection rate was 11.2 mL/min with a coefficient of variation of ±1.88 percent for 57 determinations. The concentration of the solution computed from the volumes of TBA and distilled water mixed together was 3.44×10^5 mg/L. The concentration determined by gas chromatographic analysis, using the procedure described previously, of a sample of the solution was 3.47×10^5 mg/L. Information on the water discharge was presented previously (fig. 16).

Mean water temperatures were estimated using the Lagrangian parcel approach as discussed previously. The volatilization coefficients were adjusted from these mean water temperatures to a base temperature of 25.0 °C using equation 20 with a β value of 6,550 for TBA determined in laboratory studies (Rathbun and Tai, 1988).

The TBA volatilization coefficients were converted to acetone volatilization coefficients using equations 16 and 22. The various parameters in these equations were determined using procedures described previously in the discussion of equation 22. Integral mean windspeeds for use in equation 18 were computed from equations 35 and 36 for time periods for which plateau concentrations existed at the different cross sections. Parameter values resulting from these calculations are presented in table 12.

Table 12.--*Parameters determined from the t-butyl alcohol (TBA) plateau concentration volatilization study, afternoon of day 4*

Reach (meters)	Volatilization coefficient$\times 10^4$ (minutes^{-1})	Mean windspeed (meters per second)	Gas-film coefficient (meters per day)	Mean flow depth (meter)	Overall mass-transfer coefficient (meter per day)	Liquid-film coefficient (meter per day)
59-140	9.47	1.38	285	0.0636	0.0867	0.170
140-220	6.58	1.29	279	.103	.0980	.226
59-220	7.99	1.20	272	.0845	.0972	.230

Values of the TBA volatilization coefficients and the acetone volatilization coefficients computed from equations 16 and 22 and the parameters in table 12 are presented in table 13. These coefficients will be compared with coefficients determined using other methods later in the report.

t-Butyl alcohol synoptic survey on day 4

A synoptic sampling survey of the TBA concentrations was completed at 1900 hours on day 4 just prior to the termination of the TBA injection at 1905 hours (table 8). Because there were only nine sample points for the survey and because of the small change in concentration with distance down the stream, it was not practical to break the stream into subreaches as was

Table 13.--*Volatilization coefficients for t-butyl alcohol (TBA) at 25.0 degrees Celsius, determined from plateau concentrations on the afternoon of day 4, and acetone volatilization coefficients computed from these coefficients*

Reach	Volatilization coefficient × 10^4 ($minutes^{-1}$)	
	t-Butyl alcohol	Acetone
59-140	9.47	16.7
140-220	6.58	12.5
59-220	7.99	15.4
Inj-59	6.10	10.0
Inj-140	8.18	14.0
Inj-220	7.74	13.1

done for the plateau concentrations. Therefore, only one coefficient for the overall reach between cross sections 59 and 220 was calculated for this survey.

The TBA volatilization coefficient at 25.0 °C was computed from the concentration-versus-distance data and equation 24. The traveltimes to the respective cross sections were computed from the distances and the mean water velocities determined from the day 1 dye injection to be presented shortly. The mean water temperatures were determined from water temperature data using the Lagrangian parcel approach described previously. The calculation procedure consisted of varying the volatilization coefficient until the rms error between the calculated and experimental concentrations was minimized. The rms error was calculated from equation 28.

The TBA volatilization coefficient was 8.17×10^{-4} min^{-1} with an rms error of ±2.99 percent. Converting this coefficient to an acetone coefficient using equations 16 and 22 and the procedure described in the preceding section gives a value of 15.6×10^{-4} min^{-1}. This coefficient will be compared with coefficients determined using other methods later in the report.

Lagged daily acetone concentrations

Volatilization coefficients were computed from the mean daily acetone concentrations (table 11) using a lagging procedure. The concentrations were plotted as a function of the mean times, and smooth curves were drawn through the points. These curves were used to interpolate concentrations at the proper times so that the downstream concentrations were lagged by the traveltime between the cross sections. The traveltimes between the injection point and the respective cross sections and between cross sections were computed from the reach lengths and the mean velocities which will be presented shortly.

Nine pairs of concentrations at approximately 1-hour intervals between 0800 hours and 1600 hours were used for each reach. The overall mean flow division factor of 0.296 (table 9) was used for calculations involving concentrations at cross section 59 and the injection point. The overall γ value (table 10) was used to describe the decrease of the acetone injection rate. The overall mean nighttime acetone injection rate of 3.97 mL/min was used as the initial morning injection rate at 0700 hours.

Volatilization coefficients were computed from equation 25, and the mean values and the coefficients of variation are presented in table 14. Also presented are the mean reach water velocities. Means of the day 1 and day 30 values were used in computing the volatilization coefficients.

Table 14.--*Volatilization coefficients for acetone at 25.0 degrees Celsius determined from the lagged daily acetone concentrations, the coefficients of variation of the volatilization coefficients, and mean water velocities*

[Inj, injection point]

Reach (meters)	Volatilization coefficient $\times 10^4$ ($minutes^{-1}$)	Coefficient of variation (percent)	Mean water velocity (meter per minute)
59-140	11.1	±42.9	0.672 (day 1) .683 (day 30)
140-220	8.23	±29.0	.477 (day 1) .470 (day 30)
59-220	9.80	±17.1	.559 (day 1) .557 (day 30)
Inj-59	20.1	±35.4	.317 (day 1) .410 (day 30)
Inj-140	13.0	± 3.81	.528 (day 1) .588 (day 30)
Inj-220	11.1	±13.6	.505 (day 1) .531 (day 30)

Fitted daily acetone concentrations

Volatilization coefficients between cross sections were computed from the mean acetone concentrations (table 11) by using the concentration-versus-time relation at the upstream cross section as the boundary condition. A least-squares regression of the logarithm of the concentration as a function of time was used as this boundary condition. A volatilization coefficient at 25.0 °C then was assumed, and this coefficient was adjusted to the mean Lagrangian temperature using equation 20. This was done for each of the three sample times at the downstream cross section, with the downstream time lagged by the traveltime between the cross sections. The downstream concentration was calculated using equation 25 with the appropriate upstream concentration, the assumed volatilization coefficient corrected for temperature, and the

traveltime between the cross sections. An rms error of the form of equation 28 was computed between the calculated and experimental concentrations. This entire procedure then was repeated until the error was minimized.

Volatilization coefficients between the injection point and the different cross sections were computed from a modified form of equation 23. This modification was necessary because the acetone injection rate was not constant but decreased during the daytime hours, as discussed previously. Consequently, the acetone concentration in the water at the injection point, C_0, was not constant, as assumed in equation 23.

Following Marino (1974), it can be shown for an exponentially decreasing source concentration that:

$$C(x) = C_0^0 \, [\exp(-\gamma \delta t)] \, [\exp\{(-K_V)(x/U)\}] \tag{39}$$

where C_0^0 = the concentration, in milligrams per liter, at the injection point at some arbitrary base time t_0;

γ = the rate coefficient, in minutes^{-1}, describing the exponential decrease of the acetone injection rate with time; and

δt = the time difference, in minutes, between the sampling time relative to the arbitrary base time and the traveltime, Δt, to the cross section.

This time difference is given by:

$$\delta t = (t_s - t_0) \, (60) - \Delta t \tag{40}$$

where t_s = the clock time, in hours, of the sample; and

t_0 = the arbitrary base time, in hours.

The procedure for a specific cross section consisted of selecting a volatilization coefficient at 25.0 °C, adjusting this coefficient to the mean Lagrangian temperature using equations 20, computing the downstream concentrations as a function of time using equations 39 and 40, and computing an rms error of the form of equation 28 between the experimental and computed concentrations. This procedure then was repeated until the rms error was minimized.

As in the lagging procedure for the daily acetone concentrations, the overall mean values of the flow division factor and the γ coefficient describing the exponential decrease of the acetone injection rate were used. Also, the overall mean nighttime acetone injection rate was used as the initial morning rate.

Volatilization coefficients computed by these two procedures and the rms errors of fit are presented in table 15. These coefficients will be compared with coefficients determined using other methods later in the report.

Table 15.--*Volatilization coefficients for acetone at 25.0 degrees Celsius, determined from the fitted daily acetone concentrations, and the root-mean-square errors of fit*

[Inj, injection point]

Reach (meters)	Volatilization coefficient $\times 10^4$ ($minutes^{-1}$)	Root-mean-square error (percent)
59-140	12.4	±3.39
140-220	11.4	±5.89
59-220	9.99	±6.22
Inj-59	16.2	±9.07
Inj-140	12.4	±5.10
Inj-220	10.9	±3.64

Lagged acetone concentrations on day 4 and day 30

Sample collection for the determination of acetone concentrations was limited generally to the morning, noon, and afternoon times, as discussed previously. However, on day 4, day 30, and day 33, more frequent samples were collected, and the data from day 4 and day 30 were used to compute the acetone volatilization coefficients. The data from day 33 could not be used because of perturbations in the concentrations resulting from rainfall on day 32 (table 5).

Volatilization coefficients were computed from equation 25 using concentrations lagged by the traveltime between the respective cross sections. When experimental concentrations at the downstream cross section were not available at the exact time required by this lagging process, the concentration was determined by linear interpolation between the experimental values. The computed coefficient was assumed to be for the mean temperature corresponding to that of a Lagrangian parcel moving through the system at the time the samples were collected. All computed coefficients then were adjusted to a base temperature of 25.0 °C, using equation 20. For calculations involving concentrations at cross section 59, a mean flow division factor of 0.235 was used for day 4 (table 9) and the day 31 factor of 0.416 (table 9) was used for day 30. For calculations involving concentrations at the injection point, the corresponding γ values (table 10) for day 4 and for day 30 were used to describe the exponential decrease of the acetone injection rate. The mean nighttime acetone injection rates for the previous night were used as the initial morning injection rates at 0700 hours.

Mean values of the volatilization coefficients and the coefficients of variation are presented in table 16. These coefficients will be compared with coefficients computed using other methods later in the report.

Table 16.--*Volatilization coefficients for acetone at 25.0 degrees Celsius, determined from lagged concentrations on day 4 and day 30 and the coefficients of variation*

[Inj, injection point]

Reach (meters)	Day of experiment	Volatilization coefficient $\times 10^4$ (minutes^{-1})	Coefficient of variation (percent)
59-140	4	18.6	±29.8
	30	12.8	±49.7
140-220	4	5.64	±53.7
	30	7.26	±27.1
59-220	4	10.1	±17.6
	30	8.02	±35.5
Inj-59	4	17.3	±31.9
	30	8.26	±100
Inj-140	4	17.5	±16.0
	30	9.62	±16.9
Inj-220	4	11.6	±18.3
	30	9.03	±25.0

Fitted acetone concentrations on day 4 and day 30

The procedures used in fitting the day 4 and day 30 acetone data to determine volatilization coefficients were virtually identical to the procedures used for fitting the daily acetone concentrations as described previously. The only difference was that values for three parameters approriate for day 4 and day 30 were used rather than overall values. These parameters were the flow division factor, the γ coefficient describing the decline of the acetone injection rate, and the mean overnight injection rate which was used as the initial morning rate.

Volatilization coefficients calculated by fitting the acetone concentration data on day 4 and day 30 and the rms errors of fit are presented in table 17. These coefficients will be compared with coefficients computed by other methods later in the report.

Acetone synoptic survey on day 4

A synoptic sampling survey of the acetone concentrations was completed at 1900 hours on day 4 just prior to the termination of the TBA injection at 1905 hours (table 8). The acetone volatilization coefficient at 25.0 °C was computed from the concentration-versus-distance data and equations 39 and 40. The traveltimes to the respective cross sections were computed from the distances and the mean water velocities to be presented shortly. The mean water temperatures were determined from water temperature data using the Lagrangian

Table 17.--*Volatilization coefficients for acetone at 25.0 degrees Celsius determined from fitting downstream concentrations using upstream concentrations as boundary conditions on day 4 and day 30, and the root-mean-square errors of fit*

[Inj, injection point]

Reach (meters)	Day of experiment	Volatilization coefficient $\times 10^4$ (minutes^{-1})	Root-mean-square error (percent)
59-140	4	16.9	±4.51
	30	13.2	±6.41
140-220	4	5.82	±6.06
	30	6.08	±3.32
59-220	4	9.72	±7.54
	30	9.32	±4.37
Inj-59	4	16.6	±4.79
	30	7.71	±4.59
Inj-140	4	17.4	±5.89
	30	11.3	±4.35
Inj-220	4	11.6	±8.01
	30	9.08	±3.54

parcel approach described previously. The calculation procedure consisted of varying the volatilization coefficient until the rms error (eq. 28) between the calculated and experimental concentrations was minimized.

The computed acetone volatilization coefficient was 15.8×10^{-4} min^{-1} with an rms error of ±5.39 percent. Computations were limited to one coefficient for the overall reach between cross sections 59 and 220 because of the limited number of data points.

Comparison of the Acetone Volatilization Coefficients

The acetone volatilization coefficients determined by the different procedures are summarized in table 18 for reaches between cross sections 59 and 140, 140 and 220, and 59 and 220, and in table 19 for reaches between the injection point and cross sections 59, 140, and 220. Also given in tables 18 and 19 are the mean coefficients for each reach and the coefficients of variation of the mean. The errors given in tables 18 and 19 are the coefficients of variation for computations involving lagged concentration data and the rms errors (eq. 28) for computations involving data fitting.

The volatilization coefficients were qualitatively in agreement with expectation based on the physical characteristics of the reaches. The reach between cross sections 59 and 140 had the largest water velocity (table 14) and the largest average volatilization coefficient (table 18), and the reach between cross sections 140 and 220 had the smallest values of these parameters. The overall reach between cross sections 59 and 220 had intermediate

Table 18.--*Summary of acetone volatilization coefficients at 25.0 degrees Celsius for reaches 59-140, 140-220, and 59-220*

[--, no data]

Reach (meters)	Volatilization coefficient × 10^4 ($minutes^{-1}$)	Time period	Error[1] (percent)	Concentration data used
59-140	16.7	Day 4	--	t-Butyl alcohol plateau
	11.1	Day 10-Day 34	±42.9	Lagged daily acetone
	18.6	Day 4	±29.8	Lagged acetone
	12.8	Day 30	±49.7	Lagged acetone
	12.4	Day 10-Day 34	± 3.39	Fitted daily acetone
	16.9	Day 4	± 4.51	Fitted acetone
	13.2	Day 30	± 6.41	Fitted acetone
Mean 14.5±19.5 percent[2]				
140-220	12.5	Day 4	--	t-Butyl alcohol plateau
	8.23	Day 10-Day 34	±29.0	Lagged daily acetone
	5.64	Day 4	±53.7	Lagged acetone
	7.26	Day 30	±27.1	Lagged acetone
	11.4	Day 10-Day 34	± 5.89	Fitted daily acetone
	5.82	Day 4	± 6.06	Fitted acetone
	6.08	Day 30	± 3.32	Fitted acetone
Mean 8.13±34.2 percent[2]				
59-220	15.4	Day 4	--	t-Butyl alcohol plateau
	15.6	Day 4	--	t-Butyl alcohol synoptic
	9.80	Day 10-Day 34	±17.1	Lagged daily acetone
	10.1	Day 4	±17.6	Lagged acetone
	8.02	Day 30	±35.5	Lagged acetone
	9.99	Day 10-Day 34	± 6.22	Fitted daily acetone
	9.72	Day 4	± 7.54	Fitted acetone
	9.32	Day 30	± 4.37	Fitted acetone
	15.8	Day 4	± 5.39	Acetone synoptic
Mean 11.5±27.0 percent[2]				

[1]Error is the coefficient of variation for the lagged concentration data and the root-mean-square error for the fitted concentration data.

[2]Error is the coefficient of variation.

values of both parameters as expected. The mean values in tables 18 and 19 also indicate that the reaches between the injection point and cross section 140 and between the injection point and cross section 220 had volatilization coefficients similar to those for the reaches between cross sections 59 and 140 and 59 and 220. This was expected because the reach between the injection point and cross section 59 was short and, therefore, contributed little

to the overall coefficients. Also, the coefficient for this reach had a mean coefficient (table 19) comparable to the other coefficients for the upstream part of the stream.

Table 19.--*Summary of acetone volatilization coefficients at 25.0 degrees Celsius for reaches between the injection point and cross sections 59, 140, and 220*

[Inj, Injection point; --, no data]

Reach (meters)	Volatilization coefficient × 10^4 (minutes^{-1})	Time period	Error[1] (percent)	Concentration data used
Inj-59	10.0	Day 4	--	t-Butyl alcohol plateau
	20.1	Day 10-Day 34	±35.4	Lagged daily acetone
	17.3	Day 4	±31.9	Lagged acetone
	8.26	Day 30	±100	Lagged acetone
	16.2	Day 10-Day 34	± 9.07	Fitted daily acetone
	16.6	Day 4	± 4.79	Fitted acetone
	7.71	Day 30	± 4.59	Fitted acetone
Mean 13.7±36.1 percent[2]				
Inj-140	14.0	Day 4	--	t-Butyl alcohol plateau
	13.0	Day 10-Day 34	± 3.81	Lagged daily acetone
	17.5	Day 4	±16.0	Lagged acetone
	9.62	Day 30	±16.9	Lagged acetone
	12.4	Day 10-Day 34	± 5.10	Fitted daily acetone
	17.4	Day 4	± 5.89	Fitted acetone
	11.3	Day 30	± 4.35	Fitted acetone
Mean 13.6±21.8 percent[2]				
Inj-220	13.1	Day 4	--	t-Butyl alcohol plateau
	11.1	Day 10-Day 34	±13.6	Lagged daily acetone
	11.6	Day 4	±18.3	Lagged acetone
	9.03	Day 30	±25.0	Lagged acetone
	10.9	Day 10-Day 34	± 3.64	Fitted daily acetone
	11.6	Day 4	± 8.01	Fitted acetone
	9.08	Day 30	± 3.54	Fitted acetone
Mean 10.9±13.3 percent[2]				

[1]Error is the coefficient of variation for the lagged concentration data and the root-mean-square error for the fitted concentration data.

[2]Error is the coefficient of variation.

The errors in tables 18 and 19 are much larger for computations involving lagged concentrations than for computations involving fitted concentrations. This results because pairs of single concentrations were used in the lagging

procedure; consequently, there was considerable variation in these individual volatilization coefficients. The fitting process, however, considers the data as a whole set, and the error was minimized in the fitting process.

The errors in the lagged concentration computations generally decreased as the reach length increased. This decrease resulted because of the greater change in the acetone concentration over the longer reach. Analysis of first-order rate equations of the form of equation 23 (Yotsukura and others, 1983; Rathbun, 1988) has indicated amplification of analytical errors for short reaches with small concentration changes. This amplification occurs when the logarithm of the concentration ratio is taken as required by equation 25 for computation of the rate coefficient. Conversely, for long reaches with large concentration changes, analytical errors in the concentration determinations are decreased when the logarithm of the ratio is taken. The large errors for the coefficients from the lagged concentration computations are a result of small acetone concentration changes which are a consequence of the short length of the model stream and the slow rate of volatilization.

Comparison of the coefficients for a specific time period indicates generally good agreement. It might be argued that such an agreement should be expected because the same data were used. However, the lagging and fitting computation procedures were considerably different.

Comparison of the coefficients for all time periods indicates, with the exception of those for the reach between cross sections 140 and 220, that the day 4 values were generally larger than the coefficients for the other time periods. This was true of coefficients based on both acetone and TBA concentrations. There were several factors that could have contributed to these larger volatilization coefficients.

The mean daytime windspeed on day 4 was 1.13 m/s compared with 0.463 m/s on day 30 and an overall mean daytime windspeed of 0.739 m/s (table 7). Also, the windspeeds on the afternoon of day 4 were higher than average, peaking at a value of 1.72 m/s at both 1441 hours and 1624 hours (fig. 17). These larger windspeeds would contribute to greater losses of both acetone and TBA from the model stream. Although the windspeed decreased later in the afternoon, concentrations in the model stream, particularly at the downstream cross sections, would not have time to recover before the late afternoon samples were collected. The effect of decreased concentrations at the downstream end of the stream is computed volatilization coefficients that are larger than if the complete stream were in equilibrium. Wind direction was determined only qualitatively. In general, however, the wind was almost always from the northwest.

The windspeed also has a direct effect on the volatilization coefficient through its effect on the gas-film coefficient. This effect is important for solutes with small Henry's constants such as acetone and TBA. Using equations 18, 17, and 15, it can be shown that increasing the windspeed from the day 30 value of 0.463 m/s to the day 4 value of 1.13 m/s increases the TBA volatilization coefficient about 13 percent. Similarly, increasing the windspeed from the day 30 value of 0.463 m/s to the maximum day 4 afternoon value of 1.72 m/s increases the TBA volatilization coefficient about 22 percent.

These calculations assume that the exposure of the model stream to the wind was similar to the exposure of the canal where the data were collected on which equation 18 was based. However, some error may be involved in this assumption. Comparison of the canal as shown in figures 6, 11, 12, 14, 17, 18, and 19 of Jobson and Sturrock (1979) with the model stream as shown in figures 5, 9, and 10 suggests the model stream may be much more exposed to the effect of wind than the canal because of the high banks on the canal. Greater exposure to the wind would result in greater dependence of the gas-film coefficient on windspeed than indicated by equation 18. Thus, the estimated increases in the TBA volatilization coefficient as a result of windspeed increases could be even larger than those presented previously. There has been relatively little work on gas-film coefficients for evaporation and volatilization in streams and rivers, and the effect of exposure to the wind cannot be determined quantitatively at the present time.

Another factor that could contribute to the large coefficients determined from the TBA data was the fact that the TBA injection was not continued long enough to establish a plateau concentration at cross section 220 (fig. 26). Consideration of data for other solutes discussed in the section on equilibrium of the stream system indicates the TBA concentrations should have been approaching equilibrium values. Also, the plateau concentration was estimated as accurately as possible by extrapolation as shown in figure 26. However, the tendency in extrapolating transient data of this type to equilibrium conditions generally will be to underestimate the plateau concentrations. Because cross section 220 is at the downstream end of the stream, the concentration for this cross section appears in the denominator of equation 25. Thus, underestimating this plateau concentration results in volatilization coefficients that are too large for reaches including this cross section.

The volatilization coefficients determined from the TBA concentrations (tables 18 and 19) are comparable to and, in some cases, larger than the coefficients determined from the acetone concentrations for the same time period. It was rationalized previously that TBA should be much more resistant to bacterial degradation in the model stream than acetone. Consequently, this result is consistent with the conclusion that no significant bacterial degradation of acetone occurred in the model stream during the experiment.

Rhodamine-WT Dye Results

Mean Water Velocities and Longitudinal-Dispersion Coefficients

Mean water velocities and longitudinal-dispersion coefficients were determined from the rhodamine-WT dye data. Dye concentrations at cross sections 59, 140, and 220 as a function of the elapsed time from the start of the dye injection are presented in figures 27 and 28 for the day 1 and day 2 injection and in figures 29 and 30 for the day 30 and day 31 injection. The data for the preliminary dye study were presented previously (fig. 11).

Data from the transient time period were used in the computations. Initial estimates of the mean velocities were calculated from the data using equation 27 as a basis. Initial estimates of the longitudinal-dispersion

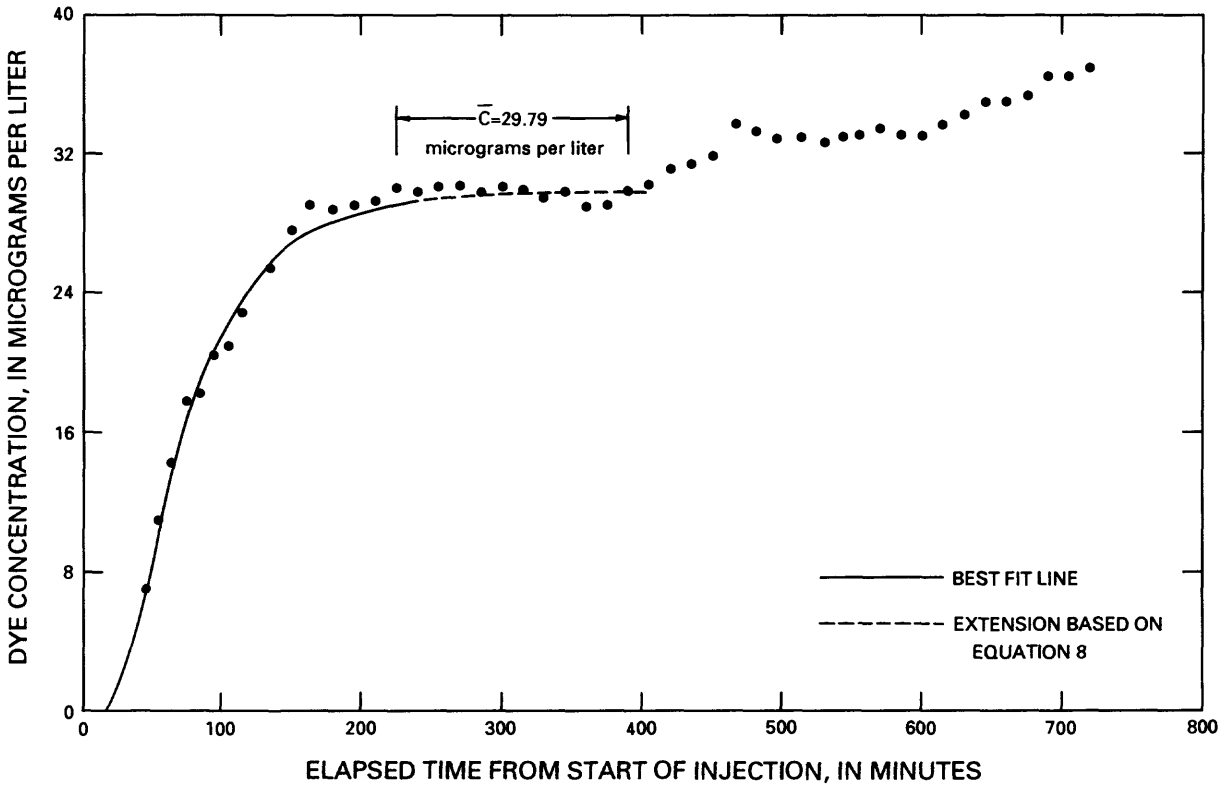

Figure 27.--Rhodamine-WT dye concentration at cross section 59 as a function of elapsed time from start of injection, day 1 dye study.

coefficients were calculated from equation 26 and the data using the procedure of Ogata (1970). These initial values then were used in equation 8, and they were adjusted to minimize the rms error difference between the experimental and calculated concentrations. The rms error was defined previously by equation 28.

The general procedure was to minimize the rms error first with respect to the dispersion coefficient, then to minimize the error with respect to the mean velocity, and finally to minimize again with respect to the dispersion coefficient. The dispersion coefficient and the rms error usually changed little during the third step. An example of this procedure is presented in figure 31 for the data from cross section 140, day 1. The initial estimates were 0.549 m/min for the mean velocity and 2.85 m^2/min for the dispersion coefficient. The first minimization step resulted in a dispersion coefficient of 2.66 m^2/min and an rms error of ±5.933 percent. The second step resulted in a mean velocity of 0.528 m/min and an rms error of ±2.848 percent. The third step resulted in a dispersion coefficient of 2.64 m^2/min and an rms error of ±2.846 percent. The rms error was much more sensitive to changes in the mean velocity than to changes in the dispersion coefficient. Such sensitivity to the mean velocity has been noted previously (Zand and others, 1976).

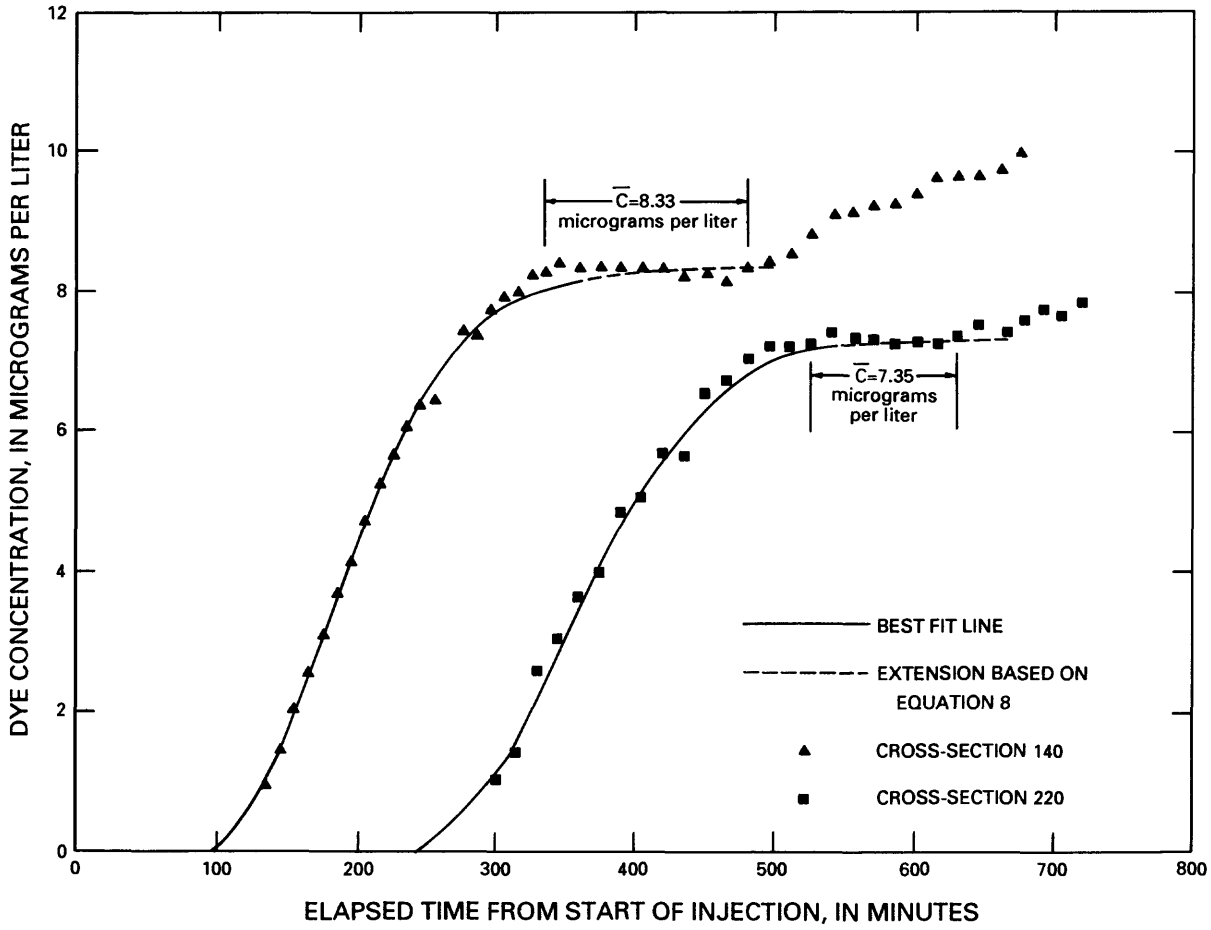

Figure 28.--Rhodamine-WT dye concentration at cross sections 140 and 220 as a function of elapsed time from start of injection, day 1 dye study.

The initial estimates of the mean velocity and the longitudinal-dispersion coefficient for this example were good approximations of the final best-fit values, with the mean velocity differing by about 4 percent and the longitudinal-dispersion coefficient differing by about 8 percent. Best-fit values of the mean velocities for the other data sets were all within 6 percent of the initial estimates, with the exception of the value for cross section 59 on day 1, where the best-fit value was 20.5 percent less than the initial estimate. In all cases, the best-fit velocity values were less than the initial estimates. Differences between the best-fit values and the estimates of the dispersion coefficient were considerably larger, ranging from -58.9 percent to +43.0 percent with a mean absolute value of 26.8 percent. The relative insensitivity of the rms error of the fitting process to the dispersion coefficient (fig. 31) probably contributed to these large differences.

Mean water velocities and longitudinal-dispersion coefficients determined by this procedure are presented in table 20. Values from the preliminary dye study are included for comparison. Also included are the rms errors of fitting defined by equation 28.

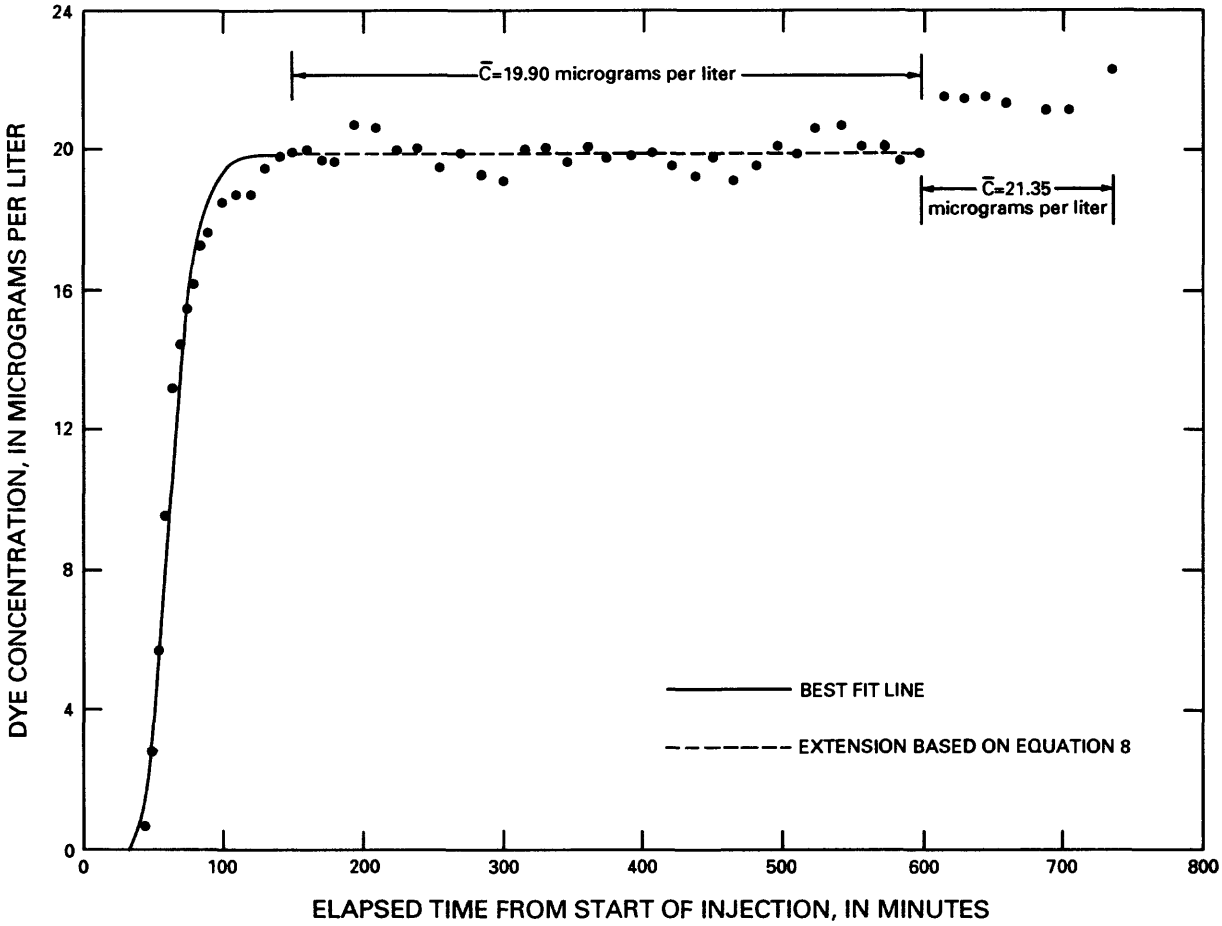

Figure 29.--Rhodamine-WT dye concentration at cross section 59 as a function of elapsed time from start of injection, day 30 dye study.

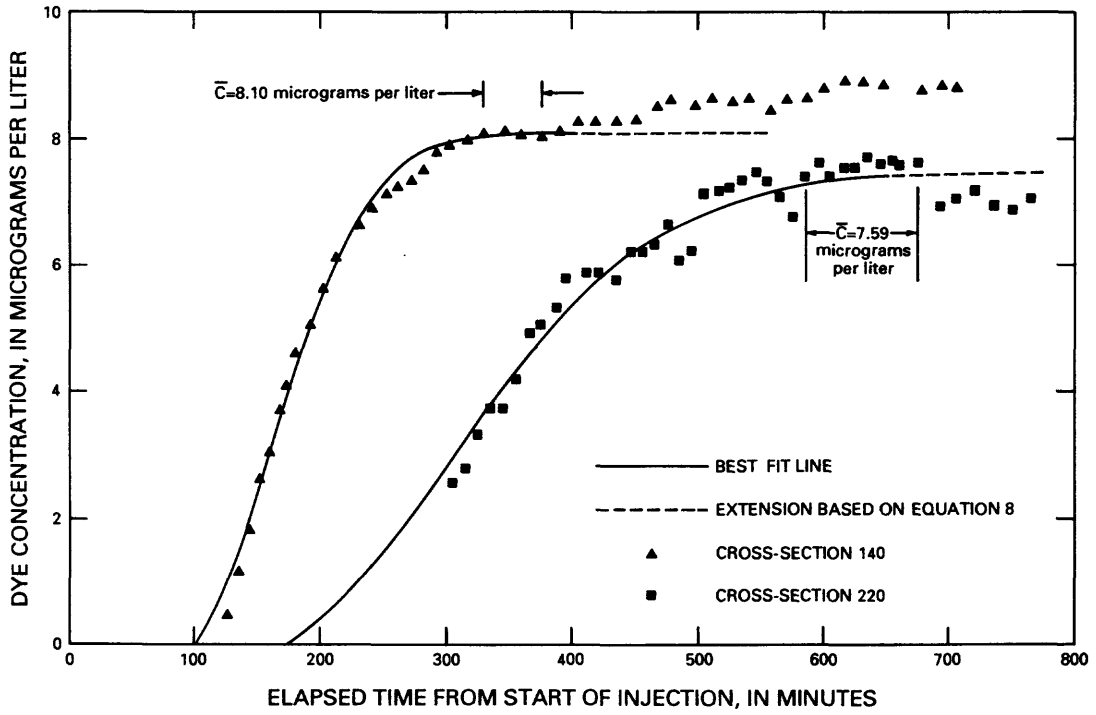

Figure 30.--Rhodamine-WT dye concentration at cross sections 140 and 220 as a function of elapsed time from start of injection, day 30 dye study.

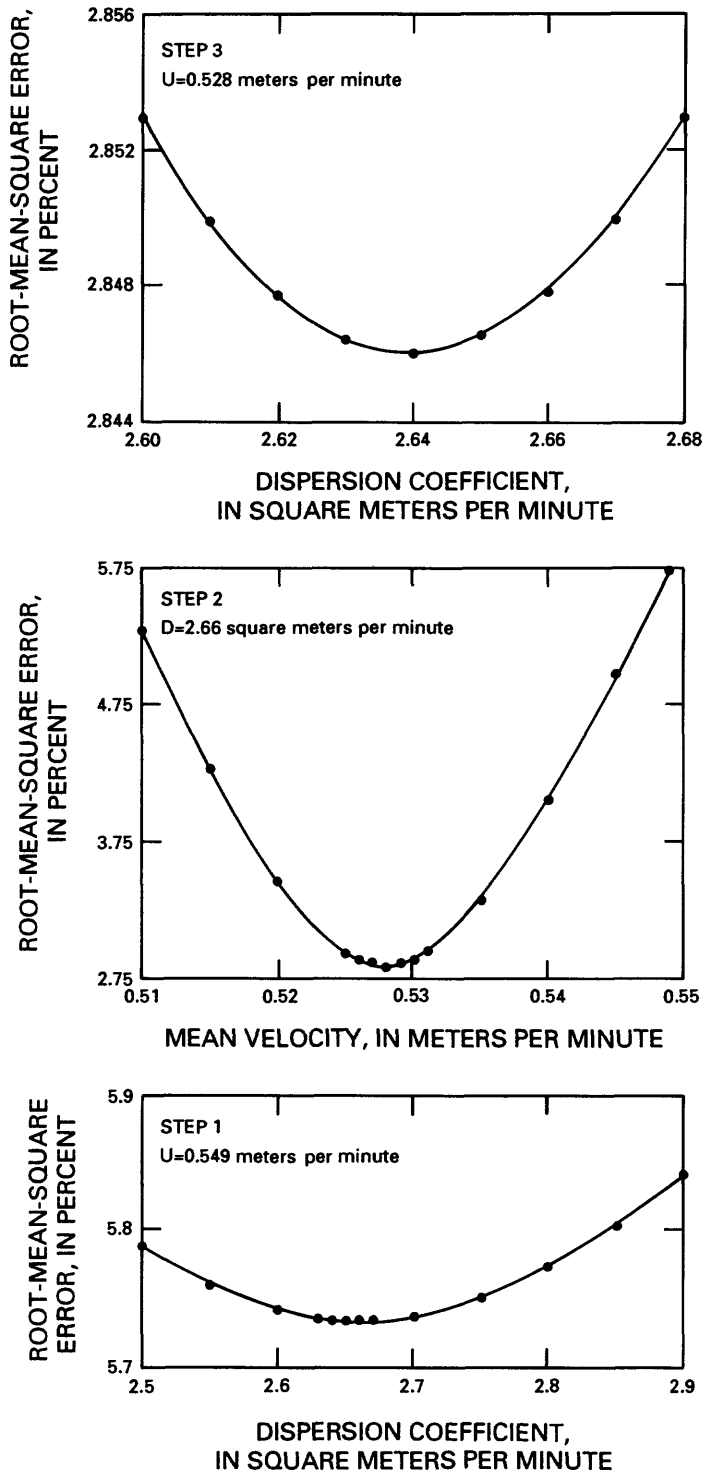

Figure 31.--Stepwise variation of the root-mean-square error with dispersion coefficient and mean velocity for rhodamine-WT dye data from cross section 140, day 1.

Table 20.--*Mean water velocities and longitudinal-dispersion coefficients determined from the rhodamine-WT data, and the root-mean-square errors of the data fit*

[Inj, injection point]

Day of experiment	Reach (meters)	Mean velocity (meter per minute)	Dispersion coefficient (square meters per minute)	Root-mean-square error (percent)
Preliminary dye study	Inj-59	0.480	0.304	±4.23
	Inj-140	.574	2.63	±3.74
	Inj-220	.510	4.62	±8.01
Day 1	Inj-59	.317	1.66	±3.75
	Inj-140	.528	2.64	±2.84
	Inj-220	.505	1.70	±4.09
Day 30	Inj-59	.410	.300	±5.48
	Inj-140	.588	2.41	±3.00
	Inj-220	.531	5.35	±4.88

The mean velocities for the three days are in reasonable agreement, with the exception of the value for cross section 59 on day 1. Comparison of the three concentration-versus-time curves for this cross section indicates a distinct difference on day 1 (fig. 27) when the concentration increased gradually. Conversely, on day 30 and during the preliminary dye study, the concentration increased rapidly with time (figs. 29 and 11) at cross section 59. The more gradual increase on day 1 also is reflected in the much larger dispersion coefficient relative to the values for the other 2 days.

The dispersion coefficients increased with distance downstream for the preliminary dye study and for the day 30 data. Such an increase is consistent with the change in the physical characteristics with distance downstream in the model stream (figs. 5, 9, and 10). Also, the dispersion coefficients were reasonably similar for the same reaches. On day 1, the dispersion coefficient for cross section 59 was much larger than expected, as just discussed. The dispersion coefficient for cross section 140 was very similar to the other two values for this cross section. The value for cross section 220, however, was considerably smaller than the other two values for this cross section. This is reflected in the relatively smooth increase in the dye concentration with time on day 1 at cross section 220 (fig. 28) compared with the scatter observed at this cross section on the other 2 days (figs. 11 and 30).

A possible explanation for the small dispersion coefficient on day 1 is that the model stream was cleaned extensively 10 days prior to the start of the acetone-injection experiment. As discussed previously, a major problem was control of the profuse growth of rooted macrophytes, particularly at the downstream end of the stream (fig. 10). Reduction of the numbers of these plants could reduce dispersion, resulting in a concentration that increased smoothly with time as was observed.

A possible explanation for the small velocity at cross section 59 on day 1 is reduced flow on the experimental side of the partition because of a change in the division of the flow by the partition. This is supported by the fact that the ratio of the plateau concentrations at cross sections 140 and 59 (figs. 27 and 28) suggests a flow division factor of 0.280. Conversely, the ratio for the day 30 plateau concentrations (figs. 29 and 30) is 0.446 which is more in agreement with the value of about 0.5 determined in the preliminary dye study. The flow division problem was discussed previously in detail.

The rms errors of fitting in table 20 were smallest for cross section 140, somewhat larger for cross section 59, and largest for cross section 220. This result is consistent with the smoothness of the concentration-versus-time curves presented in figures 11, 27, 28, 29, and 30; that is, the smoother the variation of the concentration with time, the easier it is to fit the curve. The smoothness of the concentration-versus-time curves is in turn a function of the physical characteristics of the stream at the cross section. At cross section 140, the stream was relatively free of weeds (fig. 9) and the depth was shallow (fig. 7). At cross section 220, the weeds were profuse (fig. 10) and the depth was deep (fig. 8). Cross section 59 was relatively close to the injection point; consequently, the concentration increased rapidly with time (figs. 11, 27, and 29). Fitting such rapid changes in concentration is subject to greater error than fitting gradual changes in concentration. This is supported by the fact that the rms errors for cross section 59 for day 30 and for the preliminary dye study were larger than the error for day 1 when the concentration increased more slowly.

The predicted concentration-versus-time curves for day 1 and day 30 are presented in figures 27 through 30. The predicted curves for the preliminary dye study are not presented; however, they were similar to those for day 1 and day 30 as evidenced by the similarity in rms errors in table 20. The solid lines in figures 27 through 30 indicate the part of the data set over which the fitting process was conducted. Fitting was limited to these points because the mean velocity and the longitudinal-dispersion coefficient have the greatest influence on the concentration in this transient period. The overall fit probably would have been improved by including all the plateau concentrations. However, an overall best-fit was not the objective of the fitting process; rather, it was to determine the mean velocity and the longitudinal-dispersion coefficient. The dashed lines in figures 27 through and 30 are extensions of equation 8 with the best-fit parameters.

The fitting process based on equation 8 resulted in excellent predictions of the concentration-versus-time relations for the transient time periods (figs. 27 through 30). The fitting process also gave reasonable predictions of the initial plateau concentrations. However, the day 1 concentration-versus-time distributions all indicate increasing concentrations during the latter stages of the observation period, the day 30 distribution at cross section 59 indicates an abrupt increase in concentration near the end of the observation period, and the day 30 distribution at cross section 140 indicates a series of apparent plateau concentrations. These perturbations will be discussed in the next section.

Finally, the observed equilibrium plateau concentrations indicated as $\bar{C}$ in figures 27 through 30 were used as C_0 in equation 8 in the fitting process. This procedure effectively corrects for the fact that rhodamine-WT dye is not completely conservative. It is generally recognized that the dye degrades photochemically (Tai and Rathbun, 1988) and sorbs to sediments (Scott and others, 1969). The extent of such losses depends on the sunlight conditions prevailing at the time of the study and the characteristics of the sediment in the stream. Dye loss in the model stream study will be discussed in more detail in the next section.

Other Results From the Dye Studies

The bottom of the model stream was filled with a floc of organic detritus (figs. 6, 7, and 8). Also, the areas along the banks, particularly at the downstream end, contained profuse growths of a rooted macrophyte (fig. 10). Such characteristics create dead zones which are volumes into which movement of solutes is by processes much slower than the convective transport process in the main channel of the stream.

Continuous injection of a solute into a stream with dead zones is characterized by a concentration that increases to an apparent plateau concentration, then increases again to another plateau concentration, and then perhaps a third plateau concentration or more until the solute is in equilibrium with all parts of the stream system. Examples of such behavior have been presented (Bencala and others, 1984). The first plateau concentration generally is considered to indicate equilibrium of the solute with dispersive processes in the main channel of the stream, with subsequent plateau concentrations indicating equilibrium with various parts of the dead zone structure of the stream.

Some of the dye concentration-versus-time curves appear to exhibit the multiple plateaus characteristic of dead zones. This is most evident in the curves for cross section 140 on day 30 (fig. 30) and for the preliminary dye study (fig. 11). The cross section 220 data (figs. 11, 28, and 30), where dead zones would most likely be expected, do not exhibit multiple plateaus, although interpretation is complicated by the scatter in the concentration-versus-time data. Perhaps this scatter itself is indicative of dead zone effects.

Transport models taking dead zones into account have been developed (Bencala and Walters, 1983). These models generally require the cross-sectional area for transport into the dead zone and an exchange coefficient. Because these parameters cannot be calculated from fundamentals, they must be determined by fitting of experimental data. Thus, in the present study, the fit of the experimental data probably would be improved because of the two additional fitting parameters.

However, dead zone effects were not considered in the fitting of the data in the present study for several reasons. First, the effect was not observed consistently at all times at a specific cross section, nor was it observed at all cross sections. Second, the effect observed at cross section 140 on the 2 days was relatively small as indicated by the small differences between

the apparent plateau concentrations. This contrasts with the much larger differences observed in mountain streams (Bencala and Walters, 1983; Bencala and others, 1984) which necessitated consideration of dead zones to permit adequate fitting of the experimental data. Figures 27 through 30 indicate that the dye data of this study can be adequately fitted by equation 8 without considering the effect of dead zones. Finally, the times of most importance in determining the fate of acetone in the model stream were the transient period and after equilibrium had been established. Dead zones have the greatest effect near the end of the transient period and before equilibrium is established. The dye data presented in figure 11 and figures 27 through 30 indicate that this time period was relatively short in the present study.

Dye concentrations are presented in figures 27 through 30 only to elapsed times of less than 800 min. The dye injections were continued, however, for total times of 2,162 min for the dye injection begun on day 1 and 1,420 min for the injection begun on day 30 (table 8). These data will not be presented or discussed extensively because they are not pertinent to the study of the fate of acetone in the model stream. One use of these data, which will be discussed, was the computation of the percentage recovery of the dye on day 2 and on day 31.

It is necessary, however, to consider the increasing concentrations observed during the latter part of the day 1 data (figs. 27 and 28) and the marked increase in concentration at cross section 59 at the end of the day 30 data (fig. 29). The constancy of the plateau concentrations in the model stream depend, as discussed previously, on the constancies of the concentration of the solution injected, the injection rate, and the water discharge. A single dye solution prepared at one time was injected for each study; thus, the concentration of solution injected should have been constant. The water discharge was approximately constant, although changes in the division of the flow by the partition could have affected the concentrations.

Consider first the day 1 dye injection. The solution injection rate is presented in figure 32 as a function of elapsed time from the start of the injection. The injection rate was constant between 0 min and 330 min with a mean of 8.0 mL/min and a coefficient of variation of ±0.56 percent. Between 330 min and 360 min, however, the rate increased about 4 percent and then continued to increase gradually with time during the rest of the observation period.

If the increase in rate occurred at 360 min, then the times at which the concentrations might be expected to increase at cross sections 59, 140, and 220 can be estimated by adding 360 min to the traveltimes of the leading edge times of the dye mass to the respective cross sections. Traveltimes estimated from the times of the leading edges of the dye mass (figs. 27 and 28) are about 20 min for cross section 59, 100 min for cross section 140, and 250 min for cross section 220. The corresponding times at which the concentrations should begin to increase are 380 min at cross section 59, 460 min at cross section 140, and 610 min at cross section 220. These times agree reasonably well with the actual times indicated in figures 27 and 28.

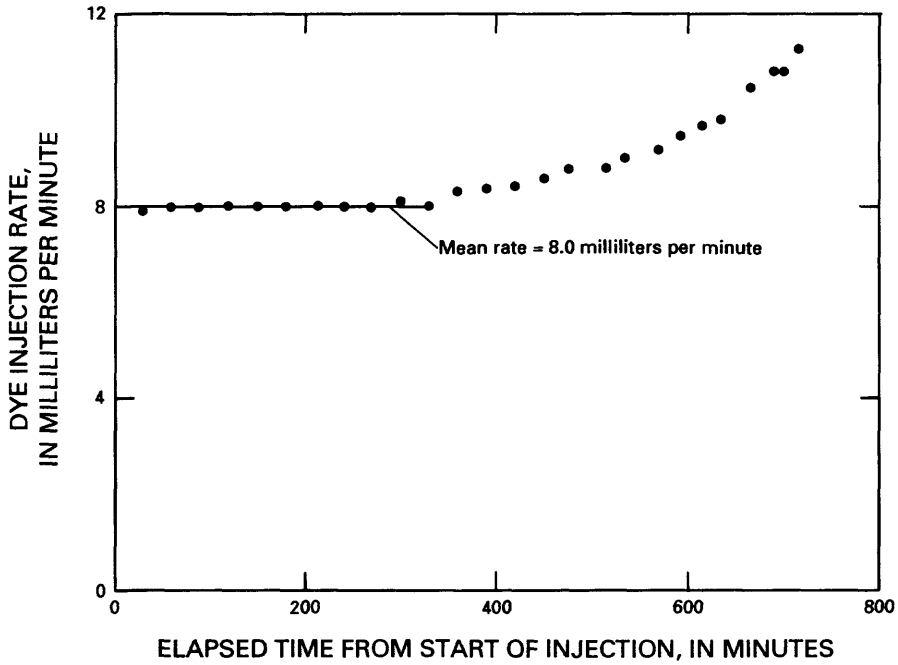

Figure 32.--Injection rate of the rhodamine-WT dye solution as a function of elapsed time from start of injection, day 1 dye study.

The dye solution injection rate for day 30 is presented in figure 33 as a function of the elapsed time from the beginning of the injection. These injection rates were determined from changes in the level of the solution in the supply vessel, whereas the rates for day 1 presented in figure 32 essentially were instantaneous rates determined with a graduated cylinder. The injection rate was reasonably constant at 8.8 mL/min with a coefficient of variation of ±1.99 percent for the first 567 min of the injection. At 567 min, the rate covering the time period from 567 min to 628 min increased about 4 percent and the rate continued to increase gradually thereafter. The increase in concentration at cross section 59 occurred between 600 min and 615 min. Because the traveltime of the leading edge of the dye mass to cross section 59 on day 30 was about 35 min (fig. 29), there is a reasonable agreement between the times. Also, the ratio of the two injection rates (9.5/8.8=1.08) is in agreement with the ratio of the plateau concentrations (21.35/19.90=1.07). These results indicate the increase in the plateau concentration at cross section 59 was a result of an increase in the dye solution injection rate.

The explanation for the increasing dye rates in both the day 1 and day 30 injections was not determined. Apparently, the speed control device on the metering pump malfunctioned after a period of use, allowing the pump to run at a higher speed.

Percentage recoveries of the dye were computed from the observed plateau concentrations and equation 31. Recoveries also were computed from equation 32 and the areas under the complete dye concentration-versus-time curves for

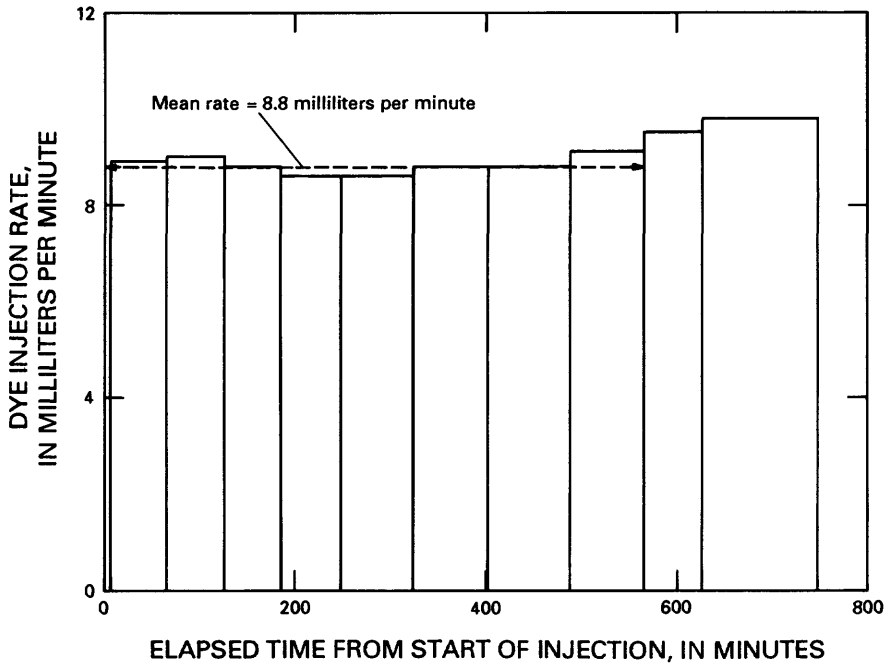

Figure 33.--Injection rate of the rhodamine-WT dye solution as a function of elapsed time form start of injection, day 30 dye study.

days 30 and 31. Results are presented in table 21. The concentration of the dye solution injected used in equation 31 was determined from samples of the solution collected at the beginning and end of each injection. The dye injection rate and water discharge were determined as discussed previously.

The dye recoveries indicated losses of about 8 percent to 10 percent. One value larger than 100 percent was obtained for cross section 59 on day 2. Values larger than 100 percent are physically impossible; thus, some error must have occurred. The flow division factor changed considerably on day 2 (table 9). Because this factor must be used to determine the water discharge on the experimental side of the partition, any error in this factor contributes to errors in the dye recovery factor computation. The recovery factor for this cross section was 100 percent on day 1, which is physically possible but probably not realistic. This again suggests some problem with the flow division factor.

The recoveries are reasonably consistent, with the exception of these two values for cross section 59 and the day 1 and day 30 values for cross section 220. The values for this cross section on the next days (day 2 and day 31) increased considerably, suggesting the stream at cross section 220 was not in equilibrium on day 1 and on day 30. In the preliminary dye study, the dye concentration at cross section 220 had not plateaued (fig. 11), but it was near the concentration at cross section 140. This indicates a recovery virtually the same as that observed at cross section 140. These differences indicate that the model stream required longer to achieve equilibrium in the day 1 and day 30 injections than in the preliminary dye study. Similar results were observed in the TBA injection discussed previously. Finally,

Table 21.--*Percentage recoveries of rhodamine-WT dye in the three dye studies*

[eq., equation; --, no data]

Day of experiment	Cross section (meters)	Dye recovery (percent)
Preliminary dye study	59	95.5
	140	93.5
	220	--
Day 1	59	100
	140	87.8
	220	76.4
Day 2	59	110
	140	90.5
	220	87.9
Day 30	59	90.2 (eq. 31)
	140	95.9 (eq. 31)
	220	81.1 (eq. 31)
Day 31	59	94.2 (eq. 31)
	140	91.4 (eq. 31)
	220	90.4 (eq. 31)
Days 30 and 31	59	92.6 (eq. 32)
	140	92.9 (eq. 32)
	220	89.9 (eq. 32)

the recoveries computed using equation 32 and the areas under the complete concentration-versus-time curves for days 30 and 31 are in good agreement with those computed using the plateau concentrations on day 31. This agreement indicates the dye observed plateau concentrations on day 31 were approximately equilibrium concentrations and, consequently, it was concluded that the model stream was in equilibrium on day 31.

Glucose and Diel Oxygen Study Results

Glucose

Results of five synoptic sampling surveys for glucose injected on day 17 are presented in figure 34. The glucose concentration decreased with distance downstream for four of the surveys, as would be expected if bacterial degradation were occuring. The concentrations for the other survey were approximately constant with distance downstream. Samples were collected for two other synpotic surveys. However, these results are not reported because the sample tines were too soon after increases in the concentration of the glucose injection solution. Consequently, the stream had not had sufficient time to establish equilibrium conditions after the change.

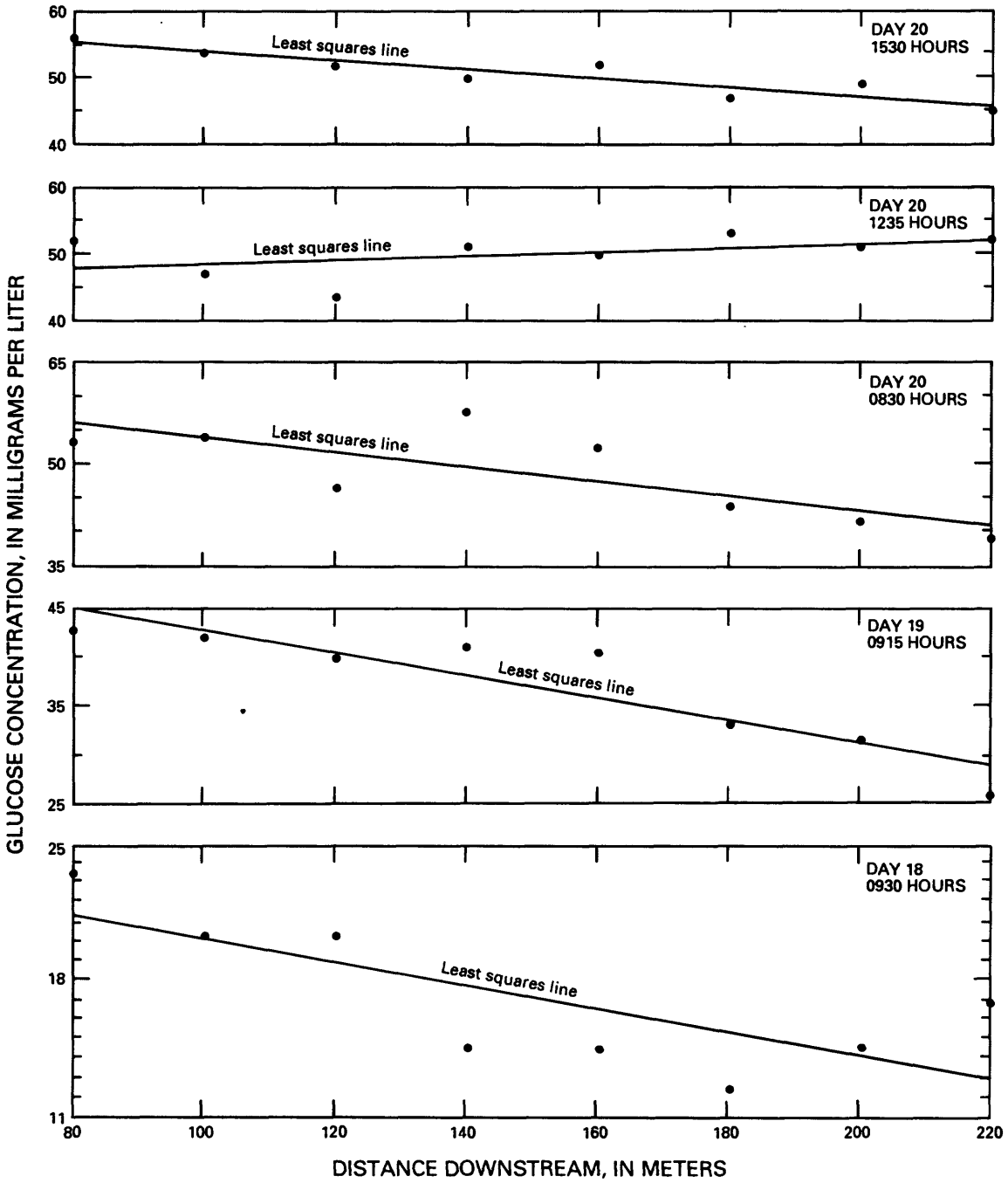

Figure 34.--Glucose concentration on a logarithmic scale as a function of distance downstream for five synoptic sampling surveys.

Least-squares regressions of the logarithm of the glucose concentration as a function of the cross-sectional distance were completed, and the slopes are given in table 22. Also given in table 22 are the root-mean-square errors of fit of the form of equation 28 and the time period since the last change in the concentration of the glucose injection solution.

Table 22.--*Results of the least-squares analysis of the glucose concentrations from the synoptic sampling surveys*

Day of experiment	Sample time (hours)	Slope × 10^4 (meters^{-1})	Error (percent)	Time period (hours)
18	0930	-34.8	±13.5	18.5
19	0915	-34.9	±7.43	22.8
20	0830	-21.9	±9.26	20.6
20	1235	+6.1	±5.02	24.7
20	1530	-14.0	±2.76	27.6

Slopes of the least-squares regressions for the four surveys indicating the expected decrease in concentration with distance downstream were significantly different from zero at the 5-percent level. The slope of the other survey was positive, but not significantly different from zero. The four slopes were in reasonable agreement with each other. The rms errors ranged from ±2.76 percent to ±13.5 percent and reflect the general scatter of the experimental points about the best-fit lines (fig. 34). The explanation for the anomalous behavior of the 1235-hours synoptic on day 20 is unknown. The flow division factor determined from this synoptic is in reasonable agreement with the ones before and after this sample time (table 9).

As discussed previously in the analysis of the daily acetone concentration data, it was concluded that a time period of somewhat less than 2 days was necessary to establish true equilibrium conditions in the model stream. Because the time periods in table 22 are less than this value, it is expected that the glucose concentrations may not have been completely in equilibrium with the stream system.

Diel Oxygen Study

Results of the diel oxygen study on days 11 and 12 are presented in terms of the percentage saturations of dissolved-oxygen concentration. These percentage saturations at cross sections 59, 140, and 220 are presented in figure 35 as a function of clock time. Similar diel variations in the pH values and the inorganic carbon concentrations were observed. As an example, the pH at cross section 220 increased from 7.96 at 0602 hours to 10.78 at 1710 hours as the inorganic carbon concentration decreased from 50.3 mg/L at 0602 hours to 18.0 mg/L at 1710 hours. These pronounced variations in the percentage saturation of dissolved oxygen, pH, and inorganic carbon concentration are indicative of the biological activity in the model stream.

Net daytime productivities and nighttime respiration rates were computed from the diel study results using the single station method (Stephens and Jennings, 1976). These values are generally reported on an areal or a volumetric basis. However, because the water discharges on the two sides of the partition were generally not equal, the results are presented in terms of the mass of oxygen, which corrects for the differences in discharge. The flow division factor from day 10 (0.289 from table 9) was used for this purpose. Results are given in table 23.

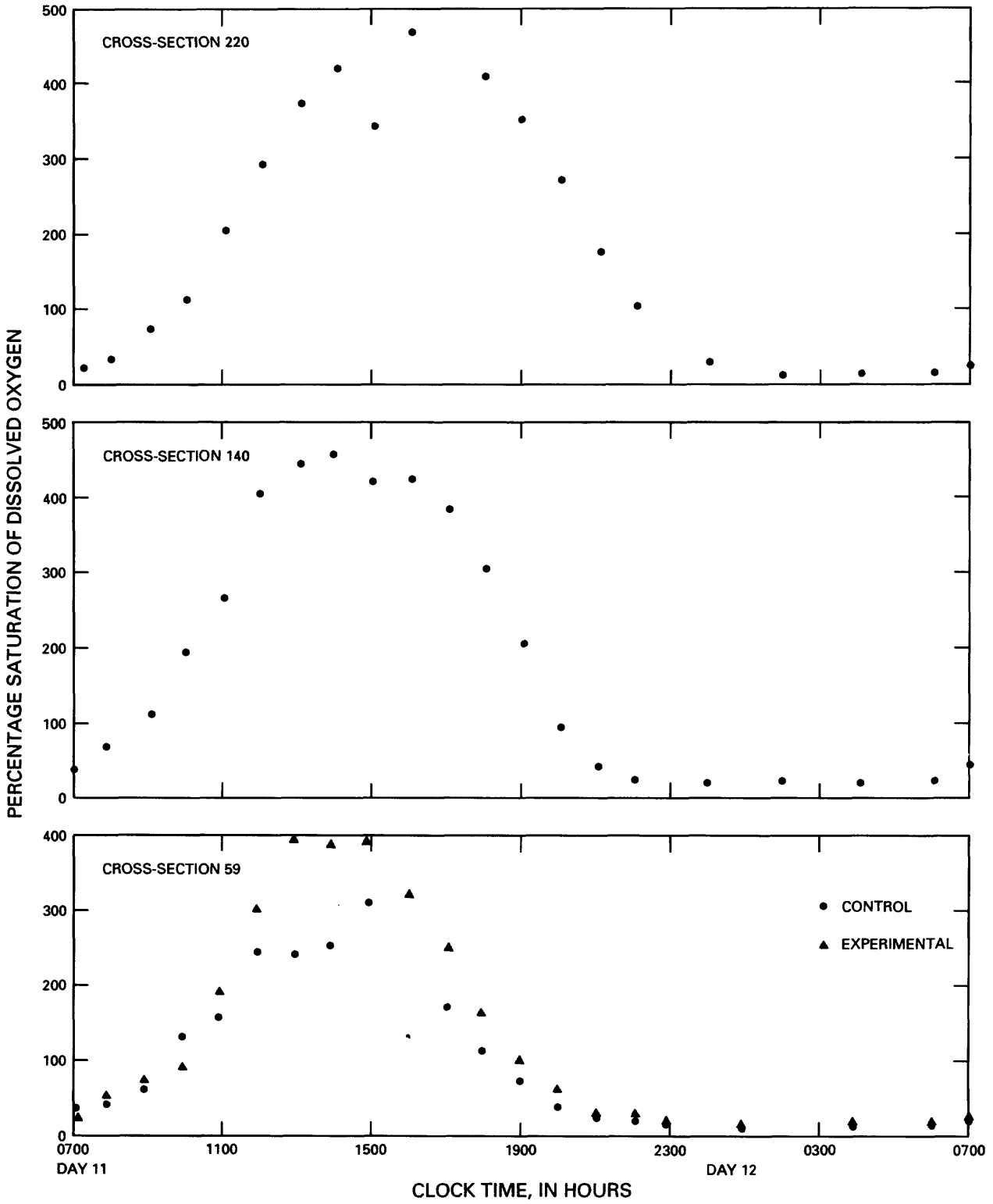

Figure 35.--Percentage saturation of dissolved oxygen as a function of clock time in the diel oxygen study at cross sections 59, 140, and 220.

Table 23.--*Results of the diel oxygen study on days 11 and 12*

[exp, experimental side of the partition; cont, control side of the partition]

Cross section (meters)	Net daytime productivity (grams oxygen)	Nighttime respiration (grams oxygen)	Ratio, productivity/ respiration
59 exp	413	-307	1.35
59 cont	475	-658	.72
140	2,780	-1,680	1.65
220	3,720	-2,480	1.50

The net daytime productivities on the experimental and control sides of the partition at cross section 59 were comparable, indicating about the same amounts of photosynthesizing biomass. The nighttime respiration of the control side, however, was more than twice that on the experimental side, probably indicating a large amount of nonphotosynthesizing biomass. As a result, the productivity/respiration ratio for the control side was less than 1.0. However, the ratios for the experimental side and for cross sections 140 and 220 were greater than 1.0, indicating biological activity in the model stream.

Modeling the Acetone Concentration-Versus-Time Distributions

The acetone concentration-versus-time distributions during the transient period on day 2 were modeled using a modified form of equation 6. This modification corrected for the fact that the acetone injection rate was not constant, but decreased with time during the daylight hours. Following Marino (1974), it can be shown for an exponentially decreasing acetone injection rate that:

$$C(x,t) = C_0^0 \, exp(-\gamma t) f'(x,t) \text{ for } 0<t\leq\tau \qquad (41)$$

where C_0^0 = the concentration of acetone in the water at the injection point at time zero, in milligrams per liter;

γ = the rate coefficient, in minutes^{-1}, describing the exponential decrease of the injection rate with time; and

$f'(x,t)$ = $f(x,t)$ as given by equation 8 except that ΣK_i-γ has been substituted for ΣK_i.

The mean velocities and longitudinal-dispersion coefficients were determined from the day 1 dye data (table 20). Volatilization coefficients were taken as the means of the day 4 values (table 19). The day 4 values were used rather than overall averages because the mean daytime windspeed on day 4 (1.31 m/s) was comparable to that on day 2 (1.06 m/s). The volatilization

coefficients at 25.0 °C were adjusted to the mean Lagrangian water temperature corresponding to each experimental concentration using equation 20. These temperatures were determined using the lagging procedure described previously.

The γ value of 0.000288 min^{-1} for day 2 (table 10) was used. The concentration of acetone in the water at the injection point at time zero was computed from the γ value, the mean day 2 daytime injection rate determined from volume changes in the calibrated supply reservoir, and the mean day 2 inlet water discharge. The mean of the three morning flow division factors (table 9) was used for computations involving cross section 59.

Predicted acetone concentrations as a function of elapsed time from the start of the injection are presented in figure 36 for cross section 59, figure 37 for cross section 140, and figure 38 for cross section 220. Also presented in these figures are the experimental concentrations. Errors of the form of equation 28 were ±9.74 percent for cross section 59, ±14.6 percent for cross section 140, and ±39.5 percent for cross section 220.

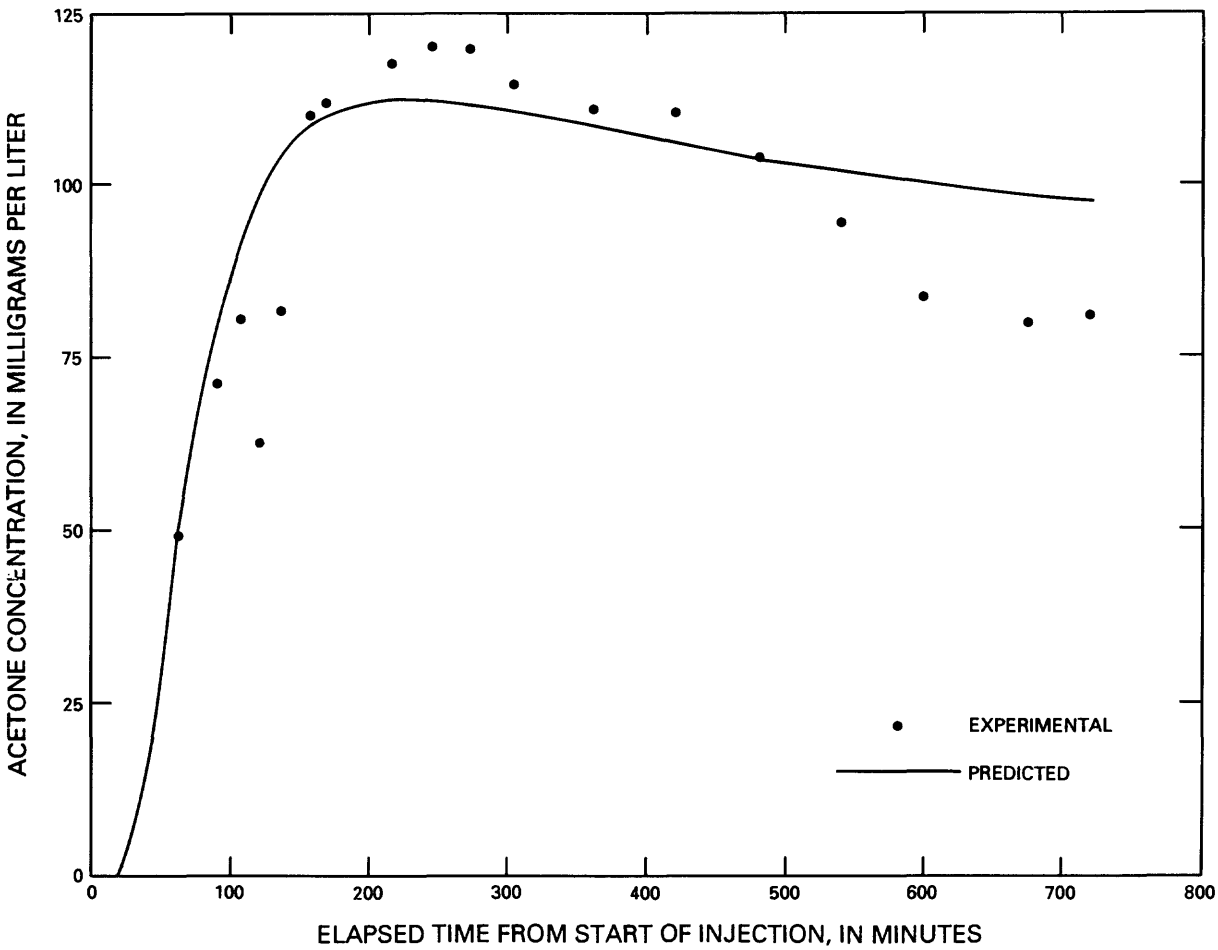

Figure 36.--Predicted and experimental concentrations of acetone at cross section 59 as a function of elapsed time from start of injection, day 2.

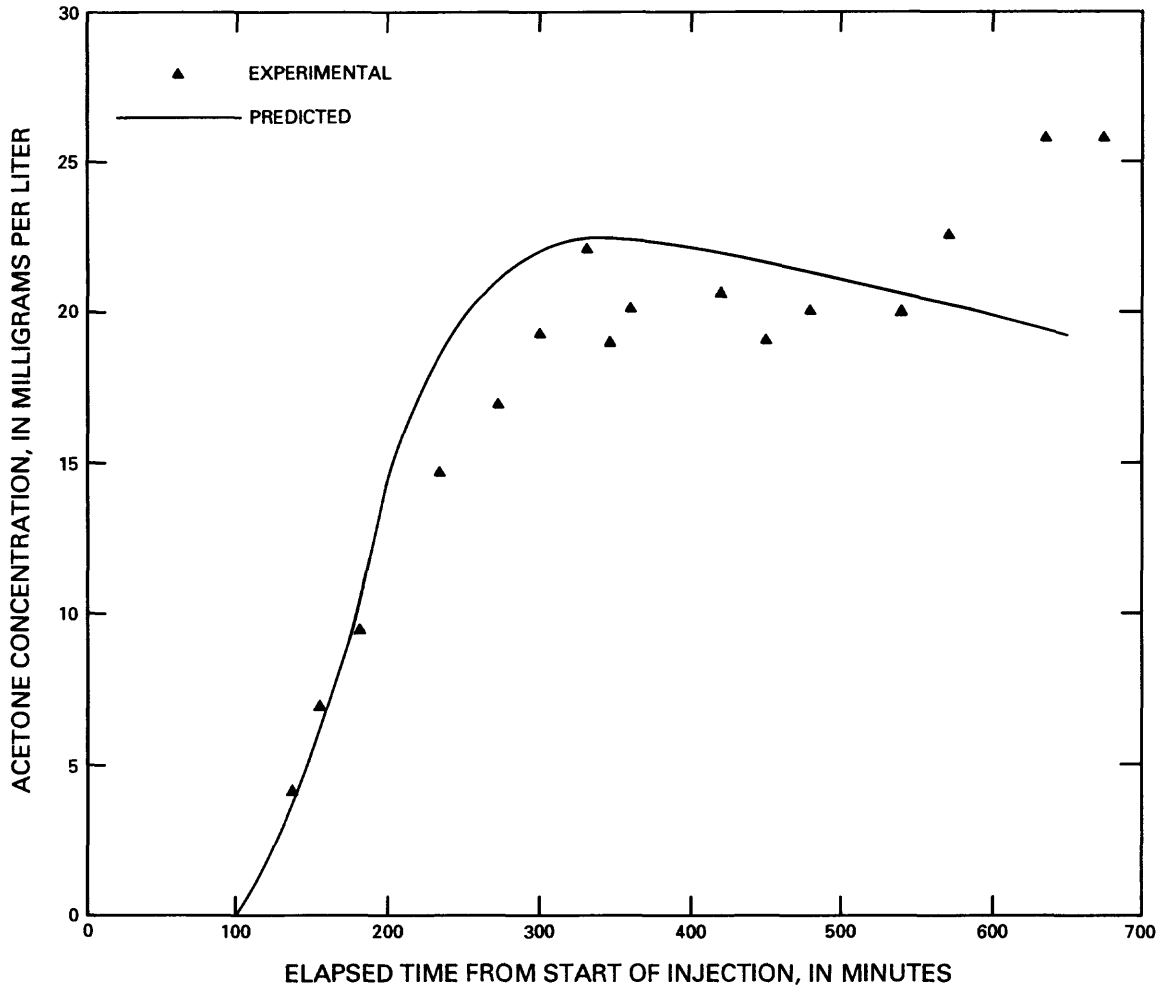

Figure 37.--Predicted and experimental concentrations of acetone at cross section 140 as a function of elapsed time from start of injection, day 2.

A reasonably good fit of the experimental data was obtained for cross section 59 (fig. 36). The experimental concentrations during the latter part of the observation period decreased faster than predicted. This difference probably is because the flow division factor (table 9) on the afternoon of day 2 increased considerably, indicating increasing flow on the experimental side of the partition. This increasing flow would result in decreasing concentrations as indicated in figure 36. An attempt was made to incorporate a variable flow division factor into the modeling. However, the fit was not improved much, because the scatter in the flow division factor precluded determining its exact dependence on time.

The fits of the experimental data for cross sections 140 and 220 are not as good as for cross section 59. The predicted concentrations at each cross section increase faster with time than the experimental points. Also, the predicted plateau concentrations generally are larger than the apparent plateau concentrations of the experimental values. Such behavior is as would

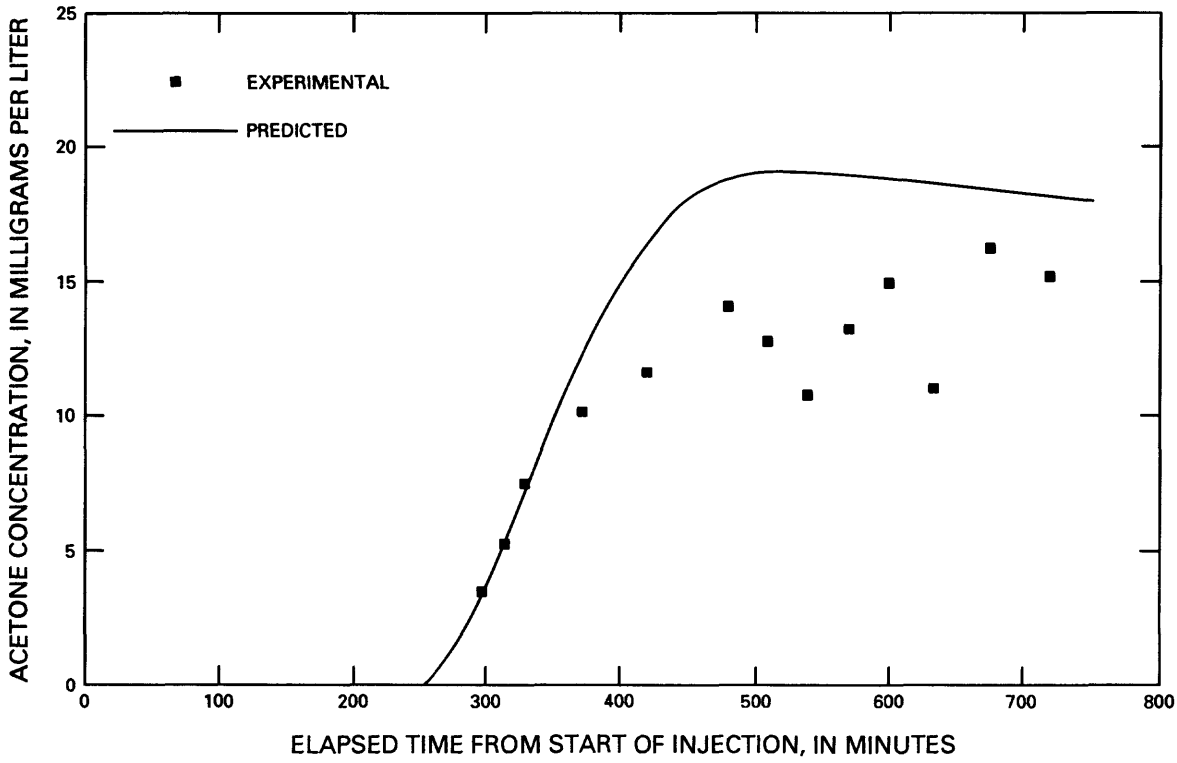

Figure 38.--Predicted and experimental concentrations of acetone at cross section 220 as a function of elapsed time from start of injection, day 2.

be expected if the dead zones in the model stream were retarding the establishment of the plateau concentrations. Also, the differences between the predicted and experimental concentrations are greater at cross section 220 than at cross section 140. This is consistent with the previous suggestion that dead zone effects are more important at cross section 220. Finally, as discussed previously, it is expected that time periods longer than the approximately 700-min periods indicated in figures 37 and 38 will be necessary for establishing equilibrium conditions in the model stream.

The predicted concentrations in figures 36, 37, and 38 were obtained completely independently of the acetone concentrations data for day 2. Consequently, it is concluded that equation 8 provides a reasonable fit to the experimental concentration-versus-time data during the transient time period.

DISCUSSION OF THE ACETONE TRANSPORT AND FATE STUDY

Lack of Acetone Bacterial Degradation

It was concluded on the basis of the analysis of the daily acetone concentration data for days 10 through 34 that significant bacterial degradation

of acetone did not occur in the model stream. This behavior was contrary to expectations based on the literature (Abrams and others, 1975; Thom and Agg, 1975; Helfgott and others, 1977), our own laboratory studies (Rathbun and others, 1982), and the rich biological composition of the model stream, all of which indicated that bacterial degradation of acetone should have occurred eventually during the course of the experiment. There are several possible explanations for the lack of active bacterial degradation of the acetone, the most likely being lack of acclimation of the bacteria in the model stream to acetone. Another possible explanation was the limited residence time in the stream system.

Acclimation

Various mechanisms have been suggested (Wiggins and others, 1987) as an explanation for the acclimation period. This period is the length of time between the addition of the compound to the stream and the initiation of degradation. Of the mechanisms proposed, the ones most likely to be important in the model stream include the time necessary for the enzymes to be induced or for the mutation or genetic exchange of enzymes to occur, the time for small bacterial populations to grow and to become large enough to cause a measurable degradation of the compound, nutrient limitations, and the preferential use of other organic compounds in the system.

Induction time period

Acetone was injected into the model stream continuously for 32 days (table 8). Literature cited previously as well as our own laboratory studies (Rathbun and others, 1982) all concluded that acetone was readily degraded by bacteria, indicating that acclimation to acetone of the bacteria in the model stream should occur readily. This indicates the 32-day period should have been adequate for acclimation. Consequently, it was concluded that the induction time period was not the explanation for the failure of the acetone to be metabolized in the model stream.

Growth time period

The 32-day injection of acetone also should have permitted sufficient time for small bacterial populations to grow to a size large enough to cause measurable degradation of acetone in the model stream. This assumes other factors were suitable for growth. One factor of primary importance is the availability of sufficient nutrients which will be discussed in the next section.

Another consideration is the relative importance of free-floating bacteria and bacteria attached to surfaces in the stream system. Significant numbers of bacteria could be produced during the growth process. However, if these bacteria are free floating, then they likely would be flushed from the system before significant degradation of the acetone could occur because of the limited residence time in the model stream. This subject will be discussed in more detail later.

Nutrient limitations

Results of monitoring the nutrient concentrations in the model stream prior to the acetone-injection experiment were presented previously (tables 2, 3, and 4). Nutrient concentrations also were determined twice during the acetone-injection experiment, and the results, together with water temperatures, are presented in table 24. Day 5 was 4 days after the initiation of the acetone injection and day 20 was the last day of the glucose injection (table 8).

Table 24.--*Nutrient concentrations and water temperatures for day 5 and day 20*

[exp, experimental side of partition; cont, control side of partition; µg/L, micrograms per liter; °C, degrees Celsius]

Day of experiment	Sampling time (hours)	Cross section (meters)	Orthophosphate (µg/L)	Nitrate-nitrogen (µg/L)	Nitrite-nitrogen (µg/L)	Water temperature (°C)
5	0930	0	281	2.9	1.7	26.8
		59 exp	249	53.0	7.1	25.4
		59 cont	259	126	7.6	26.2
		140	226	12.0	4.4	25.1
		220	238	2.0	4.3	24.2
20	1230	0	256	0.0	0	26.8
		59 exp	195	48.0	0	27.6
		59 cont	226	121	0	26.8
		140	156	12.0	0	28.8
		220	193	4.0	0	29.2

There were two differences in the nutrient samplings. First, the partition was not in place during the preliminary nutrient monitoring. Second, sampling during the preliminary nutrient monitoring was at cross sections 0, 20, 40, 140, and 234 (weir), whereas sampling during the acetone-injection experiment was at cross sections 0, 59, 140, and 220. This difference in sampling cross sections was not significant because only qualitative comparisons are of interest.

The orthophosphate concentrations in table 24 are similar to those observed during the preliminary monitoring period (table 2). The concentrations indicate what could be interpreted as a slight decrease with distance downstream. Also, the concentrations on day 20 are all less than the corresponding concentrations on day 5. The concentrations on the experimental side of the partition at cross section 59 are smaller than the concentrations on the control side, although these differences are small and may be within the sampling and analytical errors of determination.

The nitrate-nitrogen concentrations in table 24 are considerably smaller than those observed during the preliminary monitoring period (table 3), particularly at cross section 140 and at the downstream end of the stream (cross

sections 220 and 234). Also, the concentrations on the experimental side of the partition are only about 40 percent of the concentrations on the control side. However, the concentrations on each side are about the same on day 5 as on day 20. The nitrate-nitrogen concentrations indicate a definite decrease with distance downstream.

The nitrite-nitrogen concentrations in table 24 are comparable to those observed during the preliminary monitoring period (table 4). All the concentrations are very small or zero which is expected in water containing sufficient dissolved oxygen for the oxidation of nitrite to nitrate.

There are several possible explanations for the different nitrate-nitrogen concentrations on the two sides of the partition at cross section 59. These include differences in bacterial and biological activity and differences in the runoff sources of the nitrate-nitrogen. Although nutrient cycling in the model stream is an interesting problem, the objective of sampling the nutrient concentrations was to determine only if nutrient concentrations in the model stream could be limiting the bacterial degradation of the acetone. Consequently, these explanations will not be discussed further.

Opinions differ as to the nitrogen/phosphorus ratio needed for efficient bacterial degradation. If the BOD test is used as a basis, then the recommended (Gaudy and Gaudy, 1980) carbon/nitrogen ratio is about 20/1 and the carbon/phosphorus ratio is about 100/1, giving a nitrogen/phosphorus ratio of 5/1. Because the nutrient concentrations in table 24 give ratios much smaller than 5/1, it is concluded that the small nitrate concentrations in the model stream could be limiting acclimation of the bacteria to acetone and, subsequently, degradation of the acetone. Several laboratory studies were conducted to check this conclusion, and preliminary results indicated degradation of acetone in model stream water increased greatly when the nitrate concentration was increased.

Preferential use of other organic compounds

The model stream was biologically rich, as indicated by figures 4, 5, 10, and the results of the diel oxygen study presented in figure 35. Thus, various natural organic compounds are likely to be present in the model stream. Thurman (1985) classified the organic compounds present in natural waters into the general groupings of humic substances, hydrophilic acids, carboxylic acids, amino acids, carbohydrates, and hydrocarbons. It was suggested (Thurman, 1985) that the humic substances and hydrophilic acids contribute about 80 percent of the dissolved organic carbon of a typical river water.

These compounds have relatively complex molecular structures compared with the structure of acetone. Thus, bacterial degradation of these natural organic molecules might be expected to require more energy than degradation of the acetone molecules. However, the bacteria in the model stream have been seeing these complex structures since the first plant died and degradation of the plant matter began. Consequently, the bacteria are acclimated to and capable of degrading these compounds. Because of the abundance of natural organic material in the model stream, preferential use of these compounds

could be an explanation for the failure of the acetone to degrade. Such preferential use has been noted in other studies (Wilderer, 1981; Swindol and others, 1988).

Laboratory experiments were conducted using water from the model stream to test this hypothesis. It was found that acetone degradation occurred after a lag period. This could be interpreted to indicate the bacteria switched to acetone after consuming all the available natural organic compounds. However, the lag period could also be simply the time necessary for acclimation.

Residence Time in the Model Stream

Another possible explanation for the failure of the acetone to degrade is the short residence time in the stream system. The mean traveltime from the injection point to cross section 220 was about 6 hours, as determined from the dye studies. Consequently, if free-floating bacteria dominate the degradation process and if the acclimation time period is 6 hours or more, then the bacteria would be flushed from the system before significant degradation could occur.

Approximate values of the acclimation time period can be obtained from the laboratory studies (Rathbun and others, 1982). Lag periods of from 5 to 19 hours occurred after initiation of an experiment before degradation actually began. These lag periods were reduced to 1 to 3 hours if the bacteria were exposed to μg/L quantities of acetone overnight prior to initiation of the experiment. These studies, however, were under relatively ideal laboratory conditions with bacteria acclimated to acetone. In the model stream, a longer acclimation period would undoubtedly be necessary because the bacteria would not be acclimated to acetone. A longer acclimation period is supported by the results of a sediment sorption study using sediment and water from the model stream under nonsterile conditions (Rathbun and others, 1982). Loss of acetone was not observed until 90 hours of exposure. These results suggest free-floating bacteria would probably be flushed from the stream system before acclimation could occur and thus, no degradation would occur.

The laboratory degradation studies, however, differ from the model stream study in one important aspect. A respirometer was used for the laboratory studies, and the solutions in the glass chambers were stirred continuously. The only surfaces for the bacteria to attach to were the glass walls of the chambers. Because no attachment was noted, it is assumed the bacteria were largely in the solution phase. In the model stream, however, a variety of surfaces existed for the bacteria to attach to and it is assumed that most were attached rather than free floating in the solution phase. It was previously indicated (Tallon, 1969) that virtually all bacteria in a stream are attached to surfaces rather than free floating. Consequently, if most of the bacteria in the model stream are attached to the various surfaces, then these bacteria should have been exposed continuously to acetone for the 32 days of the injection. This should have been ample time for acclimation, as discussed previously. Finally, the indication that it is the attached bacteria that contribute most to the degradation of organic compounds in streams is supported by the experimental data on the degradation of pentachlorophenol in a model stream (Pignatello and others, 1985).

Analysis of Assumptions and Approximations

Several assumptions and approximations were made in the acetone-injection experiment and the analysis of the data. These include the assumption that the factor α in equation 12 was small relative to 1.0, the approximation that the first term on the right of equation 8 generally was negligible with respect to the second term, and the assumption that the floc layer on the bottom of the stream was relatively immobile. The validity of these assumptions and approximations is analyzed in the following sections.

Value of the α Factor

It was assumed in the derivation of the steady-state distribution equation (eq. 13) that the factor α in equation 12 was small relative to 1.0. Recall that α is defined by equation 9. Also, it was concluded in this study that significant bacterial degradation of acetone did not occur. Therefore, ΣK_i in the expression for α reduces to the volatilization coefficient for acetone, K_V^{AC}.

Values of α were computed for the reaches between the injection point and cross sections 59, 140, and 220. Maximum values of the volatilization coefficients from table 19 were used with maximum values of the longitudinal-dispersion coefficient from table 20 and minimum values of the mean velocity from table 20 to obtain maximum α values for the experimental conditions. Results are given in table 25.

Table 25.--*Maximum values of the α factor for the conditions of the model stream experiment*

[Inj, injection point; eq., equation]

Reach (meters)	Volatilization coefficient $\times 10^4$ (minutes^{-1})	Dispersion coefficient (square meters per minute)	Mean velocity (meter per minute)	Reach length (meters)	α	$C(x,\infty)/C_0$		Ratio
						eq.12	eq.13	eq.12/eq.13
Inj-59	20.1	1.66	0.317	26.0	0.133	0.852	0.848	1.005
Inj-140	17.5	2.64	.528	107.	.066	.706	.701	1.007
Inj-220	13.1	5.35	.505	187.	.110	.623	.616	1.011

Also given in table 25 are values of the ratio $C(x,\infty)/C_0$ computed from equations 12 and 13, and ratios of these values. It is concluded that the assumption regarding α in the derivation of equation 13 from equation 12 is valid for the conditions of this experiment.

Comparison of the First and Second Terms of Equation 8

It was previously noted that the first term on the right of equation 8 generally is negligible with respect to the second. When this approximation is valid, initial estimates can be obtained of the mean velocity from equation 27 and of the longitudinal-dispersion coefficient from equation 26, as discussed previously. This approximation did not affect the final results because the complete equation 8 containing both terms was used in the modeling procedure. It is, however, of interest to consider the magnitudes of these two terms for the conditions in the model stream.

Values of the first and second terms of equation 8 for sample times corresponding to the acetone data for day 2 are presented in table 26 for cross section 59, table 27 for cross section 140, and table 28 for cross section 220. The first terms at each cross section are appreciable percentages of the second term for the early sample times. This percentage decreases rapidly, however, with time. Also, the percentage for the initial values is greatest at cross section 59, smallest at cross section 220. It was concluded that the first term of equation 8 was negligible with respect to the second term for the conditions of the model stream experiment, with the exception of the early sample times at each cross section.

Table 26.--*Values of the first and second terms of equation 8 for cross section 59 for the acetone data for day 2*

[m^2/min, square meters per minute; m/min, meters per minute; min, minutes]

Dispersion coefficient (m^2/min)	Mean velocity (m/min)	Time from start of injection (min)	Equation 8	
			First term	Second term
1.66	0.317	62	0.19374	0.63493
		90	.20593	1.06355
		105	.18830	1.23490
		155	.11012	1.57921
		167	.09410	1.62644
		215	.04869	1.73896
		243	.03457	1.77058
		270	.02418	1.78748
		303	.01711	1.79671
		361	.02016	1.79922
		420	.00159	1.79172
		480	.00056	1.78283
		540	.00020	1.78038
		600	.00008	1.78580
		675	.00002	1.79890
		720	.00001	1.80728

Table 27.--*Values of the first and second terms of equation 8 for cross section 140 for the acetone data for day 2*

[m^2/min, square meters per minute; m/min, meters per minute; min, minutes]

Dispersion coefficient (m^2/min)	Mean velocity (m/min)	Time from start of injection (min)	Equation 8	
			First term	Second term
2.64	0.528	137	0.04278	0.17195
		153	.06336	.30592
		182	.08824	.60720
		239	.07419	1.13058
		272	.05022	1.30070
		300	.03285	1.38639
		332	.01852	1.43121
		346	.01421	1.44626
		361	.01056	1.45658
		420	.00293	1.45709
		451	.00143	1.45323
		480	.00071	1.44315
		540	.00016	1.42168
		572	.00007	1.41101

Table 28.--*Values of the first and second terms of equation 8 for cross section 220 for the acetone data for day 2*

[m^2/min, square meters per minute; m/min, meters per minute; min, minutes]

Dispersion coefficient (m^2/min)	Mean velocity (m/min)	Time from start of injection (min)	Equation 8	
			First term	Second term
1.70	0.505	298	0.02986	0.20048
		313	.03852	.29664
		330	.04610	.41958
		373	.05236	.76478
		420	.03915	1.06501
		480	.01725	1.25111
		510	.01003	1.28937
		540	.00543	1.30524
		570	.00278	1.31317
		600	.00136	1.31768
		634	.00058	1.32407
		675	.00019	1.32544
		720	.00005	1.32257

Mobility of the Floc Layer

It was assumed that the floc that filled the bottom of the stream cross section (figs. 6, 7, and 8) was relatively immobile. This assumption can be checked by comparing mean velocities computed from the stream discharge and cross-sectional areas measured at the top of the floc with mean velocities determined from the dye concentration-versus-time curves.

Cross sections of the type shown in figures 6, 7, and 8 were determined at 10-m intervals from cross section 40 through cross section 220 4 days after the termination of the acetone injection. Mean cross-sectional areas determined from these measurements to the top of the floc layer for reaches between the injection point and cross sections 59, 140, and 220 are given in table 29. Mean inlet water discharge was 1.177 L/s and mean outlet discharge was 1.166 L/s. The inlet discharge was used for the reach between the injection point and cross section 59, and the average of the two discharges was used for the other two reaches. This corrected for a small amount of evaporation. Mean velocities computed from these data are given in table 29.

Table 29. Mean cross-sectional areas, mean velocities computed from the areas, mean velocities from the day 30 dye study, and percentage differences

[Inj, injection point]

Reach (meters)	Mean cross-sectional area (square meter)	Mean velocity (meter per minute)		Difference (percent)
		Area	Dye	
Inj- 59	0.165	0.428	0.410	+4.21
Inj-140	.106	.663	.588	+11.3
Inj-220	.141	.499	.531	-6.41

Also given in table 29 for comparison are mean velocities determined from the day 30 dye study and percentage differences between the velocities. Two of the percentage differences are positive, indicating the cross-sectional areas needed to be larger for agreement between the velocities. However, the reach between the injection point and cross section 220, which includes the other two reaches, had a negative difference, indicating the cross-sectional areas needed to be smaller for agreement. Because no consistent differences were found between the velocities and also because the differences were small, it was concluded that there was no appreciable flow in the floc. Consequently, the assumption that the floc was relatively immobile was valid.

SUMMARY AND CONCLUSIONS

The transport and the fate of acetone, rhodamine-WT dye, t-butyl alcohol, and glucose in an outdoor model stream were determined. Acetone was injected continuously for 32 days, resulting in concentrations in the 20 to 200 milligram per liter range in the stream water. Rhodamine-WT dye was injected at

the beginning and at the end of the experiment to determine the dispersion and traveltime characteristics of the stream. An injection of t-butyl alcohol was used to determine the volatilization characteristics of the stream. A glucose solution was injected from day 17 through day 20 of the experiment in an attempt to stimulate the growth of bacteria in the stream water, with subsequent bacterial degradation of the acetone. Similarly, a nutrient solution containing bacteria acclimated to acetone in the laboratory was injected on days 23 and 24 in an attempt to stimulate bacterial degradation of the acetone. A diel oxygen study was conducted on days 11 and 12 of the experiment to determine the productivity of the model stream.

Conclusions resulting from this study are as follows:

1. Significant bacterial degradation of acetone did not occur in the model stream during the 32 days of the injection. This result was contrary to expectations based on laboratory studies and the literature, which indicated that acetone should be readily degraded by bacteria in streams.

2. Nitrogen/phosphorus ratios in the model stream were small, relative to values from the literature considered desirable for efficient bacterial degradation of organic compounds. It was concluded that the small nitrate-nitrogen concentrations in the model stream may have been limiting the ability of the bacteria in the stream to acclimate to the acetone.

3. The model stream was biologically rich and the bottom of the stream cross section contained a layer of organic detritus. It was concluded that preferential use of this abundant supply of these naturally occurring organic compounds could explain the failure of the bacteria in the stream to acclimate to acetone.

4. The mean residence time in the model stream as determined from the dye studies was about 6 hours. Laboratory studies indicated that a time period of about 90 hours was necessary for the bacteria in the model stream water to acclimate to acetone. It was concluded that, if free-floating bacteria dominate the degradation process, they would be flushed from the system before significant acclimation could occur. It was concluded that, if attached bacteria dominate the degradation process, acclimation should have occurred because the acetone was injected continuously for 32 days. The literature supports the hypothesis that the attached bacteria in streams dominate the degradation process, therefore, it was concluded that degradation should have occurred in the model stream.

5. Mean water velocities and longitudinal-dispersion coefficients determined in the preliminary dye study and twice during the acetone-injection experiment generally were in good agreement. Mean velocities ranged from 0.317 m/min to 0.588 m/min and dispersion coefficients from 0.300 m^2/min to 5.35 m^2/min for the different reaches of the stream. It was concluded that these parameters can be determined accurately from the transient parts of rhodamine-WT dye concentration-time curves.

6. Dead zones existed in the model stream as a result of the floc on the bottom and the growth of rooted macrophytes along the banks at the downstream end. Some of the dye concentration-versus-time curves showed the characteristics of dead zone effects; others did not. All the dye concentration-versus-time curves were modeled successfully without considering dead zone effects. Therefore, it was concluded that these effects were minimal in the model stream.

7. Volatilization coefficients for acetone determined from t-butyl alcohol concentrations were comparable to or larger than coefficients determined from acetone concentrations on day 4. This result supports the conclusion that significant bacterial degradation of acetone did not occur in the model stream.

8. Volatilization coefficients for acetone on day 4 generally were larger than the coefficients for other time periods. This difference was attributed to a greater windspeed on day 4, which increased the gas-film coefficient. This coefficient is significant in the volatilization from water of solutes such as acetone and t-butyl alcohol that have small Henry's constants.

9. Volatilization coefficients for acetone determined by the different methods for the different time periods generally were in good agreement, with the exception of the day 4 values which were larger for the most part. Mean coefficients ranged from 8.13×10^{-4} min^{-1} for the reach between cross sections 140 and 220 to 14.5×10^{-4} min^{-1} for the reach between cross sections 59 and 140. It was concluded that any of the methods could be used to compute the acetone volatilization coefficient for the model stream. It was recognized, however, that measurement of the coefficients was subject to large errors because of the limited length of the model stream and the slow volatilization rate of acetone. These two factors resulted in small concentration changes over the length of the model stream.

10. Injection of a glucose solution resulted in no significant decrease in acetone concentrations in the model stream. Bacterial degradation of the glucose occurred. It was concluded that the glucose added as a supplmental carbon source did not enhance the bacterial activity in the stream to the point where degradation of acetone would occur.

11. Injection of the nutrient solution containing bacteria acclimated to acetone in the laboratory resulted in no apparent decrease in the acetone concentrations in the model stream. Smaller acetone concentrations were observed in samples collected the morning after termination of the injection. However, it was concluded that these smaller concentrations were solely the result of dilution from rainfall the previous night.

12. Percentage saturations of dissolved oxygen in the diel oxygen study ranged from 13.2 to 470. Productivity/respiration ratios were greater than unity, with the exception of the control side of the divided channel at cross section 59. These results attest to the biological richness of the model stream.

13. The transient acetone concentration-versus-time data on day 2 were predicted reasonably well using a solution of the one-dimensional convective-dispersion equation. These concentrations were predicted completely independently of the day 2 experimental acetone concentrations. It was concluded that an analytical solution of the one-dimensional convective-dispersion equation for a continuous injection boundary condition adequately described the acetone concentration-versus-time data of this study.

14. Results of previous laboratory studies concluded that bacterial degradation and volatilization would be the two processes determining the fate of acetone in streams. It was concluded from the outdoor model stream study that significant bacterial degradation of the acetone did not occur.

Consequently, conclusions on the basis of laboratory studies regarding the fate of organic compounds in streams may not always be accurate. Differences observed in this study emphasize the utility of outdoor model-stream studies in determining such fates of anthropogenic compounds.

REFERENCES CITED

Abrams, E.F., Derkics, D., Fong, C.V., Guinan, D.K., and Slimak, K.M., 1975, Identification of organic compounds in effluents from industrial sources: National Technical Information Service Report PB-241 641, 52 p. plus appendices.

American Public Health Association, 1971, Standard methods for the examination of water and wastewater (13th ed.): Washington, D.C., American Public Health Association, 874 p.

Bencala, K.E., 1983, Simulation of solute transport in a mountain pool-and-riffle stream with a kinetic mass transfer model for sorption: Water Resources Research, v. 19, no. 3, p. 732-738.

Bencala, K.E., Kennedy, V.C., Zellweger, G.W., Jackman, A.P., and Avanzino, R.J., 1984, Interactions of solutes and streambed sediment 1. An experimental analysis of cation and anion transport in a mountain stream: Water Resources Research, v. 20, no. 12, p. 1797-1803.

Bencala, K.E., and Walters, R.A., 1983, Simulation of solute transport in a mountain pool-and-riffle stream--a transient storage model: Water Resources Research, v. 19, no. 3, p. 718-724.

Carpenter, J.H., 1965, The Chesapeake Bay Institute technique for the Winkler dissolved oxygen method: Limnology and Oceanography, v. 10, no. 1, p. 141-143.

Chiou, C.T., Peters, L.J., and Freed, V.H., 1979, A physical concept of soil-water equilibria for nonionic organic compounds: Science, v. 206, November 16, p. 831-832.

Clark, J.R., Rodgers, J.H., Jr., Dickson, K.L., and Cairns, J., Jr., 1980, Using artificial streams to evaluate perturbation effects on aufwuchs structure and function: Water Resources Bulletin, v. 16, no. 1, p. 100-104.

Dubois, M., Gilles, K.A., Hamilton, J.K., Rebers, P.A., and Smith, F., 1956, Colorimetric method for determination of sugars and related substances: Analytical Chemistry, v. 28, no. 3, p. 350-356.

Dugan, P.R., 1972, Biochemical ecology of water pollution: New York, Plenum Publishing Co., 159 p.

Falco, J.W., and Mulkey, L.A., 1976, Modeling the effect of pesticide loading on riverine ecosystems: Conference on Environmental Modeling and Simulation, Cincinnati, Ohio, Proceedings, p. 156-160.

Gaudy, A.F., Jr., and Gaudy, E.T., 1980, Microbiology for environmental scientists and engineers: New York, McGraw-Hill, 736 p.

Geyer, H., Viswanathan, R., Freitag, D., and Korte, F., 1981, Relationship between water solubility of organic chemicals and their bioaccumulation by the alga *Chlorella*: Chemosphere, v. 10, no. 11/12, p. 1307-1313.

Goldstein, R.M., Mallory, L.M., and Alexander, M., 1985, Reasons for possible failure of inoculation to enhance biodegradation: Applied and Environmental Microbiology, v. 50, no. 4, October, p. 977-983.

Handa, N., 1966, Examination on the applicablity of the phenol sulfuric acid method to the determination of dissolved carbohydrate in sea water: The Journal of the Oceanographical Society of Japan, v. 22, no. 3, June, p. 1-8.

Helfgott, T.B., Hart, F.L., and Bedard, R.G., 1977, An index of refractory organics: National Technical Information Service Report PB-272 438, 130 p.

Jobson, H.E., and Rathbun, R.E., 1984, Use of the routing procedure to study dye and gas transport in the West Fork Trinity River, Texas: U.S. Geological Survey Water-Supply Paper 2252, 21 p.

Jobson, H.E., and Sturrock, A.M., Jr., 1979, Comprehensive monitoring of meteorology, hydraulics, and thermal regime of the San Diego Aqueduct, California: U.S. Geological Survey Professional Paper 1137, 29 p.

Keith, L.H., and Telliard, W.A., 1979, Priority pollutants I--a perspective view: Environmental Science and Technology, v. 13, no. 4, p. 416-423.

Khare, M., and Dondero, N.C., 1977, Fractionation and concentration from water of volatiles and organics on high vacuum system--examination of sanitary landfill leachate: Environmental Science and Technology, v. 11, no. 8, p. 814-819.

Landrum, P.F., Bartell, S.M., Giesy, J.P., Leversee, G.J., Bowling, J.W., Haddock, J., LaGory, K., Gerould, S., and Bruno, M., 1984, Fate of anthracene in an artificial stream--a case study: Ecotoxicology and Environmental Safety, v. 8, p. 183-201.

Lewis, W.K., and Whitman, W.G., 1924, Principles of gas absorption: Industrial and Engineering Chemistry, v. 16, no. 12, p. 1215-1220.

Mackay, D., and Yuen, T.K., 1980, Volatilization rates of organic contaminants from rivers: Water Pollution Research Journal of Canada, v. 15, no. 2, p. 83-98.

Marino, M.A., 1974, Distribution of contaminants in porous media flow: Water Resources Research, v. 10, no. 5, p. 1013-1018.

Montgomery, H.A.C., and Gardiner, D.K., 1971, Experience with a bacterial inoculum for use in respirometric tests for oxygen demand: Water Research, v. 5, p. 147-163.

Ogata, A., 1970, Theory of dispersion in a granular medium: U.S. Geological Survey Professional Paper 411-I, 34 p.

Ogata, A., and Banks, R.B., 1961, A solution of the differential equation of longitudinal dispersion in porous media: U.S. Geological Survey Professional Paper 411-A, 7 p.

Overman, A.R., Chu, R.-L., and Leseman, W.G., 1976, Phosphorus transport in a packed bed reactor: Journal Water Pollution Control Federation, v. 48, no. 5, May, p. 880-888.

Paris, D.F., Steen, W.C., Baughman, G.L., and Barnett, J.T., Jr., 1981, Second-order model to predict microbial degradation of organic compounds in natural waters: Applied and Environmental Microbiology, v. 41, no. 3, March, p. 603-609.

Pellizzari, E.D., Castillo, N.P., Willis, S., Smith, D., and Bursey, J.T., 1979, Identification of organic components in aqueous effluents from energy-related processes: American Society for Testing and Materials Special Technical Publication 686, October, p. 256-274.

Pfaender, F.K., and Alexander, M., 1973, Effect of nutrient additions on the apparent cometabolism of DDT: Journal of Agricultural and Food Chemistry, v. 21, no. 3, p. 397-399.

Pignatello, J.J., Johnson, L.K., Martinson, M.M., Carlson, R.E., and Crawford, R.L., 1985, Response of the microflora in outdoor experimental streams to pentachlorophenol--compartmental contributions: Applied and Enviromental Microbiology, v. 50, no. 1, July, p. 127-132.

Rathbun, R.E., 1988, Discussion of *Wind function for a sheltered stream* by J.S. Gulliver and H.G. Stefan: American Society of Civil Engineers Proceedings, Journal of Environmental Engineering, v. 114, no. 1, p. 229-231.

Rathbun, R.E., Stephens, D.W., Shultz, D.J., and Tai, D.Y., 1982, Fate of acetone in water: Chemosphere, v. 11, no. 11, p. 1097-1114.

Rathbun, R.E., and Tai, D.Y., 1982, Volatilization of organic compounds from streams: American Society of Civil Engineers Proceedings, Environmental Engineering Division Journal, v. 108, no. EE5, p. 973-989.

_____1983, Gas-film coefficients for streams: American Society of Civil Engineers Proceedings, Journal of Environmental Engineering, v. 109, no. 5, p. 1111-1127.

_____1984a, Volatilization of chlorinated hydrocarbons from water: International Symposium on gas transfer at water surfaces, Cornell University, 1983, Proceedings, p. 27-34.

_____1984b, Volatilization of ketones: Chemosphere, v. 13, no. 9, p. 1009-1023.

_____1986, Gas-film coefficients for the volatilization of ethylene dibromide from water: Environmental Science and Technology, v. 20, no. 9, p. 949-952.

_____1988, Application of the two-film model to the volatilization of acetone and t-butyl alcohol from water as a function of temperature: U.S. Geological Water-Supply Paper 2318, 41 p.

Schmidt, S.K., and Alexander, M., 1985, Effects of dissolved organic carbon and second substrates on the biodegradation of organic compounds at low concentrations: Applied and Environmental Microbiology: v. 49, no. 4, April, p. 822-827.

Scott, C.H., Norman, V.W., and Fields, F.K., 1969, Reduction of fluorescence of two tracer dyes by contact with a fine sediment: U.S. Geological Survey Professional Paper 650-B, p. B164-B168.

Shackelford, W.M., and Keith, L.H., 1976, Frequency of organic compounds identified in water: U.S. Environmental Protection Agency Report 600/4-76-062, December, 618 p.

Stephens, D.W., and Jennings, M.E., 1976, Determination of primary productivity and community metabolism in streams and lakes using diel oxygen measurements: U.S. Geological Survey Computer Program Documentation User's Manual, March, Bay St. Louis, MS, 100 p.

Stevens, A.A., Slocum, C.J., Seeger, D.R., and Robeck, G.G., 1976, Chlorination of organics in drinking water: Journal of the American Water Works Association, v. 68, November, p. 615-620.

Stover, E.L., and McCartney, D.E., 1984, BOD results that are believable: Water/Engineering and Management, April, p. 37-40, p. 62, p. 66.

Strickland, J.D.H., and Parsons, T.R., 1968, A practical handbook of seawater analysis: Fisheries Research Board of Canada Bulletin 167, 311 p.

Subba-Rao, R.V., Rubin, H.E., and Alexander, M., 1982, Kinetics and extent of mineralization of organic chemicals at trace levels in freshwater and sewage: Applied and Environmental Microbiology, v. 43, no. 5, May, p. 1139-1150.

Swindol, C.M., Aelion, C.M., and Pfaender, F.H., 1988, Influence of inorganic and organic nutrients on aerobic biodegradation and on the adaptation response of substrate microbial communities: Applied and Environmental Microbiology, no. 54, no. 1, p. 212-217.

Tai, D.Y., 1978, Determination of acetone and methyl ethyl ketone in water: U.S. Geological Survey Water-Resources Investigation Report 78-123, 36 p.

Tai, D.Y., and Rathbun, R.E., 1988, Photolysis of rhodamine-WT dye: Chemosphere, v. 17, no. 3, p. 559-573.
Tallon, G.R., 1969, Microbes and microorganics in water--a review: American Society for Testing and Materials Special Technical Publication No. 448, p. 3-10.
Thom, N.S., and Agg, A.R., 1975, The breakdown of synthetic organic compounds in biological processes: Proceedings, Royal Society London, v. B189, p. 347-357.
Thurman, E.M., 1985, Organic geochemistry of natural waters: Boston, Martinus Nijhoff/Dr W. Junk Publishers, 497 p.
Tinsley, I.J., 1979, Chemical concepts in pollutant behavior: New York, John Wiley, 265 p.
U.S. Environmental Protection Agency, 1975, Preliminary assessment of suspected carcinogens in drinking water--report to Congress: National Technical Information Service Report PB-250 961, December, 52 p. plus appendices.
Van Genuchten, M.Th., 1981, Analytical solutions for chemical transport with simultaneous adsorption, zero-order production and first-order decay: Journal of Hydrology, v. 49, p. 213-233.
Veith, G.D., Macek, K.J., Petrocelli, S.R., and Carroll, J., 1980, An evaluation of using partition coefficients and water solubility to estimate bioconcentration factors for organic chemicals in fish: American Society for Testing and Materials Special Technical Publication 707, p. 116-129.
Warren, C.E., and Davis, G.E., 1971, Laboratory stream research--objectives, possibilities and constraints: Annual Review of Ecology and Systematics, v. 2, p. 111-144.
Wiggins, B.A., Jones, S.H., and Alexander, M., 1987, Explanations for the acclimation period preceding the mineralization of organic chemicals in aquatic environments: Applied and Environmental Microbiology, v. 53, no. 4, April, p. 791-796.
Wilderer, P., 1981, A model river test to describe the various impacts of chemical substances on microbial biocommunities: American Institute Chemical Engineers Symposium Series, v. 77, no. 209, Water-1980, G.F. Bennett, ed., p. 205-213.
Wilson, J.F., Jr., Cobb, E.D., and Kilpatrick, F.A., 1984, Fluorometric procedures for dye tracing: U.S. Geological Survey Open-File Report 84-234, 53 p.
Wilson, J.T., Enfield, C.G., Dunlap, W.J., Cosby, R.L., Foster, D.A., and Baskin, L.B., 1981, Transport and fate of selected organic pollutants in a sandy soil: Journal of Environmental Quality, v. 10, no. 4, p. 501-506.
Yotsukura, N., Stedfast, D.A., Draper, R.E., and Brutsaert, W.H., 1983, An assessment of steady-state propane-gas tracer method for reaeration coefficients--Cowaselon Creek, New York: U.S. Geological Survey Water-Resources Investigations Report 83-4183, 88 p.
Zand, S.M., Kennedy, V.C., Zellweger, G.W., and Avanzino, R.J., 1976, Solute transport and modeling of water quality in a small stream: U.S. Geological Survey Journal of Research, v. 4, no. 2, p. 233-240.

*U.S. GOVERNMENT PRINTING OFFICE: 1990-0-773-204/20024